APPLICATION OF FILTERED NEUTRONS TO PRECISE MEASUREMENTS OF NEUTRON CROSS SECTIONS

YOSHIAKI FUJITA

APPLICATION OF FILTERED NEUTRONS TO PRECISE MEASUREMENTS OF NEUTRON CROSS SECTIONS

1984

YOSHIAKI FUJITA

研究題目及び要旨和訳

フィルター中性子の高精度中性子断面積測定への応用

藤　田　薫　顕

要　　旨

現時点で入手しうる中性子断面積の実験データは、原子力エネルギーの研究・開発分野からの要求にたいし、充分には応えられていない。未測定断面積への要求もあるが、実験データ間の不一致に問題のある場合も多い。この実験データ間の不一致の原因は実験誤差の見積りの問題にあるわけであり、これを解決するためには実験誤差の入りにくい高精度測定法の開発が望まれる。

本研究はフィルター中性子をその高精度測定に応用するものである。フィルター中性子は、ある狭いエネルギー幅内で全断面積が非常に小さくなるウインドウと呼ばれるものをもつ厚い物質を用い、連続エネルギースペクトルの中性子をフィルターすることにより得られる単色エネルギーの中性子である。この中性子ビームのバックグランドは非常に少なく、このため、一般に実験誤差のうち相当な部分を占めるバックグランド差し引き手続きにおける不正確さからくる誤差が著しく小さくなる。さらに飛行時間法を併用することにより、バックグランドについての問題をほぼ取り除いてしまうことができる。フィルター中性子実験により得られるデータは少数のエネルギー点に限られているが、それらは高精度のデータであって、通常の飛行時間法により得られる断面積曲線を規格化するのに有効に利用される。

本研究の結果は次のように要約される。

1）　広く利用されるフィルター物質のうち、フィルターの設計にとって断面積データの不充分であったスカンジウムとシリコンにつき、ウインドウ近傍における全断面積を測定した。これらの物質を測定試料として用いるだけでなく、ノッチフィルターとしても利用し、必要な中性子のみをフィルターして測定した。この手法はバックグランドの少ないフィルター中性子応用の一例になっている。得られた高信頼度の断面積は従来のデータに対して著しく異なるものであった。シリコンについては５３．５ｋｅＶに新しいウインドウを見い出した。

２）　加速器におけるフィルタービームと飛行時間法を組み合わせ、鉄によりフィルターされた２４ｋｅＶの中性子を用い、全断面積と捕獲断面積測定において達成される精度を実験的に確めた。その結果、全断面積については約 0.1 %の精度が達成され、この精度は、このエネルギー領域における典型的な精度約１%に比較して相当によく、熱中性子による高精度測定と同程度のものである。捕獲断面積については約５%の精度が得られ、これもｋｅＶ領域における既存実験データ間の不一致に比較してかなり良いものであった。

３）　加速器による鉄フィルタービームを水素・ベリリウム・炭素・酸素の全断面積測定ならびに、ニオブ・インジウム・ホロミウム・ヨウ素・タンタル・ウラン－２３８の捕獲断面積測定に応用した。これらの物質については原子炉工学において重要なもののうちから選んだ。得られたデータを他の実験値やいわゆる評価値と比較した。

４）　原子炉において得られるシリコンでフィルターされた１４４ｋｅＶの中性子を用いトリウム－２３２の非弾性散乱断面積を測定した。結果は２５０ｋｅＶ以下のエネルギー領域において得られた最初のデータであって、その値の理論的説明のためには変形核の回転運動の直接励起過程の導入が必要なことを示した。

５）　原子炉において得られる鉄フィルター中性子を用い、有効平均全断面積にあらわれるドップラー効果と自己遮蔽効果の関係についてのＢｅｅの示した理論的予測を実験的に確めた。試料としては、同一核ながら化学結合状態の異なるトリウム金属とその二酸化物を用いた。結果は理論的予測の正しいことを示している。

６）　以上の経験をもとに、フィルター中性子の応用に関する若干の提言を行なった。

Synopsis

The experimetal data of neutron cross sections available at the present time do not always meet the requirements from the research and development of nuclear-energy applications. There are requirements for the unmeasured cross sections, while another kind of requirements is the settlement of the discrepancies between the experimental data. The discrepancies come from the improper estimate of experimental errors. For the settlement, it is highly expected to develop a new experimental technique which has an inherent point of excellence for precise measurements.

The present study is the application of filtered neutrons to the precise neutron-cross-section measurements. The filtered neutrons are a monoenergetic beam which is obtained by filtering neutrons of continuous energy spectrum with a thick material having a narrow energy band of small total cross section called as "window". The beam is very clean and reduces a perplexing problem in the subtraction procedure of background which usually introduces a considerable part of experimental errors. The employment of the time-of-flight technique along with the filtered beam almost solves the background problem. The data obtained in the experiment with filtered neutrons are limited to a few energy points; however, they are of high precision and effectively used to normalize a cross section curve obtained in a usual time-of-flight experiment.

The results of the present study are briefly itemized as follows:

1) The total cross sections of commonly-used filter materials, Sc and Si, have been measured near the windows, since the experimental data were scarce for the design of these filters. These materials were also used for notch-filters as well as for the samples in the measurement in order to obtain the neutrons of the energies relevant to the measurement. This technique is an example of the filtered-neutron applications. The results have provided high-quality data and they differ markedly from the previously-reported experiments. A new window has been found for Si at 53.5 keV.

2) By employing the combination of the accelerator-based filtered-beam and

time-of-flight techniques, the capability in achieving high precision has been studied for the total- and capture-cross-section measurements using Fe-filtered 24-keV neutrons. As for the total cross section, a precision of about 0.1 % was achieved. The precision is considerably better than a typical value of about 1 % in this energy range and comparable to that achieved in precise thermal-neutron cross-section measurements. For the capture cross section, the precision achieved was about 5 %, which is better than the descrepancies between the presently-available data in the keV range.

3) The accelerator-based Fe-filtered neutrons were applied for the total-cross-section measurements of H, Be, C and O. For capture cross sections, measurements were made for Nb, In, Ho, I, Ta and ^{238}U. These samples were selected from materials mainly of technological importance. The data obtained are compared with other experiments and so-called evaluated values.

4) Reactor-based Si-filtered neutrons have been applied to the inelastic-scattering cross-section measurement of Th at 144 keV. The result first provided an experimental data below 250 keV and shows the nessecity of the inclusion of the direct exitation prosess in the theoretical interpretation of the cross section.

5) Reactor-based Fe-filtered neutrons have been applied to an experimental verification of a relationship, which is theoretically predicted by Bee, between the Doppler and the self-shielding effects in the effective average total cross section. Thorium samples were used in two different kinds of chemical forms, metal and dioxide. The result satisfactorily verified the theoretical prediction.

6) Using the experience obtained in the above-mentioned studies, a few recommendations are given for the future application of filtered neutrons.

Contents

Chapter 1 Introduction[1]

1.1 Necessity of Accurate Neutron-Cross-Section Data and Purpose of Present Study

Neutron cross section, which is a physical quantity expressing the neutron interaction with nuclei, has been an extensive subject[2,3] in fundamental research and applied fields, since the neutron is used not only in experimental investigations of nuclei but also in harnessing processes of nuclear energy. With regard to the nuclear-energy applications, the requirement[4] of the data of neutron cross sections is increasing in various fields, particularly in the research and development of fission reactors and of the neutronic problems in fusion-reactor technology. Although a considerable number of cross-section data for most important materials in nuclear-energy applications have been obtained, these data are not always accurate to fully meet the technological requirements.[5] Between the data, there are often inconsistencies much larger than the appended experimental errors. Most of the explanations of the inconsistencies may be in the under-estimation and the unconsciousness of experimental errors. A user and a so-called evaluator of cross-section values are perplexed with facing to the inconsistency. Under such a situation, it is highly expected to develop a new experimental technique which has an inherent point of excellence for accurate measurements. The purpose of the present study is to propose the application of the filtered neutrons introduced in the next section to the accurate measurements, contributing towards the research activities to meet the above-mentioned requirements of reliable cross-section data.

1.2 Earlier Works using Filtered Neutrons

Monoenergetic neutrons in keV range can be obtained with placing a thick filtering material in the flight path of the neutrons leaking out from neutron sources having a continuous energy spectrum such as reactors and accelerators.[6,7] Some materials have sharp resonance minima in the total cross section of neutrons which are called as the windows of cross

section. The minima come from the interference effect between potential and compound-nucleus scatterings. The neutrons at the window pass through the material with little amount of extinction, while other neutrons and gamma-rays can be almost scattered-out from the beam. The neutrons thus obtained and the materials used are called simply as "filtered neutrons" and "filters", respectively. These simple names are used in this paper as well as a recent review paper by Block and Brugger.[6] The same expressions are often employed in the case of crystalline filters used to obtain cold neutrons; however, there may be no confusion as the neutron energies concerned are different.

Simpson and Miller[8] obtained the filtered neutrons of 2 keV by installing a Sc-filter at a beam-port of the MTR in 1968. Since then, many filtered-neutron facilities[9-17] have been built world-widely at research reactors by also using other kinds of filters - e.g. Fe, Si, O - to obtain monoenergetic neutrons from keV to MeV energy range. Filtered neutrons have been used mainly in the gamma-ray spectroscopy of neutron capture, in neutron tomography and as a standard neutron source for the calibration of neutron detectors. However, there are few applications in cross-section measurements of neutrons. This study extends the application of filtered neutrons to precise measurements of neutron cross sections.

More details of the filtered neutrons will be given in Chapter 2.

1.3 Capability of Filtered Neutrons for Precise Measurements

Filtered neutrons are intense and clean; they are monochromatized with little loss of source neutrons and the contamination of background neutrons and gamma-rays is very low. The main part of the experiments in this study were carried out by employing a photoneutron source with an electron linear accelerator. The accelerator-based filtered neutrons has another excellent characteristic, if it is a pulsed neutron source: The filtered neutrons can be seperated by their flight time from background neutrons and gamma-rays. The background can be reduced to an extremely low level and is reliably estimated in the amount. This is one of the main reasons for the accelerater-based filtered neutrons to be applied to precise measurements. The precise values of cross section obtained with the filtered-neutron

technique are effectively used to normalize the cross-section curves obtained in a wide energy range with such experiment as the time-of-flight. In this meaning, the value obtained with filtered neutrons is sometimes called as " a point cross section ".

With the inherent capabilities for precise measurements, the technique of filtered neutrons may be also used to measure a very small, but still important, change of cross sections such as the self-shielding and Doppler effects in the energy range of unresolved resonances.

Although the filtered neutrons are monoenergetic, they have an energy spread in the order of 10 % of the average energy. They can not be used, therefore, for a high-resolution measurement but can be successfully used for a cross section whose variation in the energy spread is small or can be treated with the statistical considerations.

1.4 Composition of This Study

The measurements in this study are seperated into two categories. The first consists of precise measurements of the total cross sections of filter material themselves for the neutron energies near their windows, since a reliable value of the cross section near the minimum is essential for the optimal design of a filter. In spite of the importance of the reliable value, there still remain marked discrepancies between experimental data even for the most popular filter materials such as Sc and Si. One may find the explanation for the discrepancies in the following reasons: (i) Total-cross-section measurements have been mostly carried out at the energies of resonance peak with an intension to determine resonance parameters. (ii) A material of a small cross section is highly transparent to neutrons and there are inherent difficulties in the transmission measurement for such a transparent sample. (iii) Even a small amount of impurities introduces a serious error in the result of experiment.

The measurements have been performed by making careful considerations in the above-mentioned items (ii) and (iii) for the following cross sections:

(1) Total cross section of Sc near the 2-keV minimum.

(2) Total cross sections of Si near the cross-section minima.

The measurements of the second category are the following applications of the filtered neutrons to several important cross sections:

(3) Total cross sections of Be, C, and O for 24-keV neutrons.
(4) The n-p total cross section for 24-keV neutrons.
(5) Capture cross sections of ^{93}Nb, ^{115}In, ^{165}Ho, ^{181}Ta and ^{238}U for 24 keV neutrons.
(6) Inelastic-scattering cross section of Th for 144-keV neutrons.
(7) Doppler and self-shielding effects of Th and ThO_2 for 24-keV neutrons.

In the measurement (3), the capability of precise measurements by accelerator-based Fe-filtered neutrons is studied in detail and the neutrons are successfully applied for the total cross sections of Be-, C- and O-samples. The n-p total cross section in the measurement (4) is important in fundamental physics and neutron-detection techniques. The samples in the capture-cross-section measurement of (5) are taken considering the technological importance from a fertile material U, a structural material Nb, and materials in the atomic-mass-number region of fission products In, Ho and Ta. In (6) and (7), reactor-based filtered neutrons are applied for cross sections of Th - a possible alternative fertile material to ^{238}U. The inelastic scattering in (6) is one of the processes in forming the energy spectra of neutrons in a Th-loaded assembly. The Doppler and self-shielding effects in (6) are important in various subjects in reactor physics such as the criticality, safety and control of a reactor.

This paper is composed as follows: In Chapter 2, a general description is given for the filtered neutrons; in Chapter 3, the experimental apparatuses used in this study are described for their common part so as to avoid the overlap of description in the following chapters; in Chapters from 4 to 10, the experiments mentioned above from (1) to (7) are given in the sequence of number, and each chapter individually consists of the purpose of the measurement, experimental method, results and discussions: in Chapter 11, concluding remarks are given for the present study.

References:

1) Fujita, Y., Yamamuro, N.: "Filtered Neutron Beam and Its Applications", Nihon Genshiryoku Gakkaishi (Journal of the Atomic Energy Society of Japan), (in Japanese), 23, No.2, 3 (1981).
2) CINDA82 (The Index to Literature and Computer Files on Microscopic Neutron Data), published by IAEA, (1982).
3) Proceeding of the Conference on " The Neutrons and its Applications, 1982 "; edit. by Schofield, P.; held at Cambridge; 13-17, Sept.(1982).
4) WRENDA 81/82 (World Request List for Nuclear Data); INDC(SED)-78/URSF; edit. by DayDay, N.; published by IAEA (1981).
5) Weisbin, C.R. et al.: Ann. Nucl. Energy, 9, 615 (1982).
6) Block, R.C., Brugger, R.M.: " Filtered Neutron Beam ", in chapter VIII of " Neutron Sources for Basic Physics and Applications " OECD/NEA Perort; edit. by Cierjacks, S.; Pergamonn Press (1983).
7) Mill, A.J., Harvey, J.R.: " Reactor- and Accelerator-based Filtered Neutrons ", RD/B/N4776, Berkeley Nuclear Laboratory Report (1980).
8) Simpson, O.D., Miller, L.G. : Nucl. Instr. Methods, 61, 245 (1968).
9) Tsang, F.Y., Brugger, R.M. : ibid., 134, 441(1976).
10) Greenwood, R.C., Chrien, R.E. : ibid., 138, 125 (1976).
11) Schwarz, R.B. : Proc. Int. Specialists' Symp. on Neutron Standards and Applications held at the National Bureau of Standards, p.493 (1977).
12) Alberts, W.G. : Nucl. Instr. Methods, 155, 307 (1978).
13) Condaiah, E. et al.: ibid., 111, 337 (1973).
14) Broder, D.L. et al.: Yadern. Fiz., 13, 3 (1971).
15) Kuzin, E.N. et al.: Atom. Energ., 35 (6), 391 (1973).
16) Aizawa, O. et al.: J. Nucl. Sci. Technol., 20(4), 82 (1983).
17) Tsuei, Y.F. et al.: Annual Report of Institute of Atomic Energy, Beijing, China, p.24 (1980).

Chapter 2 Filtered Neutrons

2.1 General Features

Neutrons obtained from usual sources have energies in MeV range and are called as fast neutrons. Neutrons in keV range are obtained by moderating the fast neutrons, and are in most cases contaminated, therefore, with fast neutrons and usually with gamma-rays. The keV neutrons are also obtained directly by a photo reaction using a gamma-ray source with beryllium or deuterium, and by an endothermic (p,n) reaction using an electrostatic accelerator. However, the sources obtained with these reactions are usually of low yield. The photo-neutron source is moreover associated with troublesome intense gamma-rays and the neutrons are usually applied for cross-section measurements where the gamma-ray is not a disturbing radiation, such as the shell-transmission and the activation techniques.

Some materials have a sharp minimum in total cross section of neutrons in the resonance-energy range. The energy for the minimum is called as a window. Filtered neutrons are obtained by placing such a material in the beam of neutrons having a continuous energy-spectrum. The neutrons of the energy at the window pass through the filter, while other neutrons and gamma-rays are almost scattered out from the beam. In Fig.2-1 is illustratively shown the relation of the energy spectrum of the source neutrons, that of the filtered neutrons and the total cross section of the filter material. Typical arrangements are shown in Fig.2-2 (a) and (b) for a reactor-based and an accelerator-based facilities respectively. Energy spectrum of filtered neutrons is estimated by a calculation as

$$F(E) = S(E)\cdot\exp\left\{-\sum_i N_i\sigma_i^t(E)\right\} \quad , \qquad (2.1)$$

where $F(E)$ is the energy spectrum of filtered neutrons; $S(E)$ is the energy spectrum of source neutrons; N_i is the number of nuclei of i-th material in the unit cross-sectional area of the filter; $\sigma_i^t(E)$ is the total cross section of i-th filter material at a neutron energy E.

Monoergetic neutrons thus obtained are very clean in the sense that the

contamination with background neutrons and gamma-rays is very low. There are usually plural minima in a single filter-material. In this case, auxiliary materials are needed to remove the neutrons at other minima than the interested, obtaining purely monoenergetic neutrons. The auxiliary materials are not always necessary if filtered neutrons are used in experiments with the time-of-flight technique, since the neutrons at different minima are seperated by their flight time. In this kind of experiment, the neutrons at different minima may be used, if required, to make simultaneous measurements at several energies of the minima.

A reliable value of the cross section near the minimum is important for an optimal design of a filter. For the design, a compromise is needed between the maximization of the intensity of filtered neutrons, the minimization of background and the avairable quantity of filter materials.

Expected advantages of filtered neutrons for cross section measurements are itemized as follows:

(i) Backgrounds of neutrons and gamma-rays are very low, leading to precise measurements of the cross sections.
(ii) Filter materials are available in the energy range where the methods of neutron production are scarce.
(iii) The energy spread of the neutrons is relatively large and the neutron is accordingly intense.
(iv) The facility is simple and the beam is steady and reproducible in quality and quantity.
(v) In the time-of-flight experiment, the background is measured during the experiment and it is reliably estimated from the time-of-flight spectrum.

A set of cross-section data is usually needed in a wide energy range. In this pespect, the information obtained by a filtered-neutron experiment is limited to one or a few energy points. However, the precise cross sections at the limited energy points are effectively used to normalize an energy dependent cross-section curve which is measured in a usual time-of-flight experiment.

2.2 Filter Materials

Neutron interactions with nuclei in keV range are mostly the scattering and the radiative capture. The sharp minimum in the cross section is the consequence of the interference between the potential and compound-nucleus scatterings. The scattering cross section of an isolated resonance is analytically expressed using a single-level Breit-Wigner cross-section formula. By neglecting the contributions of higher partial waves and the spin of the target nucleus, the formula is expressed as

$$\sigma_s = \frac{\pi}{k^2}\left| 2\sin(ka)\exp(ika) + \frac{\Gamma_n}{(E_n - E_r) + i\Gamma_n/2}\right|^2 , \quad (2.2)$$

where σ_s is the scattering cross section; E_n is the energy of neutrons; k is the wave number of neutrons; a is the scattering radius; E_r is the resonance energy; Γ_n is the neutron width.

The first term in the symbol of the absolute value in eq. (2.2) means the amplitude of the potential scattering and the second means that of compound-nucleus scattering. It is shown that the cross section in eq.(2.2) becomes zero at energy E_n , if

$$\tan(ka) = \frac{\Gamma_n/2}{E_r - E_n} . \quad (2.3)$$

This equation shows the interference minimum occures usually in the lower energy-side of the resonance peak. As an extreme case, the interference occures just on the resonance energy, if $E_n = E_r$ and $ka = \pi/2$, simultaneously. An example of the extreme case is that of oxygen at 2.35 at 2.35 MeV.

As shown in the above discussion, the cross section completely diminishes in the ideal case. In actual cases, however, it has a considerable amount of value at the window because of the following reasons:

(a) There are small amount of contributions of higher partial waves and capture cross sections.

(b) The target spin is not always zero.

(c) The target material is not always composed of a single isotope.

From the practical stand-point of material selection, a material can be used for a filter if the cross section at a minimum is less than about one -tenth of the values at other energies.

Explanations as filter materials are given in the rest of this paragraph for Sc, Fe, and Si which are most popular and are used in this study.

Significant features are shown in Table 2-1 for widely-used filter materials.

(i) Scandium

Scandium is one of rare-earth elements and a mono-isotope of atomic mass number 45. The spin number of the ground state is 7/2, and the discussion above-mentioned for a target of spin-zero can not directly be applied to this case. There are two kinds of s-wave interactions, spin-parallel and spin-antiparallel interactions, for a target nuclei of non-zero spin. The quantum numbers of the angular momentum of the compound-nucleus of Sc are 4 and 3 for the parallel and antiparallel interactions respectively. For Sc, sharp minima in the cross sections for two kinds of interactions coinside each other near 2 keV. The superposed value of the cross sections, each of which is written with a similar expression as eq.(2.2), still has a sharp minimum near the energy. The experimental data for the minimum cross section obtained in the earlier measurements show remarkable discrepancies between them.[1-3] More details of the discrepancies are given in Chapter 4. It is, therefore, one of the purposes of this study to make another measurement of the value by making a few effective experimental improvements.

(ii) Iron

Iron is a common structural material and most widely used as a filter. The main part of the isotopic composition is ^{56}Fe by 91.8 %. The other part is composed of ^{54}Fe, ^{57}Fe and ^{58}Fe. There is a sharp minimum near 24 keV. The ^{56}Fe is an even-even nucleus and the occurence of the mini-

mum can be physically explained by the afore-mentioned discussion of the interference minimum of a spin-zero nucleus. The values of cross section at the minium show a considerably good agreement between the existing experimental data.(4) Therefore, this study was made for the application only of the Fe-filtered neutrons to several experiments using both of the reactor-based and accelerator-based facilities. It is shown during the course of this study that the contamination of other neutrons can be reduced to less than 1 % of the main beam of relevant enegy, even in the the case of the reactor-based neutrons, by using Al and S for auxiliary filters.

The seperated isotope of ^{56}Fe has a very low value of cross section at the minimum.(5) A filter of high performance can be built if the pure isotope of ^{56}Fe is available in a necessary amount.

(iii) Silicon

The dominating isotope in natural Si is an even-even nucleus ^{28}Si by 92.23 % composition. The other part is composed of ^{29}Si and ^{30}Si. There are two significant sharp windows at 146 and 53.5 keV. The experimental data of cross section at the windows are very scarce(6). More details of the situation of the data are given in Chapter 5. One part of the study for Si is a refined measurement of the cross section minima. The window at 53.5 keV has been firstly found in this experiment. The other part of the study for Si is an application of the filtered neutrons to a measurement of the inelastic-scatteing cross section of Th.

Two kinds of monoenergetic, 144 and 53.5 keV in the average energies, neutrons are obtained using Ti and S for auxiliary filters, respectively. An adequate filter such as ^{10}B is needed to suppress thermal neutrons since a Si-sample of single crystal has a very low value of total cross section for thermal neutrons.

References:

(1) Magurno, B.M. , Mughabghab, S.F.: Proc. Conf. on Nuclear Cross Section and Technol., National Bureau of Standard Special Publication

425, No.1, 357 (1975).

(2) Liou, H.I. et al.: Nucl. Sci. Eng., 67, 326 (1978).

(3) Razbudey, V.F. et al.: Proc. Int. Conf. on Neutron Cross Section for Technol., National Bureau of Standard Special Publication 594, GD9 (1980).

(4) Kobayashi, K. et al.: Annals of Nucl. Energy, 4, 499 (1977).

(5) Liou, H.I. et al.: Nucl. Sci. Eng., 70, 150 (1979).

(6) Fields, R.E., Walt, M.: Phys. Rev., 83, 479 (1951).

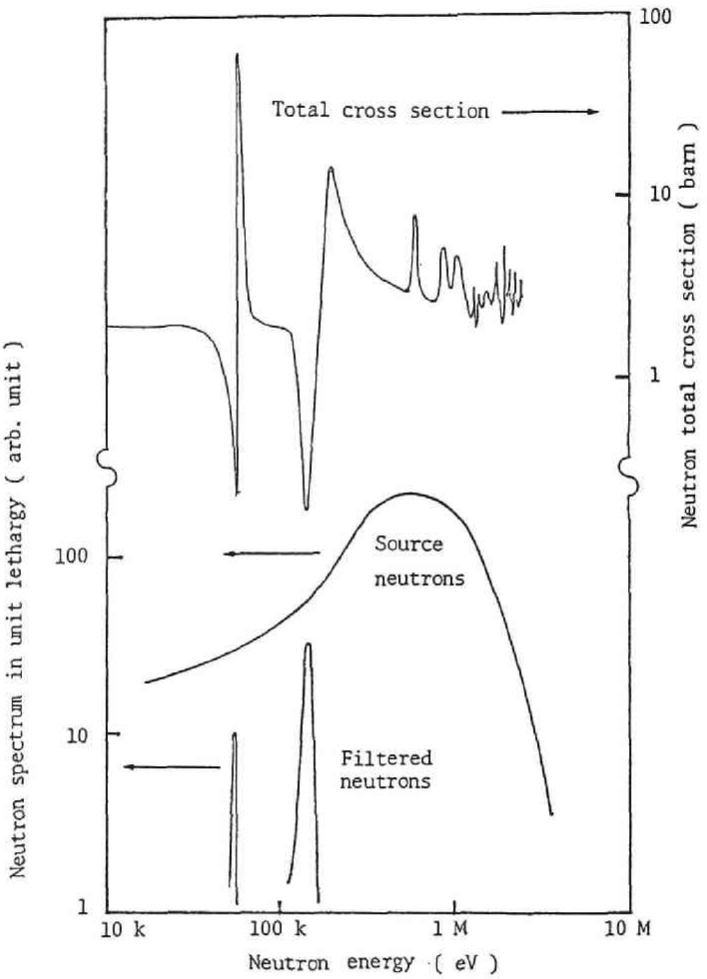

Fig.2-1 An illustrative relationship between the source neutrons, the filtered neutrons and the total cross section of the filter material.

Table 2-1 Commonly-used filter materials

Filter Materials	Main Isotope in Natural Element (%)	Spin Parity	Average Energy* (keV)	Energy Spread* (keV)	Auxiliary Filter Materials	Adoption in this study
U	^{238}U : 99.27	0^+	0.186	0.00145	Se, Mn, Ge	None
Sc	^{45}Sc: 100	$7/2^-$	2.0	0.8	Ti, ^{60}Ni, ^{64}Zn	Measurement of the cross section minimum
Fe	^{56}Fe: 91.66	0^+	24	2	Al, S	Application as a filter material
Si	^{28}Si: 92.21	0^+	144 54	24 1	Ti S	Measurement of the cross section minima and application as a filter material
O	^{16}O : 99.759	0^+	2350	100	Bi	None

* The numbers of energy are approximate values. For more detail, the values depend on the thickness of a filter and the energy spectrum of source neutrons.

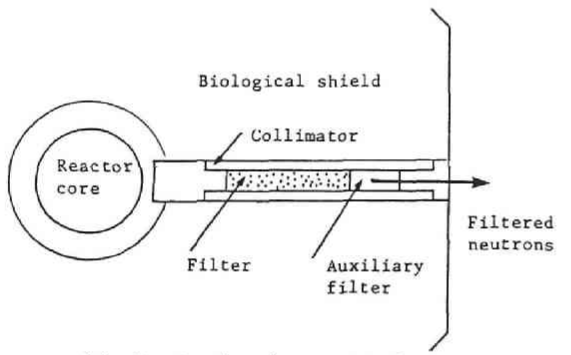

(a) Reactor-based arrangement

Typical dimensions:
- Length of beam tube ~3 m
- Diameter of beam tube ~15 cm
- Diameter of filter 2~5 cm

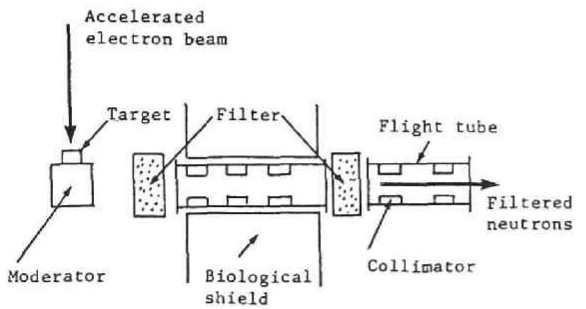

(b) Accelerator-based arrangement

Typical dimensions:
- Length of flight path 10 ~ 100 m
- Thickness of shield 2 ~ 4 m
- Diameter of flight path 10 ~ 30 cm
- Diameter of neutron beam ~5 cm

Fig.2-2 Typical arrangements of filtered neutron facilities.

Chapter 3 Installations Used in Experiments

In this chapter is given a general description of the installations commonly used in the experiments in this study. The experiments in Chapters from 4 to 8 have been carried out using a time-of-flight spectrometer at an electron-linear-accelerator facility of the Research Reactor Institute of Kyoto University (KURRI-LINAC) and the other experiments in Chapters from 9 to 10 using the versatile filtered-neutron beams at the Research Reactor Facility of the University of Missouri (MURR).

The KURRI-LINAC is a L-band two-section machine with the maximum electron energy of 46 MeV and the average beam power of 10 kW. Four neutron flight tubes are installed for experiments in neutron- and reactor-physics. Two of these, 12 and 22 m long, were used in this study. A description of the installations is given in the first half of this chapter as for the neutron source, the time-of-flight spectrometer, and the detector and data-acquisition system.

It was needed at the MURR, in advance to the utilization of the facility, to experimentally study the beam quality and to remove the other neutrons intruded to the filtered beam of interest. This preliminary study was very important for precise measurements of cross sections, and the results of the study are presented in the second half of this chapter along with the description of the versatile beam facility.

3.1 Installations Used in Measurements with Accelerator-Based Filtered Neutrons at KURRI-LINAC

3.1.1 Neutron Source

Photoneutrons were produced by bombarding a water-cooled Ta-target with high energy electrons. The neutrons have energies of MeV, and were moderated down to keV range by a polyethylene moderator placed adjacent to the the target. The energy spectrum of the neutrons directed to the spectrometer from the target assembly is shown in Fig. 3-1. In filtered-neutron experiments, the width of the electrom beam could, in general, be taken longer than in a usual time-of-flight experiments of high energy resolution

so as to obtain more intense neutrons, since the energy resolution of neutrons depends only on the shape of the cross section and the thickness of the filter material used. The intense gamma-flash coming from the target were largely reduced by the use of a thick filter and a shadow cone of Pb which intercepted the gamma-flash directed to a neutron detector placed at the end of the flight path.

3.1.2 Time-of-Flight Spectrometer

A typical arrangement of the transmission measurements is shown in Fig. 3-2. The nominal length of the flight path is 22 m. A transmission sample was placed near the middle position of the flight path. Neutrons were collimated with Pb- and B_4C-collimators, having diameters of 5 cm at the sample position and of 10 cm at both ends of the flight path. The filter material was placed between the target and the transmission sample. Main part of the material was positioned near the target to roughly remove other neutrons and gamma-rays first and to prevent their coming out from the target room. The other part of the material was placed outside the target room in order to complete the filtering.

Filtered portions of neutrons obtained by a calculation are also shown in Fig.3-1 for Sc-, Fe- and Si-filters, of 33, 30 and 75 cm in respective thicknesses. The numbers of the filtered neutrons reaching the detector under the conditions of the production rate of 1×10^{12} n/sec and of the above-mentioned aperture in the collimation were about 200, 380 and 1350 n/sec for the Sc(33 cm)-, the Fe(30 cm)- and the Si(75 cm)-filters, respectively. The intensity of 53.5 keV neutrons in the case of the Si-filter is about 160 n/sec.

A capture-cross-section measurement in Chapter 8 was carried out at a 12 m-long flight path so as to obtain more neutrons and improve the counting statistics. Diameters of the collimation of the flight path were 15 cm near the target and 5 cm at the sample position.

3.1.3 Neutron Detector and Data Acquisition System

Transmitted neutrons were detected with a ^6Li scintillation detector

of 1.27 cm in thickness and 12.7 cm in diameter, of type NE-908 of Nuclear Enterprise, Ltd., or an NaI(Tl)-detector of 5.08 cm in thickness and 12.7 cm in diameter. The NaI(Tl)-detector counted keV neutrons via the $I(n,\gamma)$ reaction. The high efficiency of the detector for the capture gamma-rays lead to a high neutron efficiency. Complete removal of other energy neutrons with the filter made the detector free from the activation of Na.

A pair of C_6F_6 scintillators, 10 cm in diameter, 4 cm in thickness, of type NE-226 of Nuclear Enterprise, Ltd., were used for prompt gamma-ray detection in the capture-cross-section measurement. The use of the scintillator as a total-energy detector is described in Chapter 8.

Neutron production rate was monitored with proportinal counters of BF_3 and ^3He for each run during the experiment. The BF_3 counter was placed in the target room to count thermal neutrons which were proportional to the production rate of fast neutrons at the target. The ^3He counter was inserted in the flight tube without intercepting the collimated neutrons but with glancing at the target in order to monitor the keV neutrons directed from the target to the flight path. These monitors were used in transmission measurements for long samples for which a sample changer could not be used. These two systems showed a consistent result of neutron monitoring. For the samples of ordinary thickness, a sample changer of rotation or push-pull type was used to minimize the drift effect of the experimental system.

Neutron signals from the transmission detector and the monitor system were analyzed in the time-of-flight mode with a crystal-oscillator-based time analyzer, and then were stored in a computer memory. In experiments where the sample changer was used, the memory was separated into four regions and each region was stored with the signals for one of the runs of different sample thicknesses during a preset-time period of data acquisition. The sequence of measurement was controlled by an automatic sample-changer and time-analyzer controller.

3.2 Versatile Filtered-Neutron Facility at MUKR and Improvement of Beam Quality

3.2.1 Versatile Filtered-Neutron Facility[1]

A versatile filtered-neutron facility is provided at a beam port of the 10 MW MURR. A cross-sectional plan view around the core of the reactor is shown in Fig.3-3. The installation of the filtered-neutron facility at the beam-port F is shown in Fig.3-4. The reactor is loaded with the MTR-type fuel of highly-enriched U. The core is built in a pressurized tube of 30 cm in diameter, and moderated and cooled with light-water coolant in the tube. The tube is concentrically surrounded with reflectors of Be metal in the inner part and graphite in the outer part. Neutrons are extracted from the outer surface of the pressure tube. The beam tube is 10.16 cm in diameter. Another tube of Al, 3 cm in diameter and 380 cm in length, and installed inside with filter materials, is inserted from the outside of a biological shield into the beam tube. There are several kinds of replacable filters at the facility and each filter has a standard composition of main and auxiliary materials. The Si- and Fe-filters of them were used in this study.

3.2.2 Silicon-Filtered Neutrons

The standard Si-filter is 208 cm in length and 2.54 cm in diameter. A 1-mm-thick plate of ^{10}B was added to the filter to surpress thermal neutrons. The beam led to the outside of the biological shield had a diameter of 3 cm (FWHM) and there were negligible amount of dispersed neutrons outside of a 5-cm circle. The beam quality was studied with a spherical H_2-gas counter of 3 atm. in pressure and 4 cm in diameter. The energy spectrum for the filtered beam is shown in Fig.3-5. The neutron flux of 144-keV neutrons was estimated from the counts of the H_2-gas counter to be approximately 6×10^4 $n/cm^2/sec$. There were negligible amount of neutrons in the higher energy region than 144 keV. The neutrons of 54 keV, however, were intruded by about 8 %. This fraction of 54 keV neutrons was close to the value obtained by calculation using the cross-section data

measured in the experiment in Chapter 5. It was experimentally shown, for the sake of future studies, that a monoenergetic beam of 53.5-keV neutrons can be obtained by adding some S as an auxiliary filter to the Si, since the S-filter scatters the 144-keV neutrons out from the beam and passes the 53.5-keV neutrons only. The effects in the pulse height spectra, with varying the amount of added S, measured with the H_2-gas counter and their unfolded spectra are shown in Figs. 3-6 and 3-7, respectively.

An unfolding code of the above-mentioned pulse-height spectrum was prepared by revising the MATXUF code[2] which was written basing upon the derivative method and for the use with the online and realtime unfolding. As is seen in Fig.3-5, the energy spread of the unfolded spectrum is larger than the reliable calculation of the energy spread. The difference is attributed to the resolution of the detector system.

3.2.3 Iron-Filtered Neutrons

The standard Fe-filter consists of 50.8 cm in Fe, 20.3 cm in Al, 5.1 cm in S and 0.1 cm in ^{10}B. The 24-keV neutrons were obtained by the order of 10^4 $n/cm^2/sec$ in intensity and 2.54 cm in beam diameter. The energy spectrum of the beam measured with the afore-mentioned H_2-gas counter showed that the beam still contained the intruded neutrons in the energy range from 100 to 600 keV by 18-% amount. The energy spectrum of the beam is shown in Fig. 3-7. An addition of auxiliary filters, 28 g/cm^2 of S and 21.5 cm of Al, reduced the contamination down to about 0.6 %. After installing the auxiliary filters, a few trial transmission measurements were carried out using a long-counter for neutron detection and using polyethylene samples of neutron-transparencies down to 0.01. The total cross sections obtained were reasonable and showed no inclination to decrease or increase with the thickness of the sample. This result indirectly assured that the contamination was satisfactorily removed. The trial measurements were also carried out with Fe-samples of thicknesses up to 10 cm. The result showed there was very little contamination of neutrons other than at the 24-keV window, especially for thermal neutrons. The neutron long-counter was used, after the above-mentioned studies, for the transmission measurement of 24-keV neutrons.

References:

(1) Tsang, F.Y., Brugger, R.M.: Nucl. Instr. Methods, 134, 441 (1976).
(2) Miller, W.H.: Nucl. Instr. Methods, 153, 533 (1978).

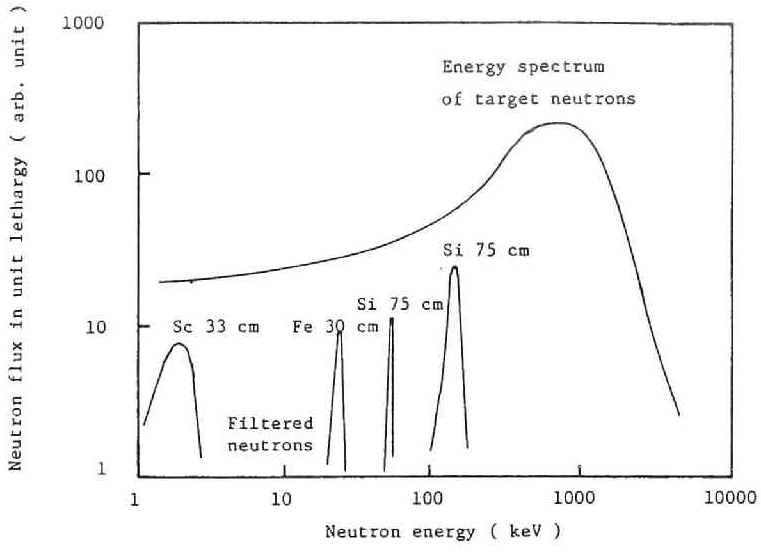

Fig. 3-1 Energy spectrum of neutrons directed from the target assembly to the flight path. Filtered portions of neutrons are obtained by an approximate calculation using cross-section values.

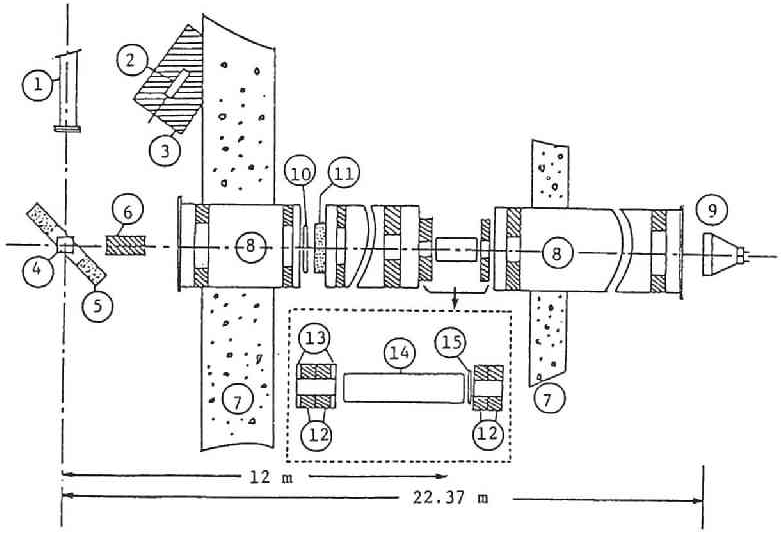

1. KURRI-Linac, 2. BF_3 neutron monitor, 3. Pb gamma-flash shield, 4. Water-cooled photo-neutron target, 5. Polyethylene moderator, 6. Pb gamma-flash shadow shield, 7. Concrete shield, 8. Flight tube, 9. ^{6}Li neutron detector, 10. ^{3}He neutron monitor, 11. Sc-notch filter, 12. Pb collimator, 13. Boron-carbide collimator, 14. Transmission sample, 15. Co notch filter

Fig. 3-2 Experimental arrangement of neutron transmission measurements at KURRI-Linac.

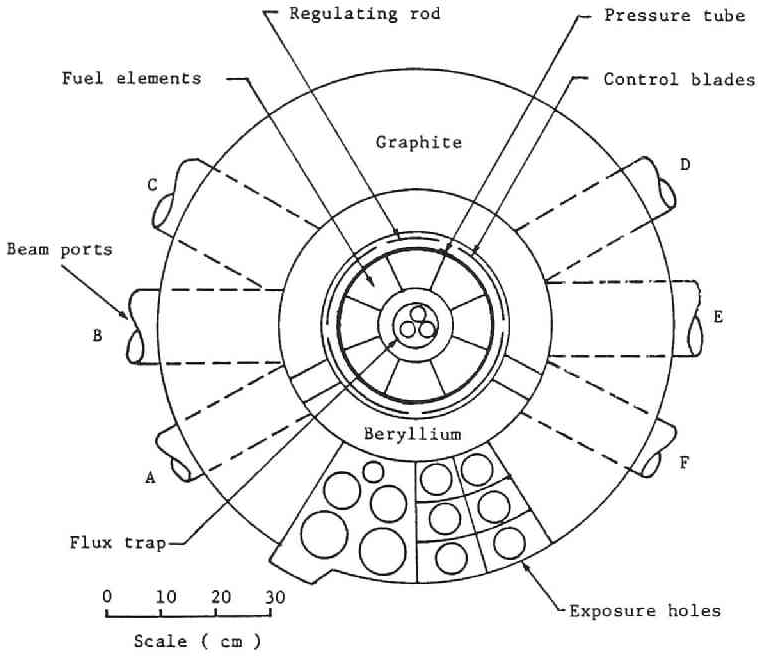

Fig. 3-3 A cross-sectional plan view around the core of MURR.

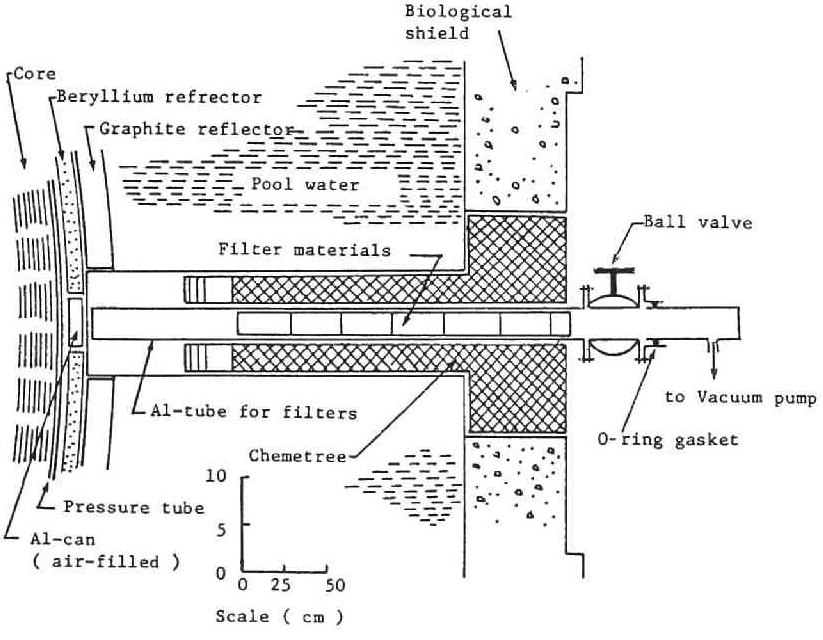

Fig. 3-4 Versatile filtered-neutron facility at MURR.

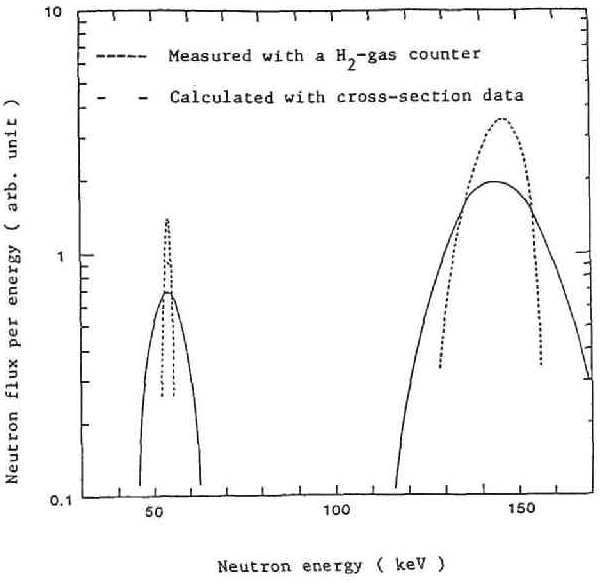

Fig.3-5
Energy spectrum of Si-filtered neutrons obtained by unfolding a pulse-height spectrum measured with a H_2-gas counter. The dotted spectrum is calculated with cross-section data. The difference of the width is attributed to the energy resolution of the gas counter.

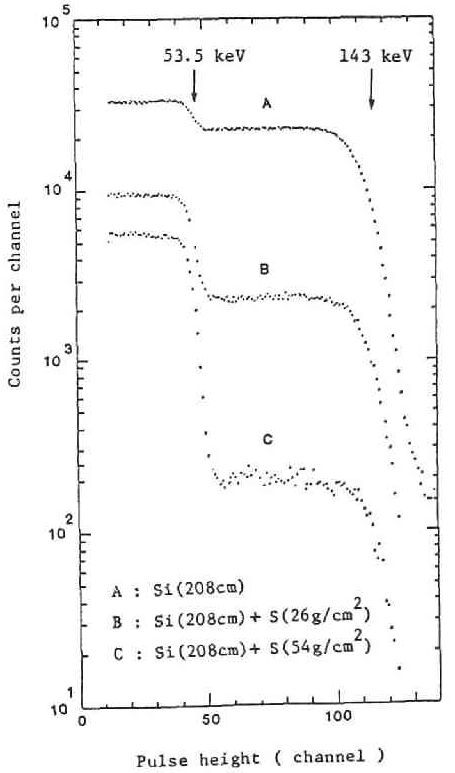

Fig.3-6
Pulse height spectra of Si-filtered neutrons measured with a H_2-gas counter. The 143-keV neutrons are removed by an auxiliary filter of S providing monoenergetic 53.5-keV neutrons.

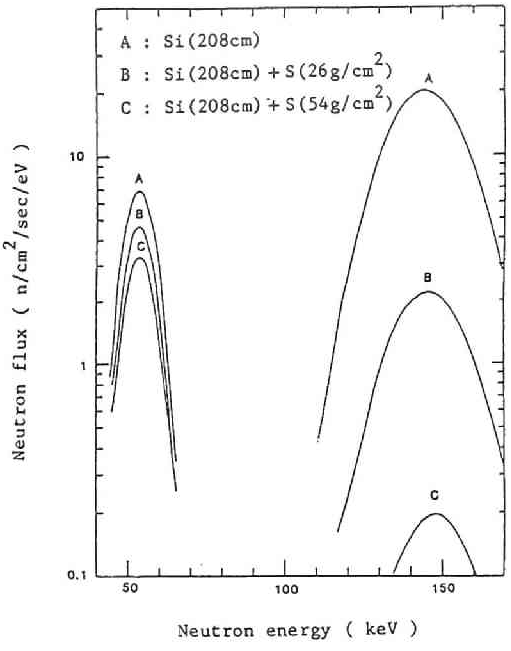

Fig.3-7

Energy spectra of neutrons obtained by unfolding the pulse-height spectra in Fig.3-6.

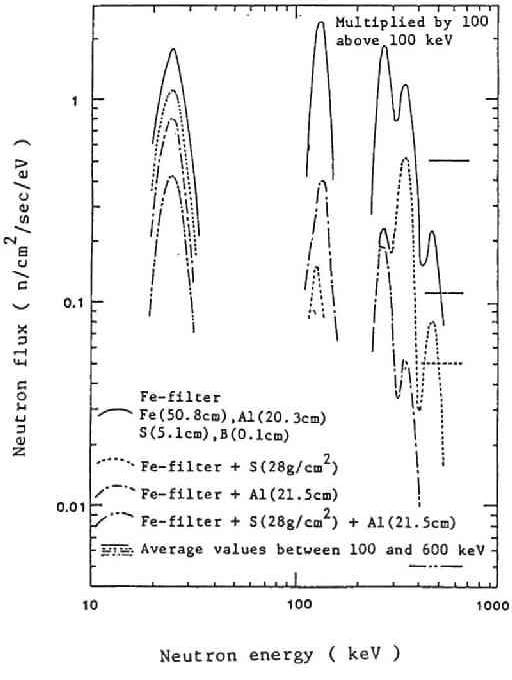

Fig.3-8

Energy spectra of Fe-filtered neutrons. The effectiveness of the addition of Al and S is shown by experiment for the removal of high energy neutrons between 100 and 600 keV. The spectra above 100 keV are multiplied by a factor 100. The thickness of S and B in the standard Fe-filter are the numbers in the pressed powder form.

Chapter 4 Measurements of Total Cross Section of Sc Near 2-keV Minimum[1]

4.1 Introduction

Scandium has a deep minimum near 2 keV in the neutron total cross section and is used as a transmission filter to provide monoenergetic 2-keV neutrons at reactor beam facilities.[2-7] A reliable value of the cross section near the minimum is important for an optimal design of the filter. Nevertheless, there still remain marked discrepancies between experiments. In 1975, Magurno et al.[8] showed about 0.085 barn for the minimum by evaluating the experimental data available at that time. Two experiments were reported thereafter: one is 0.71 ± 0.03 barn measured by Liou et al.[9] (this reference is refered as LIOU hereafter) using the standard time-of-flight method at an electron linear accelerator and at a reactor beam facility, and the other is 0.27 ± 0.07 barn measured by Razbudey et al.[10] using monoenergetic 2-keV neutrons prepared by filtering reactor neutrons with Sc itself.

There are two big s-wave resonances in the total cross section of Sc at 3.295 and 4.330 keV.[9] The former is a spin-antiparallel (the quantum number of total angular momentum of the compound state, $J = 3$), and the latter is a spin-parallel interaction ($J = 4$). The scatterings with these resonances independently interfere with the potential scattering and show respective interference minima. The superposition of these scatterings which take the main part of the total cross section still shows a marked minimum because the energies of the minima are close each other in this case of Sc. Thermal-neutron scattering is also the superposition of spin-parallel and spin-antiparallel interactions. A fitting to the measured total cross section with the Breit-Wigner multi-level formula in the energy range of these resonances down to thermal-neutron energies requires to posturate a few negative-energy resonances which correspond to the bound energy levels in the compound nucleus.

A reliable measurement near the minimum is also interested to understand the properties of the thermal-neutron interaction of Sc. According to the discussion in LIOU, their higher value (0.71 barn) at the minimum reason-

ably explains the dominant contribution of the spin-antiparallel interaction in thermal-neutron energies, which is consistent with the results of other kinds of experiments such as a spin precession experiment[11] of neutrons and a neutron capture gamma-ray spectroscopy[12]. Magurno et al.[8] showed, on the contrary, the above-mentioned lower value (0.085 barn) at the minimum which means the dominant contribution of the spin-parallel interaction. Razbudey et al.'s value[10] (0.27 barn) just mediates between these two values.

The measurement reported here of the total cross section near the minimum was performed with the standard time-of-flight technique using an electron linear accelerator as a neutron source. In order to obtain a reliable value of the small cross section near the minimum, the impurities in the sample material were carefully examined and the transmission samples were prepared to be as thick as possible so to attain an adequate transmission ratio.

4.2 Experimental Method

4.2.1 Apparatus

Measurements were carried out by using a time-of-flight spectrometer at the KURRI-LINAC. Experimental arrangements and the outline of measurement have been described in Chapter 3.

Scandium of about 5 g/cm^2 and a 1-mm-thick Co were inserted in the neutron beam as notch filters in order to determine the background levels in a time-of-flight spectrum. In a measurement of a cross-section minimum, the sample material may be also used as a notch filter since the material has a big resonance peak near the minimum. The time-width of the electron beam and the channel width of the time analyzer used were 33 and 125 nsec, respectively. The energy resolution of the experiment was estimated about 0.5 % near 2 keV. This resolution was enough for the present purpose to make a measurement in the broad interference minimum. Any typical p-wave resonance, however, could not be clearly resolved.

4.2.2 Scandium Sample

The trasmission samples were prepared using Sc-metal of 2 kg in total weight by the procedure explained below by taking care of the contamination with machining oil or with the oxidation.

The Sc-lumps were first rolled into plates of about 1 to 2 mm thickness with a mill under the room-temperature, and then the plates were cut into flakes of about 1-cm^2 area with pincers. The flakes thus obtained were packed in Al pipes of 5 cm in inner diameters and 20, 20 and 30 cm in respective lengths, and having lids of Al-plates of 1-mm thickness at both ends.

The number of Sc-nuclei in a unit cross-sectional area of each sample was needed to deduce the cross section from a transmission factor. It was simply determined by dividing the weight of the packed Sc by the cross-sectional area of the pipe. The volumes occupied by packing the same amount of Sc in the pipes of two different inner diameters, 5 and 7 cm, agreed within about 2 %. Then, the error in the number of nuclei in a unit cross-sectional area was considered to be about 2 %.

The Sc-samples packed in the Al-pipes were dried at 200°C in a vacuum vessel during 4 h, and then were sealed after being filled with dry N_2-gas; it was presumed that the Sc was free from adsorption of any moisture.

The Sc-metal was of USSR-origin and a quality certificate of the USSR-standard was attached to the lumps of the Sc-distillate. The information of the impurities quoted from the certificate is shown in Table 4-1.

After the Sc was cut into flakes, a qualitative inspection of purities was carried out at the Research Center of Mitsubishi Metal Industry Ltd. with the X-ray fluorescence analysis and no impurity other than Cu was recognized within the detective limit of the analysis. The result of the analysis qualitatively agreed with the quality certificate.

Copper was the most significant in the amount and moreover it has a big resonance in the total cross section near 2 keV; it was the only impurity which affected the measured cross-section value of Sc near 2 keV. Therefore, the content of Cu was specially analyzed using the activation and chemical titration methods. In the activation method, a chip of about 1 g taken from the Sc-flakes was irradiated with the bremstrahlung from the

linac. After the irradiation, the decay of 0.51-MeV gamma-ray was followed with an NaI(Tl)-scintillation-detector for several days. By analyzing the decay curve, the activity of ^{64}Cu was obtained after subtracting those of ^{44}Sc and ^{44m}Sc, and the absolute value of Cu content was determined by normalizing to the activity of a reference chip of Cu which was simultaneously irradiated with the Sc-chip. In the titration analysis, a few pieces of the flakes were disolved in hydrochloric acid and Cu was titrated by the iodostarch reaction. The results obtained were 0.13 $\pm$ 0.06 and 0.18 $\pm$ 0.02 w/o, for the activation and titration methods, respectively. The weighted average 0.175 $\pm$ 0.02 w/o was used to correct the measured cross section for impurity.

Physical parameters of the transmission samples are shown in Table 4-2. In the measurement, four combinations of the samples were used : (A) 20 cm only , (B) 20 cm + 20 cm , (C) 20 cm + 20 cm + 30 cm , and (D) 2.4 cm.

4.3 Experimental Results

The measurement was carried out for about 15 h and the transmission samples were repeatedly changed every 1 h to minimize the drift-effect of the measurement. Two examples of time-of-flight spectra obtained are shown in Fig.4-1 for Open- and Sample(C)-runs. In all runs, Sc and Co, and a thin sheet of Cd were placed in the neutron beam for notch filters and an overlap filter, respectively. The background in each spectrum in Fig.4-1 was estimated by linearly interpolating between the counts at about 4.33 keV (190-th channel) and at about 132 eV (1100-th channel), corresponding to the resonance energies of Sc and Co, respectively.

Five kinds of spectra, one of the open-run and the others of different sample thicknesses, were corrected for the counting loss and for the background, and normalized with monitor counts. These spectra were then used to deduce the cross section of Sc by applying the least-square method for each time-of-flight channel between 3 keV and 250 eV. The energy for each channel was calculated using the length of flight path and the flight time. The result of cross-section values obtained is shown in Fig.4-2. The fluctuation of experimental points in the figure is considered to be the counting statistics except for a small peak at 1.06 keV, which may be a

p-wave resonance appeared at 1060.4 eV in LIOU measurement. The counting statistics are typically shown for a few data points in the figure. The solid curve is a least-square fitting with a polynomial function of sixth degree to the experiment. The polynomial is given as follows :

$$\sigma(E) = 18.00 - 44.51\ E + 56.81\ E^2 - 44.351\ E^3 + 20.674\ E^4 - 5.2389\ E^5 + 0.5572\ E^6 \quad (0.2 < E < 3.0) \ ,$$

where $\sigma(E)$ is the total cross section of Sc in barn, and E is the neutron energy in keV.

The data points in Fig.4-2 are corrected for the impurity of Cu which is the most significant impurity and has a big resonance of 43 ± 1.5 eV width at 2.038 ± 0.003 keV.[13] The total cross section of Cu for the correction is calculated using the single-level Breit-Wigner resonance formula and above mentioned parameters. The data points before the impurity correction are also shown in the figure with open circles around the resonance.

In order to confirm the consistency of measurements among those of different sample-thicknesses, the numbers of counts accumulated in 1.8 to 2.2 keV channels and subtracted with the background counts in corresponding channels are plotted in Fig.4-3 by relative units in a semi-logarithmic scale as a function of sample-thicknesses. The accumulation of counts is only for the purpose of obtaining adequate counting statistics for the confirmation. Standard deviation due to counting statistics is shown for each point in the figure. The plots are expected to linearly decrease with the increase of the sample-thickness, if the transmission measurements are properly carried out. The deduced chi-square of the fitting with a straight line is 3.5. This value shows that the fitting is reasonable and there is not any implicit error which is much larger than the standard deviations of counting statistics.

The value of energy at the cross-section minimum can not be definitely determined from Fig.4-2: the first glance of the figure shows, however, the energy is near 2 keV and very probably between 1.9 and 2.1 keV. The nominal energy of 2 keV usually attributed to the filtered beam is very close

to the average energy calculated using the present data. The cross-section value at the minimum is 0.21 ± 0.02 barn obtained by averaging the data points between 1.9 and 2.1 keV, and estimating the error by the dispersion of the data points. The error caused in the estimation of impurity should be added to the above-mentioned error. The average value between 1.9 and 2.1 keV before the correction to impurity is 0.33 barn ; the cross section is decreased by 0.12 barn with the correction for the afore-mentioned content of Cu. One-fifth of the amount of correction is presumed to be the error in the correction procedure. Then, the cross section finally obtained is 0.21 ± 0.03 barn at the minimum.

4.4 Discussion

The cross section obtained in this measurement is 0.21 ± 0.03 barn at the 2-keV minimum, which is close to 0.27 ± 0.07 barn of Razbudey et al.[10] and much different from 0.085 barn of Magurno's evaluation[8] and 0.71 ± 0.03 barn of LIOU. A graphical comparison with the data in LIOU is made in Fig.4-4, where the data is represented with a solid curve (A) instead of the data pounts. The curve is a fitting to the data with the Breit-Wigner formula. Two experiments differ markedly in the small-cross-section region and gradually come to a better agreement as the cross section comes to a larger value. LIOU obtained almost the same results in both of the measurements using time-of-flight spectrometers, for common transmission samples, at an electron linear accelerator and at a reactor beam facility. This means the transmission measurement in LIOU is considered to have been properly carried out. The measurement in this study was also carried out properly as already explained. The explanation of the disagreement is considered , therefore, to be in the estimation of impurities in the sample used but not in unconscious problems in the transmission measurements.

The value obtained here is approximately one third of LIOU. This means that a thicker filter by three times can be used with the same amount of sacrifice of 2-keV neutrons. A thicker filter is favorable for reducing background neutrons and gamma-rays leaking out from the neutron source.

It is needed to discuss whether the small value obtained in this exper-

ment is consistent with the dominant contribution of the spin-antiparallel interaction in thermal-neutron energies. The dominant contribution of the spin-antiparallel interaction, as discussed in LIOU and as afore-mentioned here, is consistent with a higher value of cross section near the minimum and with the results of different kinds of experiments such as a spin-precession experiment[11] of neutrons and a neutron-capture-gamma-ray spectroscopy[12].

A trial of fitting to this experiment with the Breit-Wigner multi-level formula has been carried out following the procedure as described in LIOU. A few minor effects on the cross-section value, of p-wave resonances, of Doppler broadening , and of the energy dependence of scattering radii have been neglected for simplicity as the present analysis is of qualitative nature. The trial is carried out by modifying the resonance parameters for two negative-energy levels, one for spin-parallel and the other for spin-antiparallel interactions, and the scattering radii by keeping the resonance parameters for the positive energy levels same as those in LIOU, and by admitting some modifications in the thermal-neutron scattering parameters within an allowable limit of experimental accuracy.

A fitting is shown in Fig.4-4 with a curve (B). The curve is not the best fit but one of reasonable fittings obtained with the try and error method. The parameters modified are shown in the upper half of Table 4-3, and thermal neutron scattering parameters accordingly modified are shown in the lower half of the table. It is found in the trial that the scattering radii $R'_{\pm}$ should be decreased to around 2.5 fm in order to explain the dominant contribution of spin-antiparallel interaction ($a_- \gg a_+$) and the lower value of 0.21 barn obtained in this experiment at the cross section minimum. The scattering radius of 2.5 fm is approximately half of the nuclear radius of Sc. The value is not so small, however, as to be rejected as unreasonable, if one considers that some experiments of scattering radii and an optical-model calculation also show[14,15] considerably small scattering radii compared to the nuclear radii for the nuclei near the nuclear-mass-number of Sc. The comparison is shown in Fig.4-5.

A new measurement of the cross section was recently reported by Harvey et al.[16] Their result is 0.36 ± 0.03 barn, which is much closer to the present measurement than to the value of LIOU.

4.5 Conclusion

For an optimal design of a Sc-filter, the neutron total cross section has been measured near the 2-keV cross-section minimum using the standard time-of-flight method. The minimum value of cross section obtained is 0.21 $\pm$ 0.03 barn. The value markedly differs from 0.71 $\pm$ 0.03 barn which was measured in Liou et al.'s experiment[9] of similar method, and is close to 0.27 $\pm$ 0.07 barn of Kazbudey et al.[10] measured by a different kind of experiment carried out using reactor-based monoenergetic neutrons of 2 keV.

The lower value obtained here indicates that one may use a much-thicker filter in a filtered-beam facility. This is favorable to reduce background neutrons and gamma rays, leading to obtain a clean filtered neutron beam.

A trial of fitting the experiment with the Breit-Wigner multi-level formula shows that the lower value at the minimum near 2 keV is still consistent with the dominant contribution of the spin-antiparallel interaction for thermal neutrons.

References:

(1) Fujita, Y : J. Nucl. Sci. Technol., 20, No.3, 191 (1983).

(2) Simpson, O.D., Miller, L.G. : Nucl. Instr. Methods., 61, 245 (1968).

(3) Kuzin, E.N. et al.: Atomnaya Energia, 35, No.6, 391, (1973).

(4) Greenwood, R.C., Chrien, R.E.: Nucl. Instr. Methods., 138, 125 (1976).

(5) Schwartz, R.B.: Proc. Int. Spec. Symp. on Neutron Standard and Applications, National Bureau of Standard Special Publication 493 (1977).

(6) Alberts, W.G.: Nucl. Instr. Methods., 155, 307 (1978).

(7) Aminfar, H., Brugger, R.M.: Nucl. Instr. Methods, 188, 597 (1981).

(8) Magurno, B.M., Mughabghab, S.F.: Proc. Conf. on Nuclear Cross Section and Technol., National Bureau of Standard Special Publication 425, 1, 357 (1975).

(9) Liou, H.I. et al.: Nucl. Sci. Eng., 67, 326 (1978).

(10) Razbudey, V.F. et al.: Proc. Int. Conf. on Neutron Cross Section for Technol., National Bureau of Standards Special Publication 594, GD9 (1980).

(11) Glattli, H. et al.: Journal de Physique No.7, 629 (1979).

(12) Bolotin, H.H.: Phys. Rev., 168, 4, 168 (1968).

(13) Mughabghab, S.F. et al.: BNL-325, 3rd Edition, Vol.1 (1973).

(14) Jain, A.P.: Nucl. Phys., 50, 157 (1964).

(15) Mughabghab, S.F. et al.: Neutron Cross Sections Vol.1, Part A, p.17, Academic Press (1981).

(16) Harvey, J.A. et al.: Proc. Intern. Conf. on Nuclear Cross Sections for Science and Technology, p.856, at Antwerp, September (1983).

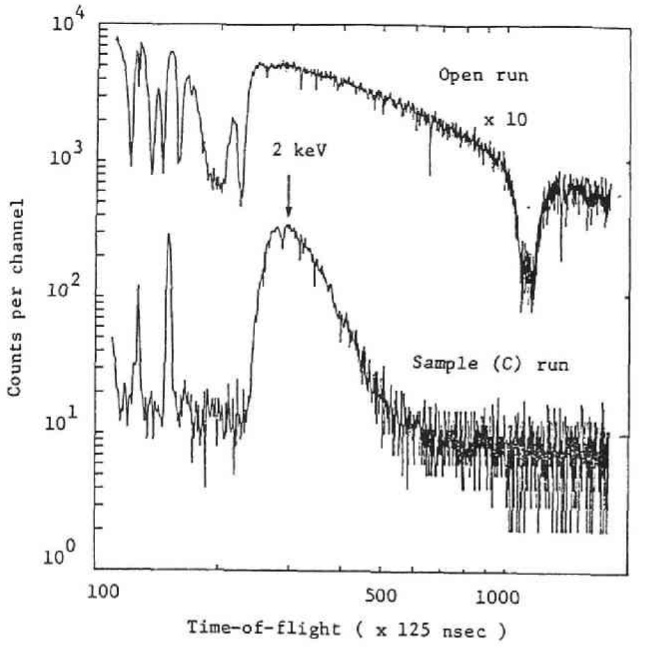

Fig. 4-1
Time-of-flight spectra. The upper is for the Open-run and the lower is for the 70-cm sample run.

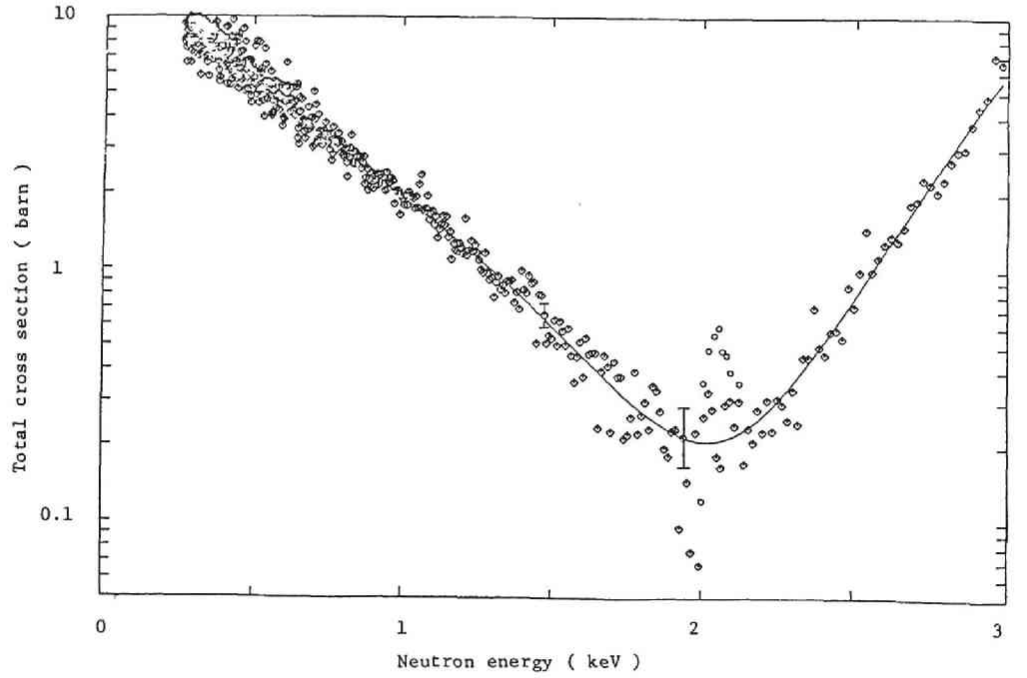

Fig. 4-2 Total cross section of Sc. The solid curve is the least-square fit to experiment with a sixth-degree polynimial of the neutron energy. The several points near 2.1 keV shown by open circles are the data before correction of Cu in the impurity.

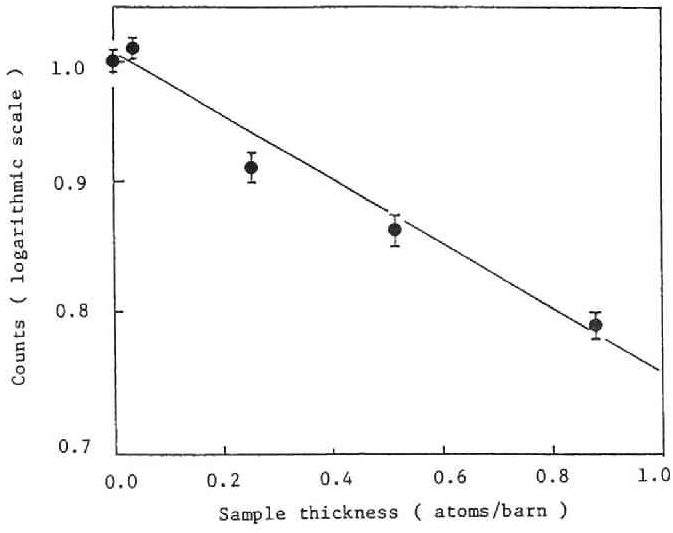

Fig. 4-3
Neutron counts in the range from 1.8 to 2.2 keV as a function of sample-thicknesses.

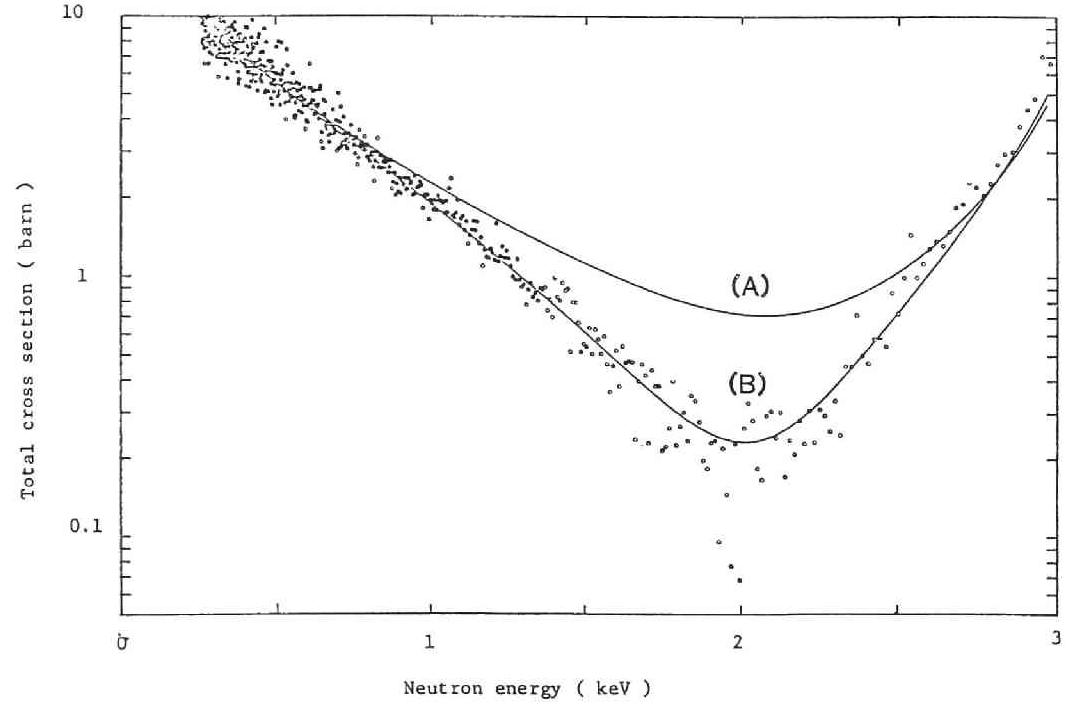

Fig. 4-4 Comparison of the obtained cross section data with two fitting curves calculated using the Breit-Wigner multi-level formula. The curve (A) is a fitting to the experimental data of LIOU and (B) is to the present experiment.

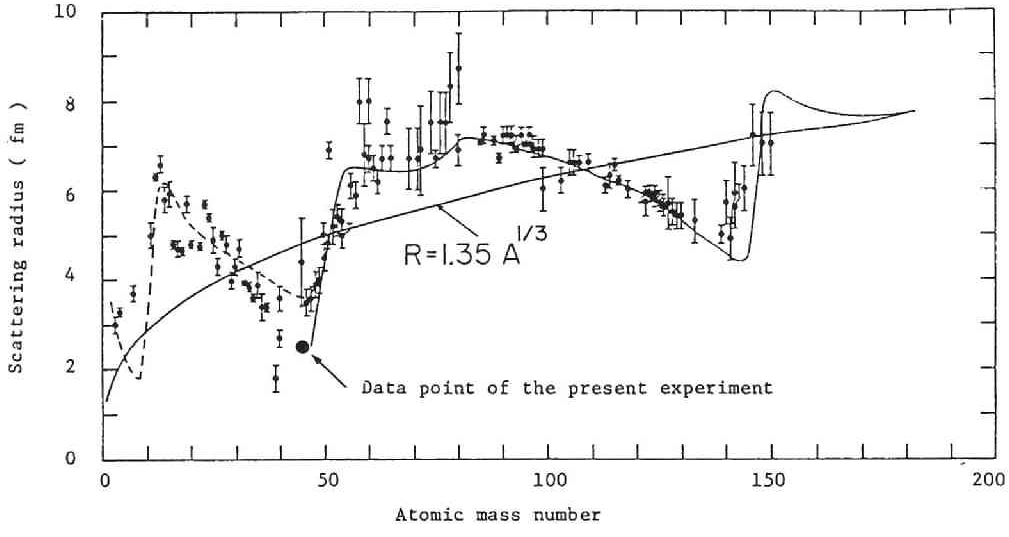

Fig. 4-5 Variation of the scattering radius with the atomic mass number. The figure is taken from a reference (15), and the real and dashed lines are optical-model calculations using deformed and spherical potentials, respectively. Details are found in the literature. The data point of the present experiment is added.

Table 4-1 Impurities in Sc-sample (w/o)

Cu	H_2	F	C	Ca	Fe	Yb	N_2	Y	Si	Zr	Ti
0.05	0.001	0.004	0.01	0.004	0.01	0.01	0.005	0.01	0.01	0.01	0.01

Table 4-2 Physical parameters of Sc-sample

Sample No.	Diameter (cm)	Length (cm)	Number of atoms per barn
1	5	20	0.265
2	5	20	0.252
3	5	30	0.356
4	6.6	2.4	0.040

Table 4-3 Parameters used in Liou's fitting and modified parameters using the data of this experiment

Name of parameter	Liou's parameter	Modified using this experiment
Scattering radius for spin-parallel interaction R'_+ (fm)	3.74	2.50
Scattering radius for spin-antiparallel interaction R'_- (fm)	3.74	2.50
Negative energy level for spin-antiparallel interaction ($J=3$) (eV)	$E=-500$ $\Gamma_n=4.0$	$E=-500$ $\Gamma_n=4.0$
Negative energy level for spin-parallel interaction ($J=4$) (eV)	$E=-220$ $\Gamma_n=0.67$	$E=-1,000$ $\Gamma_n=4.0$
Scattering cross section σ_s (b)	24	23.9
Coherent scattering cross section σ_c (b)	19.2	19.6
Scattering length for spin-antiparallel interaction a_- (fm)	19.39	19.1
Scattering length for spin-parallel interaction a_+ (fm)	6.88	7.35

Chapter 5 Measurement of Neutron Total Cross Section of Si at 146- and 53.5-keV Windows[1]

5.1 Introduction

Silicon has a marked minimum in the total cross section of neutrons at 146 keV, and is used as a filter material providing monoenergetic neutrons of about 144 keV in the effective energy. At the time when Si was used in an accelerator-based filtered-neutron experiment with a time-of-flight spectrometer at the KURRI-LINAC, it was found that the beam characteristics of filtered neutrons were much different from the calculations based on the cross sections found in BNL-325.[2] This motivated an experimental examination of the cross section using the spectrometer.[3] The result of the examination showed a very small value, one third of the evaluation of BNL-325[2] for the 146 keV window, and the existence of another marked interference-minimum near 53.5 keV. In that experiment, however, a large correction was imposed on the values by the amount up to 25 % in order to deduce the raw profile of the sharp variation of the cross-section curve which was dispersed due to the rather poor energy resolution. The correction reduced the reliability of the data and another refined experiment is needed to provide more precise data by improving the energy resolution.

There was an experiment with a very high energy resolution between 5 eV and 730 keV performed by Larson et al.[4] using the Oak Ridge National Laboratory Electron Linear Accelerator. However, the data at the windows were poor in statistics because the Si-sample was rather thin for the minimum measurement.

The experiment reported in this chapter is a refined measurement for the 53.5- and 146-keV minima by not only using thicker Si-samples, but also making several improvements of experimental conditions and apparatuses.

5.2 Experimental Method

The experiment was carried out with the 22-m TOF spectrometer at the KURRI-LINAC, which is described in Chapter 3. The improvements from the previous measurement[3] are itemized as follows:

(1) A higher energy resolution by more than three times was employed using 15 and 10 nsec for the widths of the linac-beam and the channel of a time-analyzer respectively.

(2) Higher counts were taken by more than ten times to reduce statistical errors.

(3) As a new neutron monitor, a 1-mm-thick ^{6}Li glass-scintillator was installed in the flight path instead of a BF_3 counter placed in the target room in the previous measurement.

(4) The Si-samples were 10.7, 27.2, 52.1 and 77.7 cm in thickness. The selection was better for the minimum measurements to reduce experimental errors compared to the previous samples of 20.0 and 43.0 cm.

(5) The energy scale was more carefully determined and caliblated within a 0.4 %-precision my making a transmission measurement with an Al-sample at resonance energies of 5.9035 ± 0.0015 keV and 119.75 ± 0.04 keV[4].

A ^{6}Li glass-scintillaor of 12.7 cm in diameter and 1.27 cm in thickness was used as the transmission detector. As a notch filter, a pile of Si-blocks of about 10 cm in effective thickness was placed at the entrance of the flight path in the target room. As is in the case of the Sc-experiment in Chapter 4, Si was a convenient material for the notch filter in this measurement. The background in the time-of-flight spectrum was determined with the counts in the regions blocked by the notch filter. The Si-samples were cylindrical single crystals of 6.2 cm diameter. They are the products of Komatsu Silocon Industries Ltd. and the impurity was in the order of seven-nine.

5.3 Results and Discussion

The total cross section is deduced from the five time-of-flight spectra for the open- and four sample-in runs after subtracting the background and correcting for the dead time. The results are shown in Figs.5-1 and 5-2 near the 146- and 53.5-keV windows respectively. The error-bars of counting statistics are typically shown for a few data points in the figures. The statistics takes the main of the error near the minimum value of cross section. In order to check the consistency of experiment between four samples

of different thicknesses, semi-logarithmic plots of the counts of the ^{6}Li detector are shown in Fig.5-3 as varying the sample thicknesses. The plots show the consistency of experiment between different thickneses.

The data points of open circles in Figs. 5-1 and 5-2 are the experimental results obtained by Larson et al.[4]. Their experiment was of high energy resolution and of excellent counting statistics. However, the sample used was only about 1.5 cm thick, resulting in a poor counting statistics near the windows, because the transmission of neutrons through the sample were higher than about 98 %.

In Fig.5-1, are also shown an experiment of Fields et al.[6] and a curve evaluated in JENDL-2[7]. The data points of Fields et al. are higher than the other data in the window. The discrepancy may be attributed to the poorer energy resolution in the Fields et al.'s experiment. The JENDL-2 curve, which is based on the data of Fields et al., is considerably higher than both of the present and Larson et al.'s experiments. The mimimum value near 146 keV of the present experiment, 0.187 $\pm$ 0.006 barn, agrees with 0.17 $\pm$ 0.05 barn of Larson et al.'s. However, there is a systematic descrepancy in the other energies between two experiments. In Fig.5-2, the JENDL-2 curve is shown near 53.5 keV, but no minimum can be seen in this evaluation. The results of these two experiments agree within the errors. The minimum value of the present data is 0.265 $\pm$ 0.008 barn, while that of Larson et al.'s is 0.2 $\pm$ 0.08 barn.

The sum of potential-scattering cross sections of the other isotopes than ^{28}Si in natural Si is estimated 0.16 $\pm$ 0.016 barns at the energies of the windows. The values of effective scattering-radius used for the estimation, 4.0 $\pm$ 0.2 fm for ^{29}Si and 4.3 $\pm$ 0.2 fm for ^{30}Si, are taken from the reference (5). Another estimation of the formaly-remaining cross section is given by Koester et al.[8] using the result of their scattering-length measurement to be 0.208 $\pm$ 0.007 barn. These comparisons show that the main part of minimum cross sections at the windows may be attributed to the potential scattering of other isotopes than ^{28}Si and the cross section of ^{28}Si is considered to be very small as is expected with Eq.(2.2) in Chapter 2, i.e. the Breit-Wigner cross-section formula for an even-even nucleus.

The energies 146 and 53.5 keV can be attributed to the minima with the

experimental error of 0.4 %. The effective energies of the filtered neutrons differ from these values depending on experimental conditions such as the length of a filter, the energy spectrum of source neutrons and the secondary filter used. For an example, the effective energies are 143 and 53.3 keV for neutrons obtained by filtering a 1/E source with a 2-m-long Si.

5.4 Conclusion

The study in this chapter has shown by making a refined experiment that the minimum value of the Si-cross section near 146 keV is much lower, about 50 %, than the JENDL-2 value, and that there is another marked window near 53.5 keV which can not be seen in the evaluation. The minimum values obtained at the windows indicate that the cross section of the isotope ^{28}Si is very small as is expected from the Breit-Wigner cross-section formula for an even-even nucleus.

References:

(1) Fujita, Y. et al. : To be submitted to J. Nucl. Sci. Technol.

(2) Garber, D.I. and Kinsey, R.R.: " Neutron Cross Sections ", BNL-325 (1976).

(3) Kobayashi, K. et al.: Annals of Nucl. Energy, Vol.4, Nos.9/10, 449 (1977).

(4) Larson, D.C. et al.: " Measurement of the Neutron Total Cross Section of Silicon from 5 eV to 730 keV ", ORNL/TM-5618 (1976).

(5) Mughabghab, S.F. et al.: " Neutron Cross Sections, Vol.1, Neutron Resonance Parameters and Thermal Cross Sections ", edit. by Brookhaven National Laboratory, published by Academic Press (1981).

(6) Fields, R.E., Walt, M.: Phys. Rev., 83, 479 (1951).

(7) JENDL-2 data file for Si (MAT=2140) evaluated by Asami, T. (to be published as JAERI-report).

(8) Koester, L. et al.: Zeitschrift fur Physik, A289, 399 (1979).

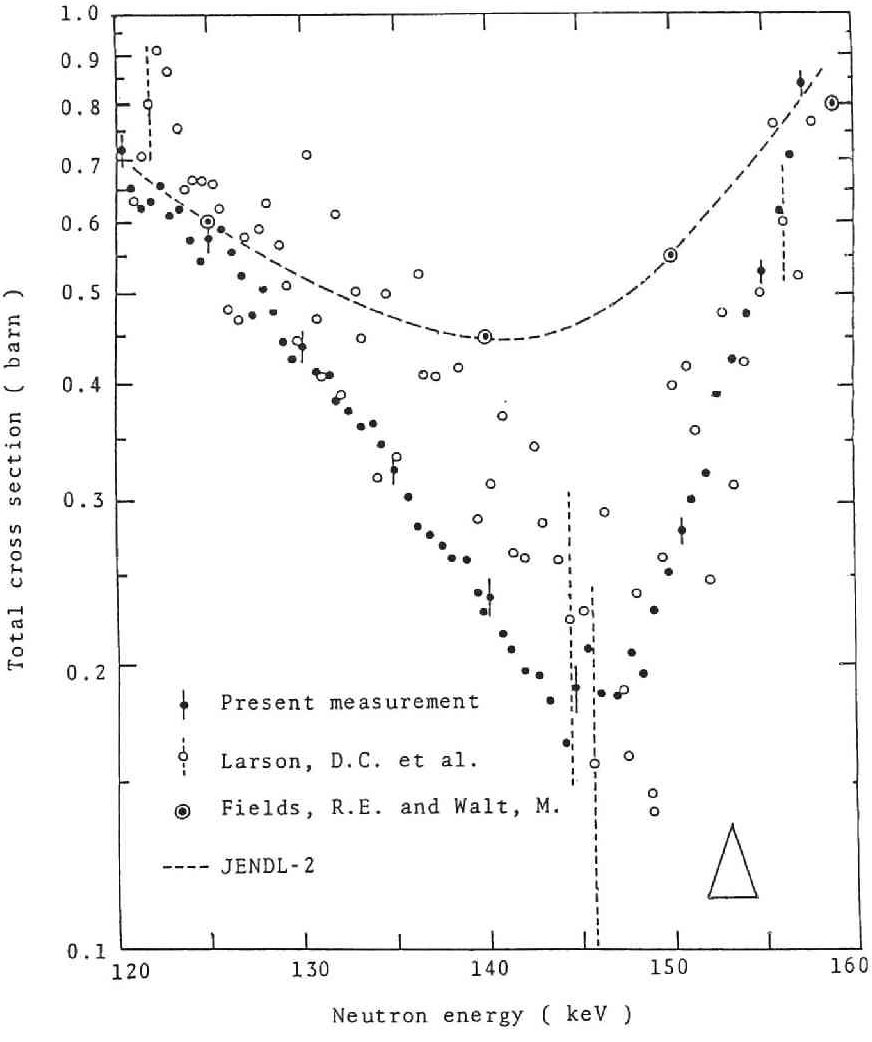

Fig. 5-1 Total cross section of Si near 144 keV. Other experiments and the JENDL-2 curve are also shown for comparison. The triangular mark shows the energy resolution of this experiment.

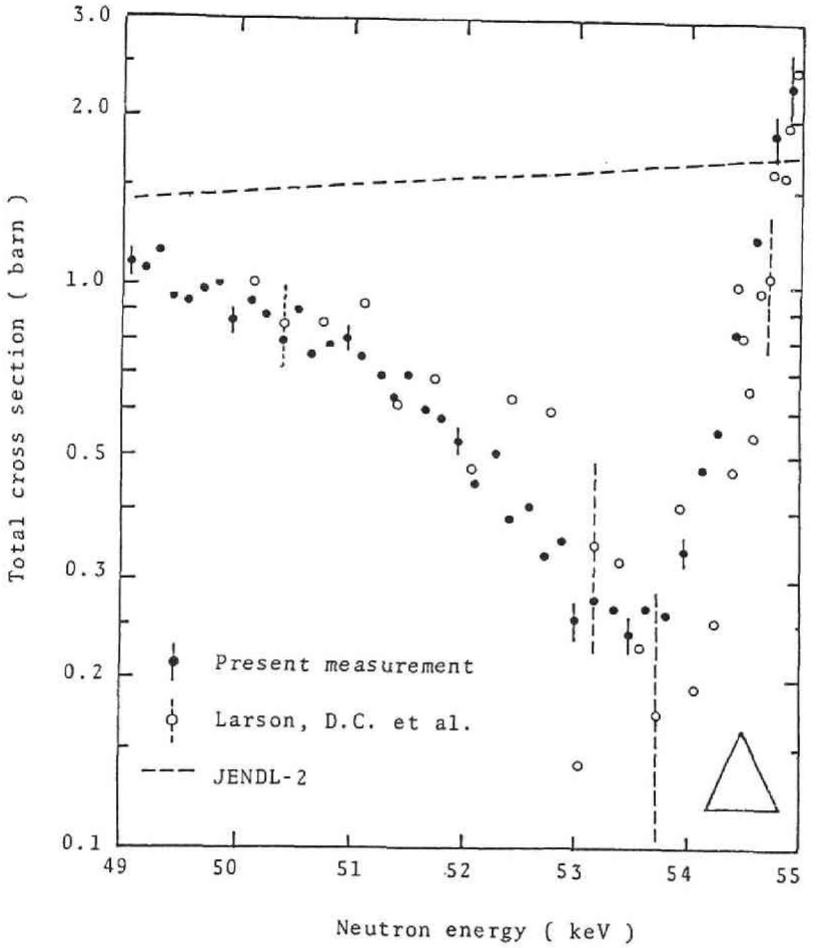

Fig. 5-2 Total cross section of Si near 53.5 keV. Other experiments and the JENDL-2 curve are also shown for comparison. The triangular mark shows the energy resolution of this experiment.

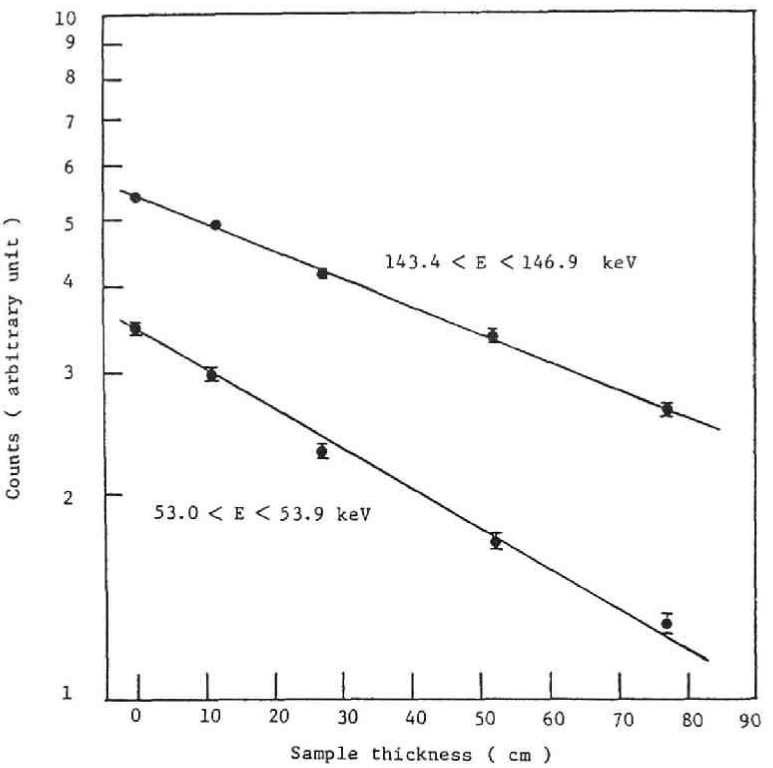

Fig. 5-3 The decrease of the counts near the windows with the increase of the sample-thickness.

Chapter 6 Measurements of Total Cross Sections of Be, C and O for 24-keV Fe-Filtered Neutrons[1]

6.1 Introduction

Prior to the application of the Fe-filtered neutrons, the applicability of the accelerator-based filtered-beam technique for precise measurements of neutron cross sections was studied using the 22-m time-of-flight spectrometer of the KURRI-LINAC. One of the essential points to achieve high precision is to attain a high signal-to-background ratio preserving the intensity of the filtered neutrons and reliably estimate the amount of the background. By installing an Fe-filter in the flight path of the above-mentioned spectrometer, time-of-flight transmission measurements were carried out for Be, C and O. These samples were selected since they are important elements in nuclear-energy applications, and the variations of cross section are very small in the energy spread of the neutrons. In this chapter are described the results of the applicability study and the applications to Be, C and O.

6.2 Experimental Method

The experimental installation is described in Chapter 3. For the improvement of beam quality, many trials were carried out to make a compromization between the minimum sacrifice of 24-keV neutrons, the improvement in signal-to-background ratio and the reduction of gamma-flash disturbance to the detector, by varying the thickness and installed position of the filter and by adding a few auxiliary filters such as Al, S and Pb. After these trials, a 30-cm filter of single material was employed for experiment. The time-of-flight spectrum of neutrons using the filter is shown in Fig.6-1. The portion C in the figure is the counts of the 24-keV filtered neutrons. The interpolation between A and B gives the background counts at the energy region of the 24-keV neutrons. The peak to valley ratio is about 700 : 1, or the background content is about 0.14 % of the foreground. In a usual time-of-flight experiment, the content is, roughly said, a few percent in a better case and often becomes worse than ten percent.

6.2.1 Samples

Considerable care had to be taken to prepare the transmission samples and determine their thicknesses. The C-samples were machined from graphite blocks of reactor-grade containing total impurity less than 30 ppm. These samples were dried under the vacuum at 120 °C to remove water, and were then sealed under the vacuum in sample cells having 0.5-mm thick Al-windows. Measurements of thicknesses and weights of the samples were made over the region where the neutron beam had passed. The results, however, indicated no density variation in the whole sample within the error of $\pm$ 0.05 %.

The Be-samples were formed by stacking plates of approximately 10 cm x 10 cm x 0.5 cm. The plates were machined from reactor-grade metal and had sharp 90 degree corners. They showed no evidence of voids near the surface.

Two O-compounds, Al_2O_3 and SiO_2, were used for this measurements, and also samples of Al and Si to determine the cross section of these elements. The cross section of O was given as the difference of values between the compound and elemental materials. The Al_2O_3-samples consisted of layers of ceramic sheets, each sheet being 1-cm thick and 7 cm x 7 cm square. A measurement using a micrometer showed that the thickness was very uniform and the faces were quite flat. In addition, the surface of the samples showed no visible evidence of voids, so it was presumed that the sample thickness in the region of the 5-cm-diameter neutron beam was the same as the average thickness over the 7 cm x 7 cm area. The SiO_2-samples consited of a stack of highly polished disk of high-purity fused SiO_2. The purities of Al-and Si-samples were better than 99.9 %. Cross sections of Al and Si are considerably smaller than that of O. Therefore, only a small amount of the error in taking the above-mentioned differences was propagated to the value of O.

The samples used in the experiments, along with their thickness and thickness uncertainties (in standard deviations), are listed in Table 6-1.

6.2.2 Data Processing

As for this experiment, the effective transmission T through a sample is

determined from an equation,

$$T = \int_{E_l}^{E_u} \exp \left\{ -N\,\sigma(E) - N_a t_a \sigma_a(E) \right\} \cdot F(E)\,dE \;/\; \int_{E_l}^{E_u} F(E)\,dE \quad , \quad (6.1)$$

where N is the sample-thickness (in molecules per unit area) ; $\sigma(E)$ the neutron total cross section of the sample at energy E ; N_a the atomic density of air ; t_a the thickness of the air displaced by the sample; $\sigma_a(E)$ the neutron total cross section of air ; and $F(E)$ the product of neutron flux and the detector efficiency at the energy E.

The $F(E)$ was obtained in an additional experiment with an energy resolution eight-times higher than that used for the transmission measurements, and are listed in Table 6-2. The limits for integration E_l, E_u were taken as 17.5 and 26.3 keV respectively.

For the sample materials used in this experiment, the energy dependences of $\sigma(E)$ and that for the air are very small over the energy spread of the beam, and then T can be reduced approximately to

$$T = \exp \left\{ - N\,\sigma\,(E_{av}) - N_a t_a \sigma_a(E_{av}) \right\}, \qquad (6.2)$$

where E_{av} is the average energy of the beam weighted with the spectrum $F(E)$. The E_{av} is equal to 23.5 keV, and accordingly all cross sections shall hereafter in this chapter be refered to this energy.

6.3 Results and Discussion

The time-of-flight spectrum of the filtered beam is shown in Fig.6-1. The spectrum contains the information of the foreground and the background simultaneously. The background at the 24 keV band, the region C, is determined by linearly interpolating between two blacked-out regions A and B. It is necessary to consider how accurate this assumption is to estimate the precision attained in the measurement.

The background in the spectrum is composed of a steady-state component due to cosmic-rays and radioactivity in the vicinity of the detector, and of a time-dependent component which varies with time-of-flight. It is the latter which causes the variation of background between A and B regions.

The attenuation of the backgrounds at A and B with transmitting through the graphite-sample indicated that the major part of this background is caused by gamma-rays, rather than by neutrons. It is difficult to conceive that a gamma-ray background would fluctuate rapidly in the time interval between A and B. As for the smaller neutron component, background neutrons are those transmitted through the higher-energy minima of Fe and then scattered by collimators. These neutrons, however, will have a slowly-varing dependence in time-of-flight. The only component which could have a significant time dependence near 24 keV is the neutrons transmitted through the filter and scattered at a small angle with collimators. The neutrons lose little energy and must be considered as a part of the signal.

With the above discussions, it has been shown that the background has a simple, smooth time dependence. The linear interpolation between A and B is a reasonable procedure determining the background at the region C. If, for example, the decrease of background from A to B is ignored, then the cross section of the (N = 1) samples is increased by 0.1 %, and that for the (N = 2) samples by 0.06 %. A reasonable upper limit of 20 % can be placed on the error produced by the linear relation assumed in the difference in the background between regions A and B, and thus the resulting uncertainty in the cross section is 0.05 %.

The detection-efficiency shift caused by a gamma-flash for the NaI(Tl) transmission-detector which is described in Chapter 3 was studied by a method of Hockenbury et al.[2] using a ^{137}Cs source. The result showed the shift produced a cross-section uncertainty of 0.06 % for the (N = 1) samples and 0.03 % for the (N = 2) samples.

The uncertainty due to the dead-time correction is small because the dead time (1.4 - 1.7 μsec) is longer than the time spread of the filtered beam. The overall uncertainty in the dead-time correction is estimated to produce a cross-section uncertainty of 0.05 %.

By combining three kinds of the above-metioned uncertainties,it has been shown that this Fe-filtered beam method is intrinsically capable of yielding an accuracy of 0.1 %, which is comparable to that achieved in precise measurements of thermal neutron cross sections.

The results of this experiments are presented in Tables 6-3 and 6-4. The cross section for air at 23.5 keV - σ_a in Eq.(6-2) - was quoted from

a literature[3].

In Table 6-3, the counting statistic is presented for each seperate run. Final results are presented in Table 6-4 for the cross sections and the uncertainties. In Table 6-5, the results are compared with the evaluated values in ENDF/B-III, ENDF/B-V , JENDL-2 and a recent measurement by Aizawa et al.[4] performed using reactor-based Fe-filtered neutrons.(The ENDF/B-III was the latest version at the time of present experiment.) The present value of Be agrees, within 0.4 %, with the result of Aizawa et al. and the ENDF/B-V. However, it is 4.5 % larger than the JENDL-2 value. As for C, the present result is larger than the others by about 0.7 to 1.2 %.

6.4 Conclusion

The applicability study of the accelerator-based Fe-filterd beam technique has shown that the technique is intrinsically capable of yielding an accuracy of 0.1 %, which is considerably better than a typical value of about 1 % in this energy range and comparable to that achieved in presise measurements of thermal-neutron cross sections.

Along with the applicability study, the technique has been applied to the neutron total cross sections of Be, C and O , giving the data with an accuracy of approximately 0.2 %. The result for Be agrees with the ENDF/B-V value by 0.4 %, and 4.5 % larger than the JENDL-2 value. For C, the present result is larger than the evaluations by 0.7 to 1.2 %.

References:

(1) Block, R.C. et al.: J. Nucl. Sci. Techol., 12(1), 1 (1975).

(2) Hockenbury, R.W. et al.: Rensselaer Polytechnic Linear Accelerator Report RPI-328-266, p.44 (1971).

(3) BNL-325, (2nd. Ed.), Suppl. No. 2, Vol. 1, (1964).

(4) Aizawa, O. et al.: J. Nucl. Sci. Technol., 20(4), 354 (1983).

(5) Ozer, O., Garber, D. : ENDF/B summary documentation, BNL-17541 (ENDF-201) (1973).

(6) ENDF/B-V data file for Be (MAT=1289) evaluated by Howerton, R.J. et al. (1979).

(7) ENDF/B-V data file for C (MAT=1306) evaluated by Fu, C.Y. et al. (1979).

(8) JENDL-2 data file for ^{9}Be (MAT=2041) evaluated by Shibata, K. et al. (to be published as JAERI-report).

(9) JENDL-2 data file for ^{12}C (MAT=2061) evaluated by Yamamoto, M. (to be published as JAERI-report).

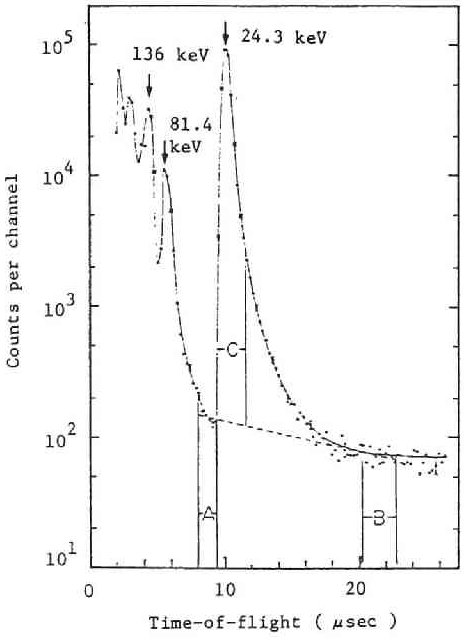

Fig.6-1 Time-of-flight spectrum of Fe-filtered neutrons for the open sample position. The regions A and B are used to determine the background and the region C represents the interval over which the foreground is determined.

Table 6-2 The $F(E)$ *vs.* neutron energy E

E_i is the energy of the upper edge of time-of-flight channel i. $\sum F_i(E)$ is arbitrarily normalized to 100.

E_i(keV)	$F_i(E)$	E_i(keV)	$F_i(E)$
26.326	0.43	21.062	1.22
25.854	2.71	20.724	1.08
25.395	8.13	20.394	0.90
24.948	13.53	20.072	0.75
24.513	15.91	19.757	0.73
24.089	14.29	19.450	0.65
23.676	11.58	19.150	0.43
23.274	8.28	18.857	0.43
22.882	6.22	18.571	0.32
22.499	4.65	18.291	0.28
22.126	3.20	18.017	0.25
21.763	2.17	17.750	0.22
21.408	1.64	17.488	

Table 6-1 Transmission samples

Sample	Composition	Thickness (mol./10^{-24}cm^2)	$N\sigma$
Be	Metallic plates	0.1840±0.0003	≈1.1
		0.3089±0.0005	≈1.8
		0.3714±0.0006	≈2.2
C	Reactor grade graphite	0.2483±0.0003	≈1.2
		0.5077±0.0003	≈2.4
Al_2O_3	Ceramic plates	0.08624±0.0001	≈1.1
		0.1293±0.0002	≈1.6
Al	Metal	0.60262±0.00003	≈0.3
SiO_2	Fused and polished disks	0.08624±0.00008	≈0.8
		0.1377±0.0001	≈1.3
Si	Single crystal	0.2720±0.0009	≈0.5

Table 6-3 Neutron total cross section for each seperate-sample run

Sample	Run	Sample thickness ($N\sigma$)	Cross section (b)	Counting statistics error (%)
C	1	1.2	4.689	0.47
		2.4	4.680	0.29
	2	1.2	4.673	0.42
		2.4	4.688	0.27
Be	1	1.1	5.873	0.47
		2.2	5.895	0.30
	2	1.1	5.899	0.42
		2.2	5.924	0.27
	3	1.1	5.891	0.43
		2.2	5.903	0.28
	4	1.8	5.905	0.27
Al_2O_3	1	1.6	12.264	0.32
	2	1.6	12.249	0.25
	3	1.1	12.284	0.40
Al	1	0.3	0.540	1.60
	2	0.3	0.535	1.30
SiO_2	1	1.3	9.235	0.25
		0.8	9.301	0.38
Si	1	0.5	1.769	3.02
	2	0.5	1.791	3.06

Table 6-4 Final results for neutron total cross section of Be, C and O

	Total cross section (b)	Total error (b)	Total error (%)	Partial errors (%) Counting statistics	Sample thickness uncertainty	Detection efficiency shift uncertainty	Dead-time correction uncertainty	Air scattering correction uncertainty	BG determination uncertainty
$_4$Be	5.903	0.011	0.18	0.14	0.09	<0.05	<0.05	<0.10	<0.05
$_6$C	4.684	0.009	0.20	0.18	0.05	<0.05	<0.05	——	<0.05
$_8$O†	3.736	0.007	0.19	0.16	0.08	<0.05	<0.04	<0.03	<0.04
$\frac{Al_2O_3-2Al}{3}$	3.735	0.009	0.23	0.18	0.12	<0.05	<0.05	<0.05	<0.05
$\frac{SiO_2-Si}{2}$	3.738	0.012	0.32	0.30	0.08	<0.05	<0.05	<0.02	<0.05

† Cross section of $_8$O is the weighted average of $(Al_2O_3-2Al)/3$ and $(SiO_2-Si)/2$.

Table 6-5 Comparison of the present results of cross sections with ENDF/B, JENDL-2 and another experiment (barn)

Element	Present result	ENDF/B-III*	ENDF/B-V*	JENDL-2*	Aizawa et al.
Be	5.903 ± 0.011	5.93 (a)	5.93 (b)	5.65 (d)	5.88 ± 0.02 (f)
C	4.684 ± 0.009	4.65 (a)	4.65 (c)	4.63 (e)	4.65 ± 0.01 (f)
O	3.736 ± 0.007	3.68 (a)	--	--	--

*) The evaluated values are the interpolated between the points near 24 keV.

(a) ref.5, (b) ref.6, (c) ref.7, (d) ref.8, (e) ref.9, (f) ref.4.

Chapter 7 Measurement of the Neutron-Proton Total Cross Section Using 24-keV Fe-Filtered Neutrons[1]

7.1 Introduction

The n-p scattering cross section has been a subject of intensive experimental[2] and theoretical studies. From the theoretical view point, the cross section is fundamentally important for the comparison of the n-p and p-p singlet interactions. It also serves as a standard cross section when it is used in recoil-proton detectors for the determination of a neutron flux.

The n-p scattering cross section is described in the energy region up to 10-20 MeV by the well-known effective-range formula[3] which are described with four empirical parameters: the effective ranges and scattering lengths for both siglet and triplet interactions. Experimental data used in the determination of these parameters are the binding energy of deuteron, the n-p coherent-scattering length and the energy dependent n-p scattering cross sections. As discussed by Houk[4], the need for precise measurements of the n-p scattering cross section still remains for the purpose of deducing the uncertainty of the parameters. For the "zero-energy" scattering cross section between a neutron and a free proton, which is particularly important for the above-mentioned purpose, Houk[4] measured 20.436 $\pm$ 0.023 barns in 1971, larger than Melkonian's value[5] of 20.36 $\pm$ 0.023 barns measured in 1949. Recently, Dilg[6] obtained an even higher value of 20.491 $\pm$ 0.014 barns by extrapolating from a measurement performed at 132 eV. The value near 24 keV, measured in this experiment, with a comparable accuracy to the above-mentioned values in the lower energy region, will contribute predominantly toward a determination of the zero-energy cross section.

A similar experimental technique described in Chapters from 4 to 6 was used for the present measurement. The areal atomic-density of transmission samples was carefully determined and the cross-section value was obtained with an overall accuracy of 0.13 %.

7.2 Experimental Method

7.2.1 Transmission Sample

Precise determination of the areal atomic-density of the transmission samples has been one of the most important problems in all of the n-p total cross section transmission measurements. In this experiment, a technique to replace a water-sample with an optically-flat SiO_2-plate was employed. An Al-case filled with pure water as is shown in Fig.7-1 was placed in the flight path. The SiO_2-sample in the water was moved into and out of the neutron beam for " Sample -In and -Out " runs, respectively. The counting ratio of these runs determined the difference between the transmission of the water layer removed by the SiO_2-plate and the plates itself. The SiO_2 was employed with the following reasons: (i) thickness and flatness of the plate can be determined with a sufficient accuracy by optical instruments, (ii) SiO_2 is stable in water, (iii) the thermal-expansion coefficient is small, and (iv) the neutron cross section is also small.

The SiO_2-plate was aligned perpendicular to the neutron beam by using a laser beam reflected from the surface of the plate. The temperature of the water was monitored with a thermocouple and the result of the cross section was corrected for the variation of water density.

7.2.2 Data Deduction

The n-p cross section varies with neutron energy within the window of the filtered beam and the precise determination of the energy scale is as important as the cross section value. The absolute energy scale was determined by the flight length and flight time, and the error was estimated to be about 0.27 %. The effective neutron energy attached to this measurement is defined by a relation,

$$\exp\left\{-\Sigma_w(E_e)d + \Sigma_{si}(E_e)d\right\} = \int_{E_l}^{E_u} \exp\left\{-\Sigma_w(E)d + \Sigma_{si}(E)d\right\} F(E)\,dE \Big/ \int_{E_l}^{E_u} F(E)\,dE \quad , \qquad (7.1)$$

where $F(E)$ is the energy spectrum shown in Fig.7-2; E_u and E_l are the upper

and lower energy limits used in data processing; $\Sigma_w(E)$ and $\Sigma_{si}(E)$ are the macroscopic total cross sections of the displaced water and the SiO_2-plate, respectively; d is the thickness of the SiO_2-plate. The value of E_e depends on sample thickness and its error is estimated to be about 0.29 %.

The n-p cross section is deduced from Eq.(7-1) to

$$\sigma_H = -\frac{1}{2}\sigma_O + \frac{1}{2}\frac{N_{si}}{N_w}\sigma_{si} + \frac{1}{2}\frac{1}{N_w}\ln\left[\frac{\sum_{i_1}^{i_u}(I_i - IB_i)}{\sum_{i_1}^{i_u}(O_i - OB_i)}\right]^{-1}, \qquad (7.2)$$

where σ_H is the n-p total cross section; σ_O and σ_{si} are the total cross sections of O and SiO_2, respectively; N_w is the areal density of the water molecules in the volume replaced by the SiO_2 plate; N_{si} is the areal density of SiO_2 in the plate; I_i and O_i are the dead-time-corrected counts for sample-in and out-runs respectively; IB_i and OB_i are the background counts for Sample-In and Out-runs respectively ; i_u and i_l are the channel numbers which correspond to E_u and E_l respectively.

7.3 Error Analysis and Corrections

Experimental errors are devided into several groups. Some of them are similar to those in the experiment in chapter 6. Only the results of the error analysis are, therefore, simply shown in Table 7-1.

The thickness of the SiO_2-plate was determined with a higher accuracy than 10^{-5}, and the overall error introduced to the cross section by the error of the areal atomic-density is estimated to be 0.017 % after the correction of the temperature variation of water density.

The 0.29 % error in E_e is equivalent to 0.038 % error in the cross section.

Corrections were made for deuterium in water, the Doppler effect and the capture cross section. They were found, however, to be lower than 0.01 % correction.

7.4 Results and Discussion

The n-p total cross section obtained are 17.767 $\pm$ 0.046 barns (E_e =

23.638 keV) and 17.732 ± 0.025 barns (E_e = 23.645 keV) for the thin and thick samples respectively. The former value is corrected for the effective energy of the latter by using the effective-range formula and found to be 17.736 barns. By taking the weighted average, the final result obtained is 17.740 ± 0.023 barns for 23.645 kV neutrons.

The result is compared with the theoretical values calculated with the parameter-sets tabulated by Lomon and Wilson[7] and Dilg[6], and using the effective-range formula. The main difference between the parameter-sets is that the former employs Houk's value and the later Dilg's value for the scattering cross section of zero-energy neutrons. The bindng energy of deuteron and the coherent scattering length[8] are commonly used for both parameter-sets. The parameters are listed in Table 7-2.

The calculated n-p scattering cross sections near 24 keV using the parameters are shown in Fig.7-3, along with the result of this experiment. The experiment is very close to the calculation based on the Houk's value and lower than the Dilg's by 1.5 standard deviations of this experiment. It can be concluded that the parameter-set of Lomon and Wilson represents the n-p cross section quite acculately and do not see the need to go to the larger cross section resulting from the Dilg's parameters.

The evaluated value for the cross section in JENDL-2[9] is 17.56 barns at 23.6 keV, which is obtained by the interpolation between the evaluated points. This evaluation is about 1 % lower than the present result.

7.5 Conclusion

The accelerator-based Fe-filtered beam, which was shown in Chapter 6 to be capable of transmission measurements of a 0.1-% intrinsical accuracy, has been applied to the cross section of the n-p interaction. The result is 17.740 ± 0.023 barns at the effective energy of 23.645 ± 0.068 keV and provides a precise value in the keV region with an accracy comparable to that of the most precise experiments in other energy range. The value was used to discuss the empirical parameters used in the effective-range formula of the n-p interaction.

References:

(1) Fujita, Y. et al.: Nucl. Phys., A258, 1 (1976).

(2) CINDA, An index to the litereture on microscopic neutron data, IAEA, Vienna 1974.

(3) Bethe, H.A.: Phys. Rev., 76, 38 (1949).

(4) Houk, T.L.: Phys. Rev., C3, 1886 (1971).

(5) Melkonian, E.: Phys. Rev., 76, 1744 (1949).

(6) Dilg, W.: Phys. Rev., C11, 103 (1975).

(7) Lomon, E., Wilson, R.: Phys. Rev., C9, 1932 (1974).

(8) Koester, L., Nistler, W.: Phys. Lett., 27, 956 (1971).

(9) JENDL-2 data file for H (MAT=2011) evaluated by Yamamoto, M. (to be published as JAERI-report).

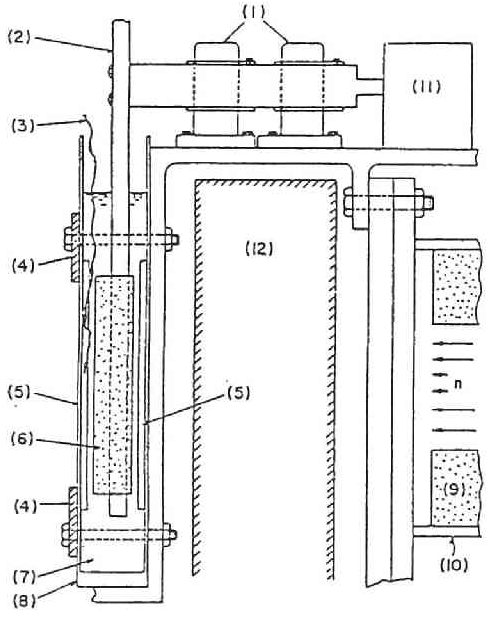

1) pillow boxes, 2) sample holder, 3) thermocouple, 4) pressing bars, 5) Al spacer, 6) SiO_2 plate, 7) pure water, 8) Al can, 9) collimator, 10) flight tube, 11) driving motor, 12) Fe filter.

Fig. 7-1 Cross-sectional view of the sample changer.

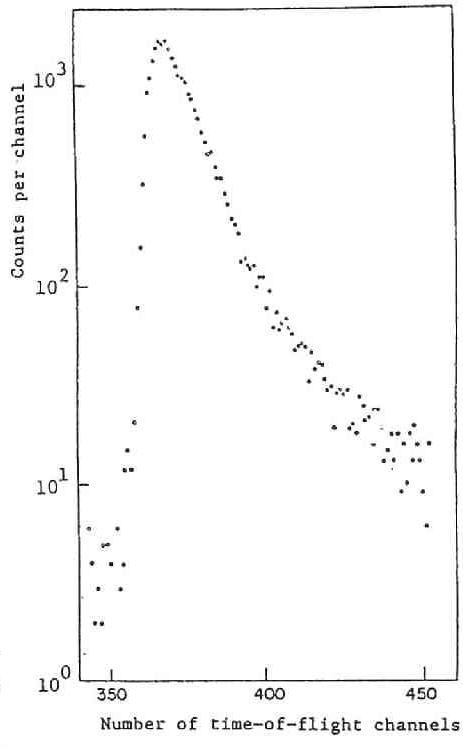

Fig. 7-2 Time-of-flight spectrum of the filtered neutrons counted by the NaI(Tl) detector.

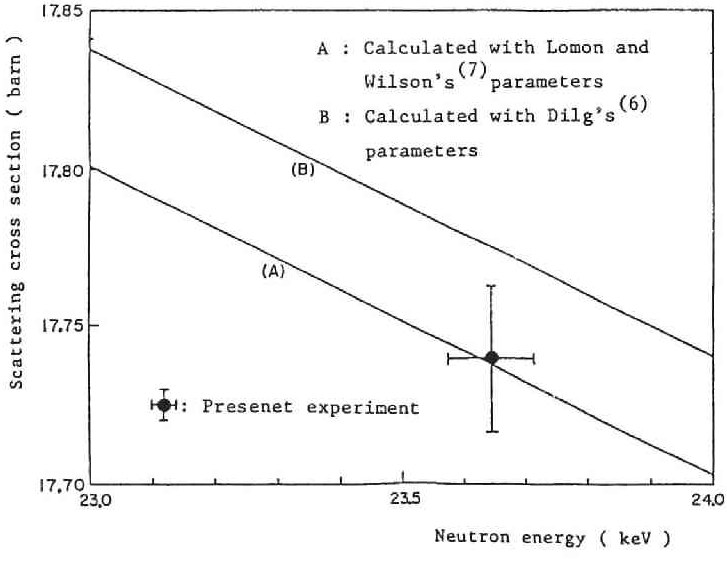

Fig. 7-3 The n-p scattering cross section near 24 keV.

Table 7-1 Neutron-proton total cross section and its errors

Neutron-proton total cross section at the effective energy 23.645 ± 0.068 keV: 17.740 ± 0.023 b	
Partial errors (%) :	0.13
Counting statistics	0.096
Sample thickness uncertainty	0.017
Detection efficiency shift uncertainty	0.04
Dead time correction uncertainty	0.05
Background determination uncertainty	0.05
Effective energy uncertainty	0.038

Table 7-2 Effective-range parameters (fm)

Parameters		Lomon and Wilson values[7]	Dilg value[6]
Triplet scattering length	a_t	5.414 (± 0.005)	5.423 (± 0.004)
Singlet scattering length	a_s	-23.719 (± 0.013)	-23.749 (± 0.009)
Triplet effective range	r_t	1.750 (± 0.005)	1.760 (± 0.005)
Singlet effective range	r_s	2.76 (± 0.005)	2.81 (± 0.005)

Effective-range formula : $$\sigma = \frac{3\pi}{k^2 + \left(\frac{1}{2}k^2 r_t \quad 1/a_t\right)^2} + \frac{\pi}{k^2 + \left(\frac{1}{2}k^2 r_s \quad 1/a_s\right)^2}$$

Chapter 8 Measurement of Capture Cross Sections of ^{93}Nb, ^{115}In, ^{127}I, ^{165}Ho, ^{181}Ta and ^{238}U for 24-keV Fe-Filtered Neutrons[1]

8.1 Introduction

Neutron capture cross section plays an important role in various aspects of reactor engineering; for instance, neutron economy, fuel breeding, reactor control, material activation, radiation shielding etc.. The accuracy of the presently-available data of capture cross sections can not meet in most cases the need of reactor engineering. To obtain more reliable experimental data, several kinds of improvement are needed in the technique of measurement. The study in this chapter extends an application of the accelerator-based filtered neutrons to the capture-cross-section measurement. Filtered neutrons are obtained by installing a thick Fe-filter in the flight path of a time-of-flight spectrometer. The advantage of filtered neutrons for this kind of experiment is reliable subtraction of the background in the measurement. The background is low in level and is simultaneously determined in the measurement. This leads to an accurate measurement of cross sections. The result, a point cross section, can be used to normalize an energy-dependent cross section obtained in a usual time-of-flight measurement.

The pulse-height-weighting technique is needed to obtain a capture cross section. The outline of the technique employed in the present measurement is as follows. Capture events are counted by detecting the prompt capture gamma-rays with a pair of C_6F_6-liquid-scintillation detectors. The pulse-height response of the detectors is analyzed by a multi-channel pulse-height analyzer. The counts of all channels are summed up with imposing appropriate respective weights. The sum gives the number of capture events irrespective of the prompt gamma-ray spectrum emitted. The number of neutrons impinging on the sample is measured with the same detectors by detecting the 480-keV gamma-ray following the reaction of $^{10}B(n,\alpha\gamma)$. In other words, the cross section of $^{10}B(n,\alpha\gamma)$ is used as the standard.

The samples selected for measurements are a fertile material ^{238}U, a structural material ^{93}Nb, and several nuclei of atomic-mass-number near those of fission products ^{115}In, ^{127}I, ^{165}Ho and ^{181}Ta.

8.2 Experimental Method

8.2.1 Experimental Layout

The experiment was carried out at the 11.7-m time-of-flight spectrometer at the KURRI-LINAC. The arrangement is shown in Fig.8-1. Neutrons filtered with a 15-cm-thick Fe were collimated within a 46-mm diameter onto a sample. Two C_6F_6-scintillation detectors, of type NE-226 of Nuclear Enterprise Ltd., 10 cm in diameter and 4 cm in thickness, mounted on EMI-9818 photo-multipliers, were placed on both sides of the sample. The detectors were shielded with a 5-cm-thick wall of Pb-bricks. The pulse signals from the detectors were stored in an analyzer by the two-parameter mode of 32 x 32 channels - i.e. time-of-flight of neutrons and pulse-height of capture gamma-rays.

A preliminary study of the energy profile of the filtered neutrons was carried out with a combination of the C_6F_6-detectors and a thick ^{10}B-sample of about 5 g/cm^2. The profile obtained is shown in Fig.8-2, where the straight base-line means the background level. The peak of the spectrum is 24.3 keV; the width is about 2 keV; the effetive energy is 23.7 keV, which is attributed to this experiment. The resonance-shaped dips in the spectrum are caused by the resonances in the Mn-impurity in the Fe-filter.

8.2.2 Pulse-Height-Weighting Technique[2,3]

Capture cross section measurements by detecting prompt capture gamma-rays are based on an equation,

$$C = \Phi Y \eta \quad , \tag{8.1}$$

where C is the count rate of the gamma-ray detector; Φ is the neutron flux incident upon a sample; Y is the probability of capture of the incident neutrons; η is the detection probability of a capture event. It is essential to prepare a value of η which is irrespective of the cascade mode of the decay of the compound nucleus produced by neutron capture from an exited to the ground level. The pulse height weighting technique is one of

the methods to assure such a characteristic to η .

Let a pulse-height response of a gamma-ray detector, i.e. the probability of count in a channel of a pulse-height analyzer, to a photon of the energy w under a certain experimental arrangement be denoted by $R(i,w)$, where i (=1,2,..,m) is the channel number. A weighting function W is defined as a set of weights $W(i)$ (i= 1,2,..,m) which satisfies the following relation:

$$\sum_{i=1}^{m} W(i)\ R(i,w) \ = \ k\ w \ , \tag{8.2}$$

where k is a proportional constant independent of the photon energy w.

The pulse-height response $R(i,w)$ can be obtained by a computer calculation for an arbitrary W and the validity of the calculation can be experimentally checkd.[3] The weighting function W is deduced regarding Eq.(8.2) as a matrix equation and can be used to assure the afore-mentioned characteristic to η as explained below.

Let a set of energies of the gamma-rays emitted by a neutron capture be given by $w_1,w_2,w_3....,w_n$; then the response $C(i)$ (i=1,2,...,m) of the detector to the gamma-rays can be written as

$$C(i) \ = \ \sum_{j=1}^{n} R(i,w_j) \tag{8.3}$$

for the count in the i-th channel of the pulse-height analyzer.

The gamma-ray spectrum differs from cature event to event; however, there is a restriction for the sum of the gamma-ray energies as

$$\sum_{j=1}^{m} w_j \ = \ (\ SE\ ) \ + \ E_n \tag{8.4}$$

where (SE)is the neutron seperation energy from the compound nucleus and E_n is the kinetic energy of the captured neutron.

If one takes a sum of $C(i)$s over all channels by weighting with $W(i)$, the sum $<CW>$ is given as

$$<CW> \ = \ \sum_{i=1}^{m} W(i)\ C(i) \ . \tag{8.5}$$

By using Eqs.(8.3), (8.2) and (8.4) the $\langle CW \rangle$ is rewritten as follows:

$$\langle CW \rangle = \sum_{i=1}^{m} W(i) \sum_{j=1}^{n} R(i,\omega_j) = \sum_{j=1}^{n} \sum_{i=1}^{m} W(i) R(i,\omega_j), \tag{8.6}$$

$$\langle CW \rangle = \sum_{j=1}^{n} k\,\omega_j = k \left\{ (SE) + E_n \right\}. \tag{8.7}$$

Eq.(8.7) shows that the sum $\langle CW \rangle$ is proportional to the number of capture events irrespective of the cascade mode of the compound nucleus and may be used as the count rate C in Eq.(8.1).

The value of Y in Eq.(8.1) which is closely related to the cross section of the relevant sample can be obtained by determining the flux Φ and the proportional constant k in Eq.(8.7). For the determination of these two values, the cross section of $^{10}B(n, \alpha\gamma)$ reaction was used as the standard and an Ag-sample was used as a so-called saturated-resonance sample at 5.2 eV. The $^{10}B(n, \alpha\gamma)$ reaction emits only one 480-keV gamma-ray and the weighting is not needed in this case. Four measurements mentioned below were carried out to obtain a capture cross section of the relevant sample at 24 keV:

$C_B^r = \Phi(5.2)\, Y_B^r\, \eta_B^r$ for the B-sample at the resonance, (8.8)

$\langle CW \rangle_{Ag}^r = \Phi(5.2)\, Y_{Ag}^r\, k \left\{ (SE)_{Ag} + 5.2 \right\}$ for the Ag-sample at the resonance, (8.9)

$C_B^{24k} \quad \Phi(24k)\, Y_B^{24k} \eta_B^{24k}$ for the B-sample at 24 keV, (8.10)

$\langle CW \rangle_S^{24k} = \Phi(24k)\, Y_S^{24k}\, k \left\{ (SE)_S + 24k \right\}$ for the relevant sample at 24 keV. (8.11)

By manipulating Eqs.(8.8)-(8.11) and taking $\eta_B^r = \eta_B^{24k}$ and $Y_B^r = Y_{Ag}^r = 1$ into consideration, one may obtain

$$Y_S^{24k} = \frac{\langle CW \rangle_S^{24k}}{\langle CW \rangle_{Ag}^r} \frac{C_B^r}{C_B^{24k}} \frac{\left\{ (SE)_{Ag} + 5.2 \right\}}{\left\{ (SE)_S + 24k \right\}} Y_B^{24k} \tag{8.12}$$

From the value Y thus obtained by Eq.(8.12), the capture cross section was deduced after correcting for the attenuation of capture gamma-rays and the multiple scattering of neutrons in the sample.

8.2.3 Samples

The ^{10}B-sample was in the powder-form and packed in an Al-capsule by 0.9 g/cm^2 in weight. The powder was chemically analyzed for the content of B and isotopically analyzed for ^{10}B. The portion of B was 93.23 w/o of the powder and that of ^{10}B was 93.93 w/o of B. The sample of I was prepared by PbI_2-powder packed in an Al-capsule. The other samples were metallic plates.

The standard cross section of ^{10}B was taken from an evaluation by Sowerby et al.[3].

For the correction of the multiple scattering, an analytical method[5] was employed since the thicknesses of the samples were relatively thin and only an approximate correction was needed. In Table 8-1 are summerized the sample thicknesses and the calculated multiple-scattering correction factors.

8.2.4 Processing of Spectra

In Fig.8-4 are typically shown the time-of-flight spectra of the prompt gamma-rays for the samples of ^{127}I and ^{238}U. One part of the background ground in the time-of-flight spectra was caused by the 24-keV neutrons scattered with the sample. This background was determined by a measurement for a graphite sample which had practically no capture cross section and had the thickness to scatter the same number of neutrons as the relevant sample. The other part of background was irrespective of the scattered neutrons and determined by linearly-interpolating between the counts in the lower- and the higher-energy regions in the time-of-flight spectra. The counts between the vertical lines in Fig.8-4 are summed up after the subtraction of background giving the respective pulse-height spectra in Fig. 8-5. The spectra weighted with W are also shown in Fig. 8-5. The $\langle CW \rangle$ needed in Eq.(8.12) for each sample is obtained by integrating the weighted spectrum in Fig.8-5. As is seen in Eq.(8.12), the weighted sum for the Ag-sample which was used for a reference in the saturated-resonance technique was needed only for the measurement at 5.2 eV. For the B-sample, measurements were needed for 24 keV and 5.2 eV, not for the spectrum but

for the counts above a discrimination level.

8.2.5 Uncertainty of Data

The statistical errors estimated from the numbers of counts appeared in Eq.(8.12) were between 2.5 and 6 % for the values of Y. These errors are shown in Table 8-1 for each sample material.

As for the systematic errors, there are several kinds of sources. The inherent uncertainty in the weighting function, or the uncertainty in η, was experimentally studied[3] using the capture gamma-rays of Au, Ta and Ag at the neutron energies of respective resonances in the eV-region. The result showed the uncertainty in η was about 2 %. The uncertainties come from that of $^{10}B(n,\alpha\gamma)$ cross section[4] and that of the multiple scattering correction, were also about 2 %. Thus the overall systematic error was estimated to be about 4 %.

Since natural element of In contains ^{113}In by 4.28 % whose cross section at 24 keV is not well known, the cross section of ^{113}In was assumed to be same as that of In in the subtraction procedure. Due to the assumption, a 2-% error was imposed on the cross section of ^{115}In.

8.3 Results and Discussion

The results of the 24-keV capture cross sections are shown in Table 8-2 along with the evaluated values in ENDF/B-IV[6]. The experimental errors are about 5 % (between 4 and 7 % depending on samples) except for ^{238}U. For ^{238}U, the error is about 8 % because of poor counting statistics.

There have been several measurements for the elements used in this study which were carried out with different kinds of experimental techniques. The data of these measurements are also shown in Table 8-2. Chaubey and Sehgal[7] made an activation-cross-sections measurement using an Sb-Be photo-neutron source. The standard cross section in their experiment was the 820 mbarns of $^{127}I(n,\gamma)$. Belanova et al.[8] made a shell-transmission measurement with an Sn-Be source , which was an absolute measurement of an absorption cross section. The experiment of Rimawi and Chrien[9] was an activation measurement with the reactor-based Fe-filter-

ed neutrons, where the $^{10}B(n,\alpha\gamma)$ cross section was used as the standard.

Although the present value of the ^{115}In cross section agrees with other experiments, those of ^{93}Nb, ^{165}Ho and ^{238}U differ from the values both of Chaubey et al.[7] and Belanova et al.[8]. A Monte-Carlo interpretation of the ^{238}U-experiment of Belanova et al.[8] was carried out by Miller and Poenitz[10] resulting in the capture cross section of 495 ± 40 mbarns at 24 keV. This revised value satisfactorily agrees with the other data in Table 8-2. The present value of ^{127}I agrees with the data of Rimawi and Chrien.[9].

As for the comparison to ENDF/B-IV values, the present data show good agreements for ^{127}I, ^{181}Ta and ^{238}U, but show large discrepancies for ^{93}Nb and ^{165}Ho.

There are three high resolution measurements[11,12,13] for ^{238}U. In Table 8-3 are shown the values of these measurements averaged over the energy interval between 20 and 30 keV, comparing with the experiments with monoenergetic neutrons. Spencer & Kaeppeler[14] measured the shape of the ^{238}U-capture cross section and showed an intermediate structure below 100 keV. If de Saussure at al.'s cross section[11] is folded with the energy spectrum of the present measurement, 575 mbarns is obtained. It is important to take into consideration of the effect of the intermediate structure in comparing the data between the point cross section and the cross-section curve. However, there still remain larger descrepancies between the cross-section curves than the effect of the intermediate structure. Therefore, the point-cross-section experiment is effectively used for the normalization of a cross-section curve. The values obtained in the present experiment have already been used for the normalization of the cross-section curves between 3.2 and 80 keV obtained at the KURRI-LINAC.[15]

8.4 Conclusion

The accelerator-based Fe-filtered beam has been applied to point capture cross section measurements. The accuracy attained is about 5 % and is considerably better than the descrepancies which exist between the presently avairable experimental data. This technique can be used as one of the

effective techniques to settle the problem of the descrepancies between the existing data. The sample materials taken up for the measurements are a fertile material ^{238}U, a structural material ^{93}Nb, and four nuclei of atomic-mass-numbers near those of fission products ^{115}In, ^{127}I, ^{165}Ho and ^{181}Ta.

References:

(1) Yamamuro, N. et al.: J. Nucl. Sci. Technol., 15 (9), 637 (1978).

(2) Macklin, R.L., Gibbons, J.H.: Phys. Rev., 159, 1007 (1969).

(3) Yamamuro, N. et al.: Nucl. Instr. Methods, 133, 531 (1976).

(4) Sowerby, M.G. et al.: Proc. Symp. Neutron Standards and Flux Normaliza-tion, AEC Symp. Ser.23, p.151 (1970).

(5) Schmitt, H.W.: Sample scattering corrections in neutron beam experiments, ORNL-2883 (1960).

(6) Evaluated Nuclear Data File /B -IV, ^{93}Nb(MAT=1189), ^{127}I(MAT=565), ^{165}Ho(MAT=820), ^{181}Ta(MAT=1285) and ^{238}U(MAT=1262) evaluated by Howerton, R.J. et al., Schmittroth, F. et al., Schenter, R.E. et al., Howerton, R.J. et al. and Paik, N.C., respectively.

(7) Chaubey, A.K., Sehgal, M.L.: Nucl. Phys., 66, 267 (1965).

(8) Belanova, T.S. et al.: J. Nucl. Energy, A/B, 20, 411 (1966).

(9) Rimawi, K., Chrien, R.E.: Proc. Conf. Nuclear Cross Sections and Technology, NBS special. publ. 425, p.920 (1975).

(10) Miller, L.B., Poenitz, W.P.: Nucl. Sci. Eng., 35, 295 (1969).

(11) de Saussure, G. et al.: Nucl. Sci. Eng., 51, 385 (1973).

(12) Moxon, M.C.: The neutron capture cross section of ^{238}U in the energy region 0.5 to 100 keV, AERE-R-6074 (1969).

(13) Friesenharn, S.J. et al.: Neutron capture cross sections of Mo, Ta and ^{238}U, GA-10194 (1970).

(14) Spencer, R.R., Kaeppeler, F.: Ref.(3), p.620.

(15) Yamamuro, N. et al.: J. Nucl. Sci. Tech., 17(8), 582 (1980).

(16) Quan, B.L. et al.: Precision Neutron Cross Section Measurements in Support of the LMFBR Program, COO-2479-10, p.17 (1976).

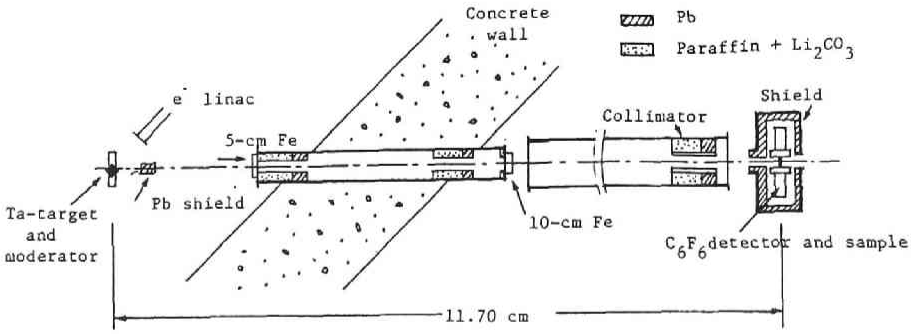

Fig. 8-1
Experimental arrangement of the capture-cross-section measurement at the KURRI-linac.

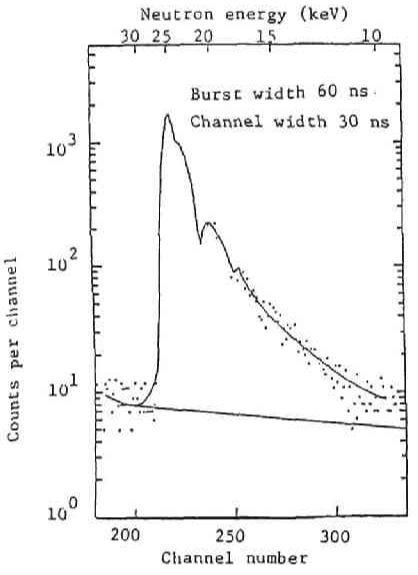

Fig. 8-2
Time-of-flight spectrum of Fe-filtered neutrons measured with a combination of the C_6F_6 detector and a ^{10}B-sample.
The line at the base is the background estimated by linearly-interpolating the block-out regions in the upper and lower energies.

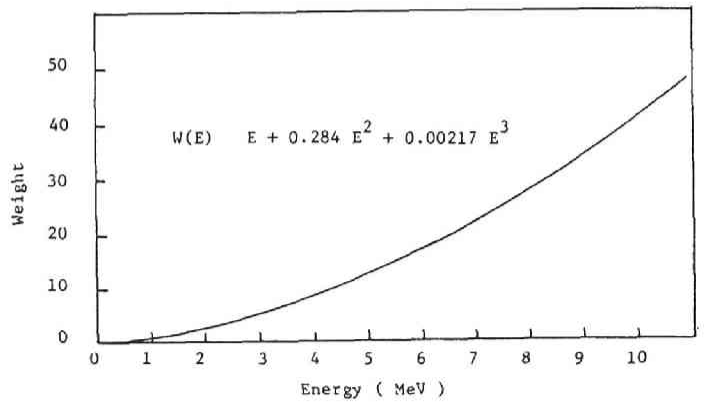

Fig. 8-3 Weighting function of the C_6F_6-detector.

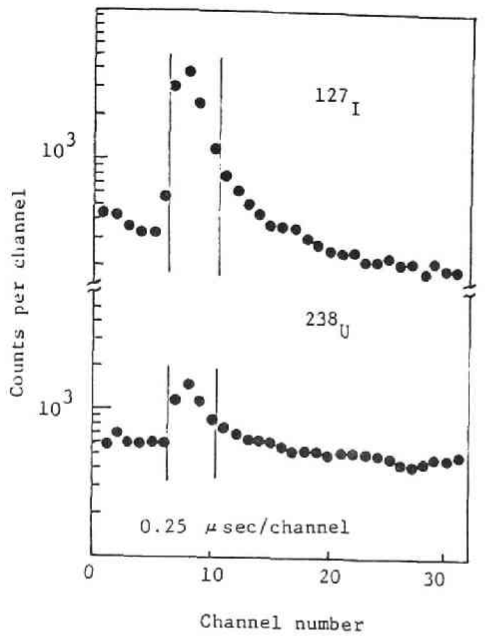

Fig. 8-4
Typical time-of-flight spectra for 24-keV neutrons for PbI_2 and U.

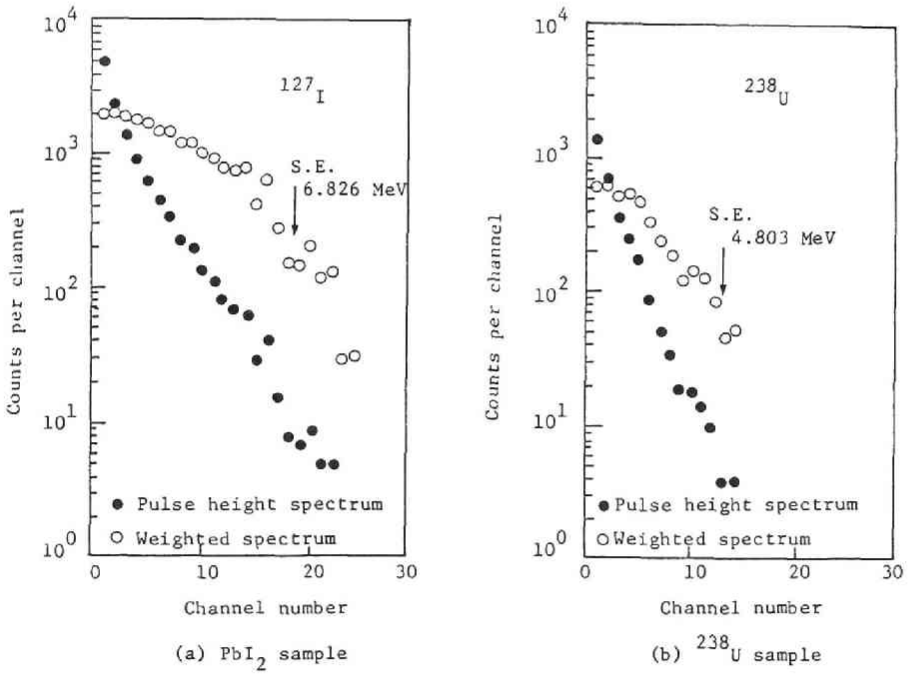

Fig. 8-5 Pulse-height and weighted spectra for 24-keV neutron capture in PbI_2 and ^{238}U.

Table 8-1 Samples and the factors in the analysis of experimental data

Target nucleus	Sample thickness (10^{-3} atoms/barn)	Multiple-scattering correction factor (%)	Statistical error of capture pribability (%)
^{93}Nb	5.26	7.0	3.0
^{115}I	3.64	4.5	4.3
^{127}In	4.96	7.2	2.7
^{165}Ho	6.63	11.6	2.5
^{181}Ta	4.52	7.8	4.2
^{238}U	1.30	3.8	6.0

Table 8-2 Capture cross sections for 24-keV neutrons

Target nucleus	Cross sections (mbarn)				
	Present	Chaubey & Sehgal[7]	Belanova et al.[8]	Rimawi & Chrien[9]	ENDF/B-IV[6]
^{93}Nb	340 ± 17		270 ± 15		275
^{115}In	770 ± 50	800 ± 50*	776 ± 66	583 ± 32**	
^{127}I	780 ± 40			767 ± 50	780
^{165}Ho	1280 ± 60	990 ± 70			1450
^{181}Ta	880 ± 50				910
^{238}U	520 ± 40		412 ± 18***	500 ± 38	490

*) The sum of 580 ± 40 mbarn for the transition to the isomeric states $^{115}In(n,\gamma)^{116m_1,m_2}In$ and 220 ± 30 mbarn for the transition to the ground state $^{115}In(n,\gamma)^{116}In$.

**) The cross section of $^{115}In(n,\gamma)^{116m_1,m_2}In$.

***) The Monte Carlo interpretation for the Belanova et al.'s experiment carried out by Miller and Poenitz[10] showed 495 ± 40 mbarn for ^{238}U capture cross section.

Table 8-3 Comparison of experimental results for ^{238}U for capture cross sections near 24 keV

Energy (keV)	Capture cross section (mbarn)	Authors
20 - 30	551 ± 30 *	de Saussure et al.[11]
20 - 30	462 ± 30 *	Moxon[12]
20 - 30	476 ± 30 *	Friesenhahn et al.[13]
24.3	499 ± 15	Quan et al.[16]
24.3	500 ± 38	Rimawi & Chrien[9]
23.7	520 ± 40	Present experiment

*)The values are quoted from Table VI of de Saussure et al.'s paper(11).

Chapter 9 Measurement of Nuclear Inelastic-Scattering Cross Section of Th for 144-keV Si-Filtered Neutrons[1]

9.1 Introduction

In recent years, there have been several measurements[2] and several theoretical evaluations[3-5] of the neutron cross sections of ^{232}Th. These investigations have been motivated by the need to assess Th as an alternative nuclear fuel. For the inelastic scattering, however, which is the prime interaction for the slowing down of neutrons in the higher energy region, neither the quality nor the quantity of the experimental information is satisfactory to guide the evaluations even when theory is used to extend the data. Experimental data are quite limited above 2 MeV while there seem to be no measurements below 250 keV.

The inelastic scattering cross section can be measured by detecting the inelastically-scattered neutrons[6-9] or by detecting the associated gamma-rays emitted from the excited residual nucleus[10]. Accelerator-produced neutrons are commonly used for such measurements by applying the time-of-flight technique. The Si-filtered 144-keV neutrons are intense and clean, and were successfully utilized at the MURR for a precise point-cross-section measurement of the inelastic scattering of ^{238}U[11]. The scattered neutrons were detected by a spherical hydrogen-gas counter. In the measurements reported in this chapter, the same technique with improvements in counting statistics has been applied at the MURR to measure the cross sections of ^{232}Th.

Thorium-232 is an even-even nucleus and has a simple structure in the low excited levels. These are the collective rotational states in a deformed nucleus. The first level is at 49.5 keV[3] and the second at 162.5 keV[3]. Thus, concerning the inelastic scattering, the 144-keV neutrons cause only the scattering for the first level. The inelestic scattering consists of two different mechanisms. One is the compound nucleus formation and the other is the direct interaction. The experimental information obtained from the present measurements is analyzed in terms of the coupled-channel calculation combined with the statistical-model calculation.

The angular distribution of the elastically-scattered neutrons at 144

keV was also obtained in the measurement. The distribution is compared with the calculations which are mentioned in the discussion of the inelastic cross section.

9.2 Experimental Method

9.2.1 Facility

A versatile filtered-neutron beam facility has been installed at a beam port of the 10 MW MURR[12]. A Si filter, 208 cm in length and 2.54 cm in diameter, was used in these measurements. A 1 mm-thick plate of ^{10}B acted as a thermal-neutron suppressor. Prior to the measurement, the beam characteristics of the filtered neutrons were experimentally studied with a spherical hydrogen-gas counter of 3 atm. pressure and 4 cm diameter which was used in the measurement of the present scattering cross sections. The beam had a diameter of 3 cm (FWHM) and there was a negligible amount of neutrons outside a 5 cm circle. The neutron flux of the beam was approximately 6 x 10^4 n/cm^{2}sec. Very little contamination of other energy neutrons was detected at energies higher than 144 keV. On the lower energy side, the contamination of 54-keV neutrons was about 8 % of the-144 keV neutrons. However, the 54-keV neutrons caused almost no problem in this measurement, as this energy is much lower than the 95 keV of inelastically-scattered neutrons.

9.2.2 Scattering Measurement

The scattering sample of Th was two metallic plates each 5.08 x 5.08 x 0.318 cm^3. Oxygen is the significant impurity in the metal by about 0.15 w/o. The sample and the spherical detector mentioned above were installed on a goniometer as shown in Fig.9-1. The filtered neutrons were collimated with a lead pre-collimator of 2.5 cm in diameter. The goniometer was moved around the axis as is indicated in the figure. The detector was fixed on the goniometer keeping its anode-wire parallel to the axis of the goniometer to maintain the axial symmetry of the counting efficiency for scattered neutrons. The sample was fixed on the axis at an angle of 60 degree

between the sample surface and the incident beam. Measurements were carried out at nine scattering angles from 30 to 150 degrees by a 15 degree increment.

With the arrangement in Fig.9-1, the angular-dependent scattering cross sections were measured by unfolding the measured pulse-height spectrum. However, in order to reduce the time drift effect, the elastic and the inelastic cross sections were obtained from two series of separate runs, respectively. For elastically scattered neutrons, the distance was set at 15 cm so as to take adequate counts in a few hours at each scattering angle. For the inelastic-cross-section measurements, the distance was reduced to 9 cm to obtain adequate counts within 40 hours for each scattering angle.

9.2.3 Background

The background counts in these measurements originated mainly from the air-scattered neutrons and from gamma-rays. The gamma-rays came both from the reactor and from the daughter nuclides of Th in the scattering sample. These introduced, however, only minor problems in subtraction of background as the pulse height of the gamma-rays was lower than that of neutrons in the energy region of interest. The background in the elastic-cross-section measurement was determined by a run with the Th sample removed. In the inelastic-cross-section measurement, elastically-scattered neutrons were,in a sense, one of the background components. This was simulated by replacing the Th-sample with a Pb-plate which has no inelastic scattering for 144-keV neutrons.

9.2.4 Data Processing

The unfolding of the pulse-height spectrum to an energy spectrum was performed with a FORTRAN program written for use with a mini-computer. The formalism in the program is based on an unfolding program developed by Miller[13]. The statistical error for the unfolded spectrum was estimated by calculating for a typical case the statistical dispersion of many unfolded values for a train of short-time runs.

The multiple-scattering correction was performed with an analytical method developed for a thin plate sample assuming that i) collisions occur spatially uniformly inside the sample,ii) the flight direction is isotropic for the neutrons colliding two or more times, and iii) inelastic scattering is isotropic.

9.3 Experimental Results

9.3.1 Incident Neutrons

The energy spectrum of incident neutrons obtained by the unfolding procedure is shown with a solid line in Fig.9-2, where one may see two groups of monoenergetic neutrons. The energy scale for the hydrogen-gas counter was calibrated at the neutron energies of 144 $\pm$ 0.5 and 54 $\pm$ 0.5 keV which are the average energies of the calculated energy spectra using the total-cross-section data available in a time-of-flight transmission measurement[14]. The dotted line in the figure shows the spectrum calculated using the total cross section of Si and assuming the so-called " 1/E spectrum " for the source neutrons. The FWHM of the 144-keV neutrons is approximately 15 keV.

The neutron cross sections of Th and the counting efficiency of the neutron detector vary with the neutron energy in the profile of the 144-keV neutrons. The effective energies for several experimental situations were calculated and, since these differed by no more than 1 keV, the 144 keV was employed as the quoted energy for this experiment.

9.3.2 Inelastically-Scattered Neutrons

In Fig.9-3 are shown typical pulse-height spectra of the hydrogen-gas counter for the scattered neutrons at a scattering angle of 60 degree. The difference in the spectra of Th and Pb is more clearly shown in the central part of the figure by using a linear vertical scale. The difference between the shapes of these spectra comes from the inelastic scattering of Th. These spectra were unfolded and the results are shown in Fig.9-4, where the spectra are normalized at 144 keV. The thickness of the Pb-sample was

chosen to scatter approximately the same number of neutrons as the Th-sample in order to make the experimental situation similar between Th and Pb. Subtracting the Pb-spectrum from that of Th gives the portion of the inelastically-scattered neutrons from Th. More precisely stated, the subtracting spectrum is prepared as a superposition of two kinds of spectra: one is the Th-spectrum for 144-keV neutrons extrapolated down to lower energies and the other is the Th-spectrum for 54-keV neutrons extrapolated up to higher energies, along with the respective shapes of the Pb-spectra for 144- and 54-keV neutrons. The subtracting spectrum is shown as a dot-dash-line in Fig.9-4. The gamma-ray and neutron background taken without the sample is also shown in the figure. Both the Th- and Pb-spectra contain the background and cancel each other in the subtracting procedure.

The inelastically-scattered portion of the spectrum is shown as a dotted line in Fig.9-4. The ratio of intensities between the elastically- and inelastically-scattered neutrons is obtained as the ratio of these respective spectra.

9.3.3 Angular Distributions

The measurements at the nine scattering angles were repeated a few times in order to minimize the long-time drift effects caused by the impinging neutrons, the amplifier gain, so forth. The background was determined by a measurement without any sample.

Relative intensities of scattered neutrons at the nine scattering angles both before and after the multiple-scattering correction, are listed in the upper halves of the second and fourth columns in Table 9-1.

The lower halves of the second and the fourth columns in the table were obtained by combining the ratios of intensities between the elastically- and inelastically-scattered neutrons and the angular dependence of the elastically-scattered neutrons.

9.3.4 Normalization of the Cross Section

The sum of the elastic and inelastic cross sections were normalized to the total cross section minus the capture cross section in order to obtain

the absolute value of the scattering cross sections. The value used for the total cross section was 11.8 ± 0.1 barns which was obtained in this experiment by making a good-geometry transmission measurement. The total capture cross section is 0.18 ± 0.017 barn adopted from reference[15] and the sum of the scattering cross sections are normalized to 11.62 ± 0.1 barns. The cross sections obtained are shown in the last column of Table 9-1 and in Fig.9-5. The angle-integrated inelastic cross section is 0.74 ± 0.05 barn. The uncertainty of this value is estimated in the next paragraph.

9.3.5 Estimation of Uncertainties

The numbers in the parentheses in the second column of Table 9-1 are the uncertainties in the meaning of the standard deviations which consist mainly of the counting statistics, the reproducibility of measurements and the arbitrariness in the backgrounds. The uncertainties are statistical and are not correlated between those different scattering angles.

Another factor that causes uncertainties in the cross section values is in the multiple scattering correction procedure. For the inelastic cross section, this correction is approximately 25 %. An uncertainty of 5 % is imposed, without any rigorous estimation, on the inelastic cross section at each scattering angle. The uncertainties of the 5 % are thought to be fully correlated between scattering angles. The uncertainty which comes from the correction procedure for the impurities in the sample is so small that it may be neglected.

As for the systematic error in the unfolding procedure, the estimation of uncertainty is generally a difficult problem. There are fortunate factors, however, in this experiment. The response functions of the elastically- and inelastically-scattered neutrons are similar each other. Moreover the response of 144-keV neutrons is given in the Pb-measurement. By considering these fortunate factors, the systematic error in the unfolding can be neglected for the ratio between the numbers of the elastically- and inelastically-scattered neutrons, which is the essential quantity to be measured in this experiment.

The spreads in scattering angles are about 10 and 16 degree for the

elastic and inelastic scatterings respectively. These were estimated by taking into account the finite sizes of the detector and the neutron beam.

The uncertainty in the angle-integrated inelastic cross section is estimated, by including the above-mentioned considerations, to be approximately 7 %.

9.4 Discussion

The angle-integrated inelastic-scattering cross section is compared in Fig.9-6 with other experimental data below 1 MeV. Also shown are three cross-section curves in the figure. The dotted curve is a calculated result[5] using a combination of the optical model of a spherical nucleus and the Hauser-Feshbach statistical model[16] modified according to Moldauer[17] for the level-width fluctuations and resonance interference effects. The parameters used are found in reference (5). The calculation treats the inelastic scattering as a compound-nucleus-formation process only. In order to prepare the recommended values for the cross section in JENDL-2, Ohsawa[5], therefore, included the contribution of the direct-scattering process by multipling the above-mentioned calculated values for the lowest three excited levels by respective correction factors. These correction factors (1.4 for the first level) were determined by utilizing the experiment of McMurray[10]. The evaluation is shown as a solid curve in Fig.6 and shows good agreement with the present measurement. The dot-dash-line in the figure is the evaluated curve in INDC(RUM)-10[3], which was estimated as the difference between the evaluated total cross section and the other components in the evaluation. This evaluation is lower than the present measurement.

Figure 9-5 shows the present results of the angular-dependent elastic and inelastic cross sections, along with three kinds of calcuations. The group A curves in the figure are the evaluation of JENDL-2[5]. The curve D stands for the statistical (Moldauer) model, and corresponds to the dotted curve in Fig.9-6. Evidently the calculation underestimates the inelastic scattering. Better fits to the data could not be obtained simply by varying the potential parameters of the spherical-optical-model within a reasonable range. Thus, calculations have been made to include the direct

inelastic-scattering process by employing the coupled-channel theory[18]. Computer codes, JUPITOR-1[19] as rewritten at the Japan Atomic Energy Research Institute and ELIESE-3[20], were used in the calculation. The results are shown in Fig.9-5 with the curves labeled with B and C. The parameters used are from Lagrange[21] for group B, and from Haouat et al.[22] for group C. The experimental errors prevent the detailed discussion of the angular dependence of inelastic scattering. The angle integrated value of C agrees with the experiment, while that of B is lower. For the elastic scattering, A and C almost agree with the measurement, while B shows slight enhancement in the forward direction.

The present measurement shows that the experimental data of inelastic scattering at 144 keV can be reasonably explained by taking into account the direct interaction effect, and that the present elastic and inelastic data can be interpreted with the potential parameter set of Haouat et al.[22] which was obtained from analysis at higher energies (0.6 - 3.4 MeV).

9.5 Conclusion

The 144-keV Si-filtered beam at the 10-MW MURR has been used to measure the inelastic-scattering cross section of ^{232}Th. The result is 0.74 $\pm$ 0.05 barn and first provided an experimental data below 250 keV. This value is in good agreement with the evaluation JENDL-2 and with a coupled-channel calculation where the inelastic scattering through the direct-exitation process of the collective rotational motion of a deformed nucleus is included as well as that through the compound-nucleus-formation process.

References:

1) Fujita, Y. et al.: To be published in J. Nucl. Sci. Technol.
2) CINDA 82, IAEA, Vienna (1982).
3) Vasiliu, G. et al.: INDC(RUM)-10, Nuclear Data Evaluation for Th-232, (1980).
4) Meadows, J. et al.: ANL/NDM-35, (1978).
5) Ohsawa, T., Ohta, M.: J. of Nucl. Sci. Technol., 18(6), 408 (1981).

6) Smith, A.B.: Phys. Rev., 126, 2, 718 (1962).
7) Glazkov, N.P.: At. Energy(USSR), 14, 900(1963); Sov. At. Energy, 14, 405 (1964).
8) Holmberg, M. et al.: Nucl. Phys., A127, 149 (1969).
9) Batchelor, R. et al.: ibid., 65, 236 (1965).
10) McMurray, W.R. et al.: Proc. Int. Conf. Interactions of Neutrons with Nuclei, Lowell, p.1329 (1976).
11) Tsang, F.Y., Brugger, R.M.: Nucl. Sci. Eng., 65, 70 (1978).
12) idem: Nucl. Instr. Methods, 134, 441 (1976).
13) Miller, W.H.: Nucl. Instr. Methods., 153, 535 (1978).
14) Kobayashi, K. et al.: Annals of Nucl. Energy 4, 449 (1977).
15) Kobayashi, K. et al.: J. of Nucl. Sci. Technol.,18(11), 823 (1981).
16) Hauser, W., Feshbach, H.: Phys. Rev., 87, 2, 366 (1952).
17) Moldauer, P.A.: Phys. Rev., 135, B622 (1964).
18) Tamura, T.: Rev. Mod. Phys., 37, 679 (1965).
19) Wakai, M. et al.: JAERI-memo-3833 (1969).
20) Igarasi, S.: JAERI-1224 (1972).
21) Lagrange, Ch.: JAERI-M-5984, p.58 (1975).
22) Haouat, G. et al.: Nucl. Sci. Eng., 81, 491 (1982).

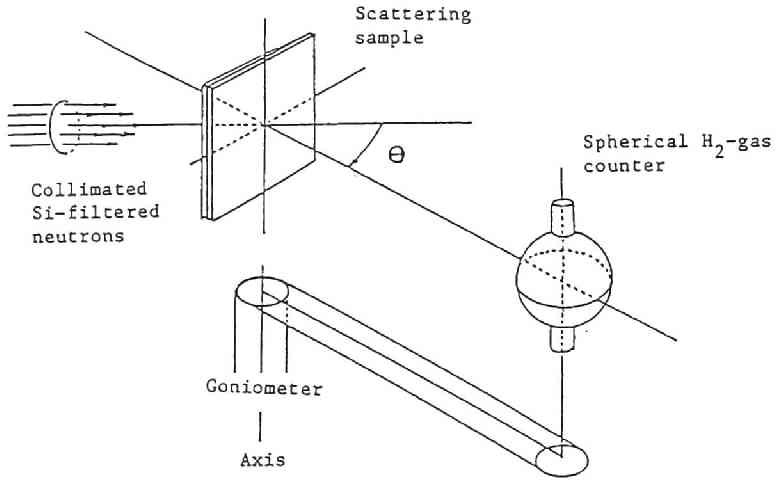

Fig. 9-1 Experimental arrangement for the scattering measurement.

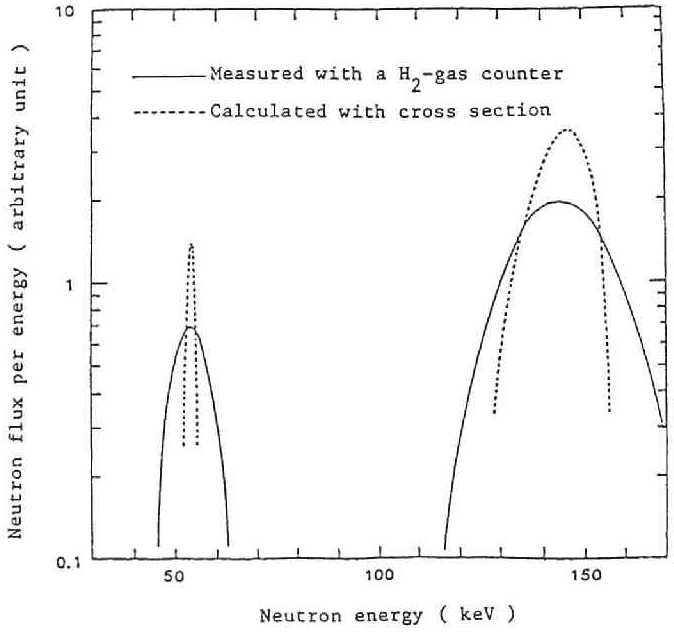

Fig. 9-2 Energy spectrum of the Si-filtered neutrons.

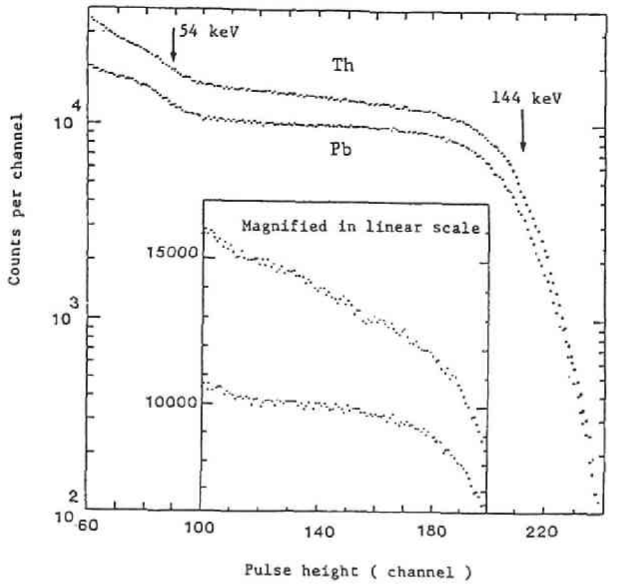

Fig. 9-3 Responces of the hydrogen-gas counter for neutrons scattered with the Th and Pb samples.

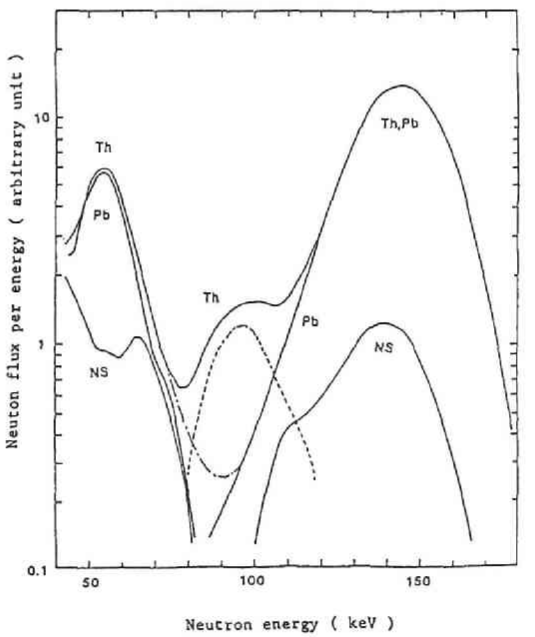

Fig. 9-4 Unfolded energy spectra of scattered neutrons with Th(Th), Pb(Pb) and without samples (NS). The dotted curve is the inelastically-scattered neutrons.

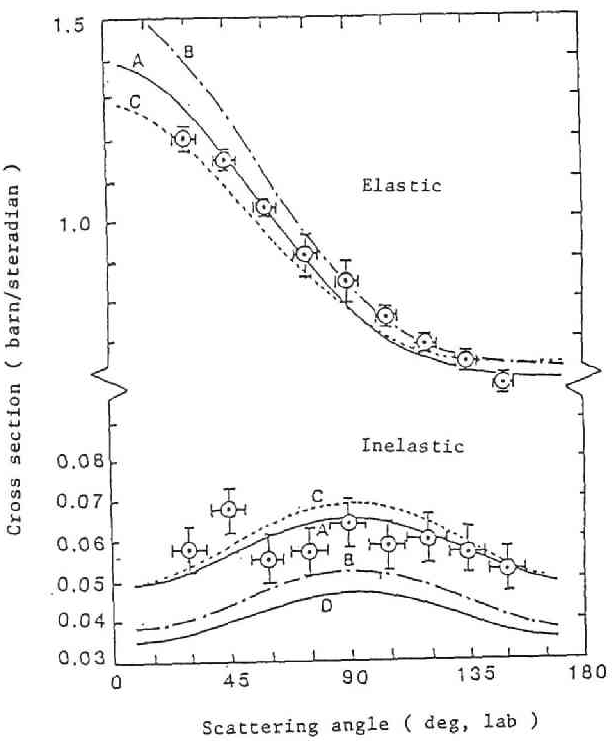

Fig. 9-5

Angular dependences of the scattering cross section of ^{232}Th.

A : Ohsawa 81 (JENDL-2)[5]

B : Coupled-channel calculation with parameters of Lagrange.[21]

C : Coupled-channel calculation with parameters of Haouat et al.[22]

D : Statistical-model calculation.[5]

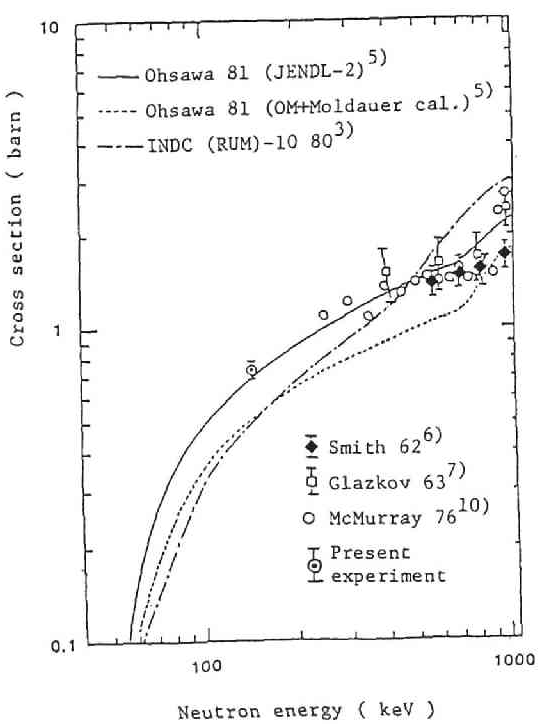

Fig. 9-6

Inelastic scattering cross section of ^{232}Th below 1 MeV.

Table 9-1 Experimental results of the elastic and the inelastic cross sections with the multiple-scattering correction factors.

Scattering angle in lab. system	Intensity of scattered neutrons (relative unit)	Multiple scattering correction factor	Multiple scattering corrected intensity	Cross sections obtained (barn/sterad)
Elastic scattering				
30	269 (7)	1.02	274	1.211 (0.032)
45	260 (6)	1.01	263	1.162 (0.027)
60	233 (5)	1.01	235	1.038 (0.022)
75	204 (12)	1.02	208	0.919 (0.054)
90	180 (11)	1.06	191	0.844 (0.052)
105	176 (6)	0.98	172	0.760 (0.026)
120	167 (5)	0.94	157	0.694 (0.021)
135	162 (7)	0.91	147	0.649 (0.028)
150	149 (7)	0.89	133	0.588 (0.028)
Inelastic scattering				
30	18.0 (1.8)	0.73	13.1	0.0579 (0.006)
45	20.7 (2.1)	0.74	15.3	0.0676 (0.007)
60	16.9 (1.7)	0.74	12.5	0.0552 (0.006)
75	17.0 (1.7)	0.76	12.9	0.0570 (0.006)
90	17.9 (1.8)	0.81	14.5	0.0641 (0.006)
105	17.4 (1.7)	0.76	13.2	0.0583 (0.006)
120	18.2 (1.8)	0.74	13.5	0.0596 (0.006)
135	17.3 (1.7)	0.74	12.8	0.0566 (0.006)
150	16.2 (1.6)	0.73	11.8	0.0521 (0.005)

i) The cross sections in the last column are obtained by normalyzing the angle-integrated scattering cross section to 11.62 barn.

ii) Numbers in the parentheses are the estimated uncertainties, the standard deviation, mainly consisting of the counting statistics, the reproducibility of measurement, and the arbitrariness in the subtraction of background.

Chapter 10 Measurement of a Relationship between Doppler and Self-Shielding Effects in Th by 24-keV Fe-Filtered Neutrons[1]

10.1 Introduction

The Doppler effect in neutron cross sections is the broadening of the resonance shape of the cross section. The broadening is caused by the thermal motion of the target nuclei, depending on the relative velosities between the incoming neutrons and the target nuclei. Unless the target is infinitely thin, the neutrons penetrating into the inner part of the target are shielded by the outer part of the target itself, resulting in the change of the number and energy-spectrum of the neutrons. This effect is called as the self-shielding. In another view point, the change is taken as a change of the effective cross section with the target thickness. These two effects are mutually related if the resonance appears in the energy spread of the incoming neutrons, and play a significant role in reactor safety and control. The treatment of these effects is one of the fundamental problems in reactor physics. The knowledge of the structure of the cross sections and the thermal motion of nuclei is needed for the computation of these factors. For neutronic computations, the cross sections in the unresolved energy range are often synthesized using an appropriate cross section formula, and a set of average resonance parameters and their statistical properties. For the thermal motion, the free-gas model is usually employed. Atomic binding effects are taken into consideration by adopting an effective temperature proposed by Lamb[2].

The apparent value of the total cross section depends on the thickness of the target, if it is measured with neutrons of energy spread wider than the resonance structure. The value is often called as " Effective Average Total Cross Section" and is abbreviated hereafter as EATCS or $< \sigma_t^{eff} >$. The EATCS depends on the physical states of the target such as the temperature and the chemical form, since the resonance width is broadened by the thermal motion of the target nuclei. Bee[3] has proposed a scaling law between the Doppler and the self-shielding effects, which will be introduced in the next section. Qualitatively Bee shows that EATCS decreases with increasing sample thickness, and increases with increasing sample

temperature. The scaling law predicts that there is a relationship between the thickness- and temperature-dependences in EATCS under the condition of high temperature limit. He compared the prediction with the available experimental data in ^{238}U. Not all the data satisfactorily agree with the prediction.

Tsang and Brugger installed an Fe-filtered-neutron facility at the 10 MW-MURR[4], and used the neutrons for the EATCS measurements of Sn[5] and ^{238}U[6] in order to study the chemical-form dependence of the Doppler effect. The filtered beam is intense and clean, and is effectively used for the precise measurement of EATCS in the good geometry transmission experiment.

The purpose of the present measurement is to first provide experimental data of the temperature dependence of EATCS for ^{232}Th and more precisely verify the scaling law. The measurements were carried out using 24-keV Fe-filtered neutrons provided at the above-mentioned facility, varying the thickness, the temperature, and the chemical form of the sample. Thorium-dioxide was used as a sample of a different chemical form.

Prior to the measurement, the beam quality of the Fe-filtered neutrons was carefully studied and improved by adding more S and Al as auxiliary filters. The study is described in Chapter 3.

10.2 Scaling Law between Doppler and Self-Shielding Effects

For the discussions of the present study given in a following section, the scaling law expressed in terms of the temperature and thickness of a transmission sample is briefly introduced here following the paper of Bee[3]. The resonance structure of a total cross section is described by the Breit-Wigner multi-level formula. If the conditions, (level spacing) >> (Doppler width) >> (total width), are fulfilled, the formula is adequately approximated as

$$\sigma_t = \sum_{\ell} \sigma_t^{\ell} \quad , \tag{10.1}$$

$$\sigma_t^{\ell} \simeq (2\ell + 1)\sin^2\phi_{\ell} \frac{4\pi}{k^2} + \sum_r \sigma_o^r \frac{\sqrt{\pi}}{\beta_r} \left\{ \exp(-X_r^2 / \beta_r^2) + \alpha^r \frac{2}{\sqrt{\pi}} F(X_r/\beta_r) \right\} . \tag{10.2}$$

Here the total cross section is written as a sum of conponents with orbital angular momentum ℓ and resonance identifier r. The three terms in the right-hand side of Eq.(10.2) are the potential, resonance and interference cross sections, respectively. The notations in the equations are commonly used ones, some of which are as follows:

$\sigma_o^r = \frac{4\pi}{k^2} g_J \cdot \Gamma_{rn} / \Gamma_r \cdot \cos 2\phi_\ell$, the peak height of unbroadened resonance, where ϕ_ℓ is the potential scattering phase shift;

$X_r = (2/\Gamma_r) \times (E - E_r)$, where E is the neutron energy and E_r is the the resonance energy;

$\beta_r = 2\Delta / \Gamma_r$, where Δ is the Doppler width (= $\sqrt{4 k \Theta E m/M}$), and Θ is the effective temperature;

$a^r = \tan(2\phi_\ell)$, the coefficient of interference term, for which a more detailed expression is given if the inclusion of the multi-level effect are needed;

$F(z) = \exp(-z^2) \int_0^z \exp(t^2) dt$, Dawson's integral.

The condition, (Doppler width) >> (total width), means the high temperature limit and is practically fulfilled for Th above the room temperature.

The EATCS is defined as an apparent total cross section obtained from a transmission factor $\langle T \rangle$ averaged over the region of energy width W. The brackets mean the averaged value. The value <T> is written as follows:

$$\langle T \rangle = \langle \exp(- N\sigma_t) \rangle = \exp(-N\sigma_c) \langle \exp(-N \sum_r \sigma_r) \rangle . \qquad (10.3)$$

Here N is the number of nuclei of target material in a unit area; σ_c is the potential scattering cross section including the effect of distant levels; σ_r is the resonance part of the cross section; the summation over r is performed for the resonances in the width W.

If the Doppler width is much less than the level spacing, the averaged transmission $\langle T \rangle$ is approximated as

$$\langle T \rangle = \exp(- N\sigma_c) \times \left[1 - (1/W) \sum_r A_E^r \right], \qquad (10.4)$$

where A_E^r is the standard transmission area function, which is given by

$$A_E^r = \int_{-\infty}^{\infty} \left\{ 1 - \exp(-N\sigma_r) \right\} dE \ , \tag{10.5}$$

$$A_E^r = \Delta \int_{-\infty}^{\infty} \left[1 - \exp - \left\{ \frac{N\ \sigma_o^r\ \pi}{2\ \Delta}\ \Gamma r \left(\exp(-\xi^2) + a^r \frac{2}{\pi}\ F(\xi) \right) \right\} \right] d\xi \ . \tag{10.6}$$

As $\Delta \propto \sqrt{\Theta}$, A_E^r/N depends only on the variable $N/\sqrt{\Theta}$ in the high temperature limit, and then

$$<T> = \exp(-N\sigma_c) \left\{ 1 - N \times f(N/\sqrt{\Theta}) \right\} \ . \tag{10.7}$$

As far as N × f is small, Eq.(10.7) can be replaced by

$$<T> = \exp \left\{ - N \left(\sigma_c + f(N/\sqrt{\Theta}) \right) \right\} \tag{10.8}$$

and the effective average total cross section or EATCS is simply

$$< \sigma_t^{eff} > = \sigma_c + f(N/\sqrt{\Theta}) . \tag{10.9}$$

If the resonances within the width W follow the Porter-Thomas distribution of neutron width, the EATCS is expressed as,

$$< \sigma_t^{eff} > = \sigma_c + \sum \frac{\pi}{2}\ \sigma_o^o\ \rho\ \bar{\Gamma}\ G\left(\frac{N\ \sigma_o^o \bar{\Gamma}_n}{2\ \Delta} \right) , \tag{10.10}$$

where $G(\nu) = \frac{1}{\pi\nu} \int_{-\infty}^{\infty} d\xi \left[1 - 1/\sqrt{1 + 2\nu\sqrt{\pi} \left\{ \exp(-\xi^2) + (2a/\sqrt{\pi})F(\xi) \right\}} \right]^{-1}$ (10.11)

and $\sigma_o^o = 4\ \pi\ g_J\ /\ k^2$,

where ρ is the level density and $\bar{\Gamma}_n$ is the average neutron width.

Eqs.(10.9) and (10.10) show that the EATCS depends on a parameter $N/\sqrt{\Theta}$ and there is a scaling law between the sample thickness N and the effective absolute temperature Θ. The EATCS expressed by Eq.(10.9) has no restriction on the number of resonances in taking the average. The value of EATCS fluctuates if the number is small, as a case of a Th-sample for Fe-filtered neutrons in this measurement, while the law holds irrespective of the fluctuation.

10.3 Experimental Method

The experiments were carried out at a versatile filtered-neutron beam facility installed at the 10 MW MURR. The experimental arrangement is shown in Fig.10-1.

10.3.1 Filtered Neutrons

The standard Fe/Al filter used at the MURR consisted of 50.8 cm of Fe, 20.3 cm of Al and 5.1 cm of S, and a 1-mm thick ^{10}B which suppressed the thermal neutrons. The study of the beam quality and the improvement are described in Chapter 3.

It is shown by a calculation using the total cross section data of the filter materials that the average energy of the beam is 24.0 $\pm$ 0.1 keV and the width in energy is 1.2 keV (FWHM).

10.3.2 Transmission Samples

Several metallic plates of 5.08 cm square with two kinds of thickness, 0.318 and 1.27 cm, were used for the Th samples. Samples from 0.318 to 3.81 cm thickness obtained by piling up these plates were adopted for the self-shielding measurements at room temperature. Three of them, 1.27, 2.54 and 3.81 cm, were used for the measurements of the temperature-dependence. The impurities which have the significant effect in the total cross section at 24 keV are O, C and H whose contents are less than 3000, 1000, and 20 ppm in weight, respectively.

For ThO_2, two discoid samples made of sintered dioxide were used. These were 5.08 cm in diameters, and 1.49 and 3.18 cm in thicknesses. The measurements at room temperature were made for 1.49-, 3.18-, and 4.67-cm-thick samples, and for 3.18- and 4.67-cm-thick samples at the elevated temperature. The atomic ratio O/Th was 2.00 $\pm$ 0.01.

10.3.3 Electric Furnace

The transmission sample was heated from room-temperature up to about

1170 K in an evacuated pipe of Inconel installed in an electric furnace. A thermo-couple of Chromel-Almel was used for the temperature measurement making contact with the sample. The temperature was raised and lowered very slowly,i.e. quasi-statically, imposing more than 10 h and by manual adjustment of the input electric power. The temperature showed a steady value within a few minutes of the counting period. It may be said that the thermo-couple indicated the correct sample temperature, even if the contact was imperfect, since consistent results were obtained between measurements taken under the raising and lowering processes.

10.3.4 Neutron and Gamma-Ray Counters

The incoming neutrons were monitored by a Cd-covered ^{3}He proportional counter placed in the beam, and the transmitted neutrons were measured by a long-counter, i.e. a bundle of three BF_3 counters installed in a paraffin moderator as shown in Fig.10-1.

The change of the atomic density of the sample in a unit cross sectional area caused by the thermal expansion should be corrected using data[7] of linear thermal expansion coefficients. Reliability of the data was confirmed by a transmission measurement of the reactor gamma-rays by using two NaI (Tl) detectors for the incident gamma-ray monitor and the gamma-ray transmission detector. Linear thermal expansion coefficients obtained are almost independent of temperature. They are $1.22 \times 10^{-5}(\pm 2\ \%)/K$ and $0.9 \times 10^{-5}(\pm 5\ \%)/K$ for Th and ThO_2 respectively, and are satisfactorily consitent with the data in Ref.(7).

Four pulse signals from the above mentioned detectors were accumulated in a multi-channel pulse height analyzer operating in the live-time mode; the correction was made automatically for counting-loss due to the dead time.

10.4 Experimental Results

10.4.1 EATCS at Room Temperature

Raw experimental data were normalized with the monitor counts and back-

grounds were subtracted. The neutron and gamma-ray backgrounds were measured by placing a thick polyethylene plate and a thick lead block in the neutron beam, respectively. The deduction of EATCS at room temperature was straight forward. The value of the total cross section of O was subtracted from the result for ThO_2 by adopting the value 3.736 $\pm$ 0.02 barns[8] obtained by the study in Chater 6. The results for EATCS at room temperature are shown in Fig.10-2.

There are two kinds of uncertainty in EATCS of Th metal. The first one is of statistical nature - the reproducibility of the transmission measurement including the statistics of counts and the error in the areal atomic density of the sample. The reproducibility is estimated to be about 0.15 % and the error in the areal density is about 0.3 to 0.4 %. The uncertainties in EATCS originated from these are about 0.4 to 0.5 % for overall samples with different thicknesses except 1.2 % for the thinest. The second kinds of uncertainties is one that comes from the correction procedure for the impurities, having the values from 0.9 to 1.3 %. Then the overall uncertainty for EATCS is from 1.0 to 1.8 %, as shown as the experimental errors in Fig.10-2. These uncertainties are highly correlated between the data points since the latter type of uncertainty dominates. The dotted error bars in Fig.10-2 are the total errors, and the solid bars are those of the first type uncertainties.

For ThO_2 at room temperature, the uncertainties estimated in the similar way are in the range from 0.4 to 0.5 %. The value of the O cross section should be subtracted from the EATCS of ThO_2 to obtain the EATCS of Th bound in ThO_2. The uncertainies of the O cross section and of the atomic ratio O/Th increase the uncertainty of EATCS. The overall uncertainty for the EATCS of Th bound in ThO_2 is about 0.9 %.

10.4.2 Temperature Dependence of EATCS

In order to deduce the temperature dependence of EATCS, we use a relation between this quantity and percent changes of neutron and gamma-ray transmissions. The relation is derived in the following.

Transmissions of neutrons $P_n(N,T)$ and gamma-rays $P_g(N,T)$ at temperature T and thickness $N(T)$ are written as follows:

$$P_n(N,T) = \exp(- N(\sigma + A \sigma_{ox})), \qquad (10.12)$$

$$P_g(N,T) = \exp(- N(\mu + A \mu_{ox})), \qquad (10.13)$$

where σ and μ are the Th cross sections of neutrons and photons respectively; the suffix ox means the values for O; the parameter A is zero for the metal and 2 for the oxide.

By taking into account that the values σ_{ox}, μ, μ_{ox} and A do not depend on temperature, the temperature dependence of EATCS for Th is expressed using Eqs. (10.12) and (10.13) as

$$\left(\frac{d\sigma}{dT} / \sigma\right) = \frac{1}{N\sigma}\left\{\frac{(\sigma + A\sigma_{ox})}{(\mu + A\mu_{ox})}\left(\frac{dP_g}{dT}\right) / P_g \quad \left(\frac{dP_n}{dT}\right) / P_n\right\} . \qquad (10.14)$$

The percent change $\Delta\sigma(T,T_o)/\sigma(T_o)$ in σ , caused by a temperature change from a reference temperature T_o to an elevated temperature T, is expressed from Eq.(10.14) using $\Delta P_n/P_n(T_o)$ and $\Delta P_g/P_g(T_o)$ - percent changes of transmissions for neutron and gamma-rays respectively - as

$$\Delta\sigma(T,T_o) / \sigma(T_o) = \frac{1}{N\sigma}\left\{\frac{(\sigma + A\sigma_{ox})}{(\mu + A\mu_{ox})} \Delta P_g / P_g(T_o) \quad \Delta P_n / P_n(T_o)\right\} , \qquad (10.15)$$

where N and σ are quantities at room temperature, and ΔP_g is considered to be proportional to N.

The results of temperature dependence of EATCS are shown in Figs.10-3 and 4 for Th and ThO_2 respectively. As for the experimental errors in the figures, almost all of systematic errors cancelled each other between room and elevated temperatures since the measurements were made relative to the room temperature. The dispersion of experimental points in the figures may be of a statistical nature, and roughly estimated systematic errors are shown in the figures as typical examples.

10.5 Discussion

The first discussion is given for a comparison between EATCS obtained at room temperature, a theoretically calculated EATCS and two evaluated values [9,10] of the total cross section. The second one is given for the rela-

tionship between the thickness and temperature dependences of EATCS: the verification of the scaling law which is the main purpose of this study.

For the first discussion, a typical set of average resonance parameters of Th is adopted from an evaluation work[11] and is shown in Table 10-1. The EATCS at room temperature is calculated using this parameter set and Eq.(10.11) for the resonances having the Porter-Thomas distribution. The calculated EATCS is shown with the dotted curve in Fig.10-2. In the calculation, the effective temperature is taken to be equal to the real temperature T, since they are very close to each other in the case of Th metal above room temperature. Two evaluated total cross sections[9,10] corresponding to an infinitely thin sample are also shown in Fig.10-2. The solid curve in Fig.10-2 is a fitting to the experiment of Th with a parabolic function of thickness.

An estimation is needed for the statistical fluctuation of EATCS in a limited energy band to make the above mentioned comparison. The expected number n of resonances in an energy band W is $W/\langle D\rangle$; the ratio of W to the average level spacing $\langle D\rangle$. Two formulas of the statistical properties of resonance parameters - Wigner and Porter-Thomas distributions - give that the sampling fluctuation of n is $\sqrt{0.27/n}$ and that of the accumulated reduced neutron width is $\sqrt{2/n}$, respectively. Then, the sampling fluctuation of the strength function is approximately $\sqrt{2.27/n}$. The fluctuation mainly comes from that of the accumulated reduced neutron width. The width W is about 1.2 keV (FWHM) in this experiment. The estimation of the fluctuation using the parameters in Table 10-1 and taking s-and p-waves into consideration shows that the averaged resonance cross section is 3.4 $\pm$ 0.5 (14 %) barns for an infinitely thin sample. By increasing and decreasing the strength function by 14 %, two dot-dash-curves (A) and (B) of EATCS in Fig.10-2 are calclated by the same way as for the dotted curve in the figure. For large N ($> 4 \times 10^{-2}$ atoms per barn), the experiment and the calculation (the dotted curve) differ by about two times of the fluctuation. For small N ($< 2 \times 10^{-2}$ atoms per barn), the experiment mediates between the evaluated total cross sections. However, a precise comparison is largely limited because of the fluctuation. There was an experiment[12] of EATCS of Th at room temperature. The data in the experiment is considerably larger than the present result. The author studied about the inconsistency and found

no other explanation than the neglection of the correction of impurities in the sample used in the previous experiment.

Proceeding to the second discussion, it is stated again that the scaling law holds irrespective of the distribution of resonance widths. By using the parameter $\bar{n}/\sqrt{\Theta}$, the thickness dependence in Fig.10-2 and the temperature dependence in Figs.10-3 and 4 are compared in Fig.10-5. The solid curve in the Fig.10-5 is the same as in Fig.10-2. Experimental points in Figs.10-3 and 4 are converted to the points in Fig.10-5 taking a reference temperature at 296 K. Fig.10-5 shows clearly the scaling law holds in the case of Th metal (upper). For the oxide (lower), the measured EATCS seems to be slightly less sensitive to the temperature change. The close comparison should not be made, since the solid curve is characteristic of the metal and not of the oxide.

A more precise comparison may be made by showing the predicted curves of the changes of EATCS with temperature in Figs.10-3 and 4. The temperature dependence is predicted using one of the curves in Fig.10-2, if one admits the scaling law. The predicted curves are shown in Figs.10-3 and 4. For the metal in Fig.10-3, the curves - the solid curve from the experiment and the dotted curve from the calculation - are close to the experimental data.

The effective temperature is introduced at this stage of discussion. The temperature Θ is expressed[13] by using the Debye temperature Θ_d as

$$\Theta = T \left(1 + 0.05\, \Theta_d^2 / T^2 - \ldots \right). \qquad (10.17)$$

The Θ_d for Th metal is 163 K[14]. For such a small Debye temperature, the difference of curves in Fig.10-3 is very small between adoptions of T and for the effective temperature. For the oxide, Θ_d of 393 K [15] is adopted though the meaning of the Debye theory may not be so clear for a diatomic substance. The upper dotted curves in Fig.10-4 are the predicted temperature dependence adopting T, and the lower ones adopting Θ for the effective temperature respectively. The difference between two kinds of predictions is small at least above room temperature. The upper curves, considering the agreement between the experiment and the prediction for the metal shown in Fig.10-3, are close to the temperature dependences for metal samples having the same thicknesses of the respective oxide samples. Figure

10-4 indicates, therefore, that the difference of the temperature dependence between the metal and oxide is within the experimental confidence band of this measurement. This experiment did not show any marked difference between Th and ThO_2 in both of the thickness and temperature dependences of EATCS, as seen in Figs. 10-2 and 10-4 respectively, though one experiment[6] showed marked differences between U and U_3O_8.

10.6 Conclusion

The present study experimentally verified using Th-samples the theoretical prediction that the temperature and thickness dependences of EATCS are scaled by one parameter $N/\sqrt{\Theta}$ in the high temperature limit , N being the thickness and Θ the effective temperature. The difference of EATCS between Th-metal and ThO_2 is small and within the error of this experiment at least above room temperature, though some dependence on atomic binding was expected.

References:

(1) Fujita, Y. et al.: To be submitted to J. Nucl. Sci. Technol.

(2) Lamb, Jr., W.E.: Phys. Rev., 55, 190 (1939).

(3) Bee, N.J. : " The Relationship between the Nuclear Doppler and Self-Shielding Effects and the Local s-Wave Strength Function in ^{238}U ", IAEA/NEA Consltants' Meeting on Uranium and Plutonium Resonance Parameters, Vienna, (1981).

(4) Tsang, F.Y., Brugger, R.M.: Nucl. Instr. Methods, 134, 441 (1976).

(5) Tsang, F.Y., Brugger, R.M.: Nucl. Sci. Eng., 74, 34 (1980).

(6) Tsang, F.Y., Brugger, R.M.: Nucl. Sci. Eng., 72, 52 (1979).

(7) Touloukian, Y.S., ed.: " Thermophysical Properties of High Temperature Solid Materials ", The MacMillan Co., New York (1967).

(8) Block, R.C. et al.: J. of Nucl. Sci. Technol., 12(1), 1 (1975).

(9) Meadows, J. et al.: ANL/NDM-35 (1978).

(10) Ohsawa, T., Ohta, M.: J. of Nucl. Sci. Technol., 18(6),408 (1981).

(11) Vasiliu, G. et al.: INDC(RUM)-10, Nuclear Data Evaluation for ^{232}Th,

(1980).
(12) Kobayashi, K., Fujita, Y. et al.: Nucl. Sci. Eng., 65, 347 (1978).
(13) Fröhner, F.H.: Applied Neutron Resonance Theory, KfK-2669, (1978).
(14) Gordon, J.E. et al.: Phys. Rev., 152, 1, 432 (1966).
(15) Willis, B.T.M.: Proc. Roy. Soc. London, 133, 274 (1963).

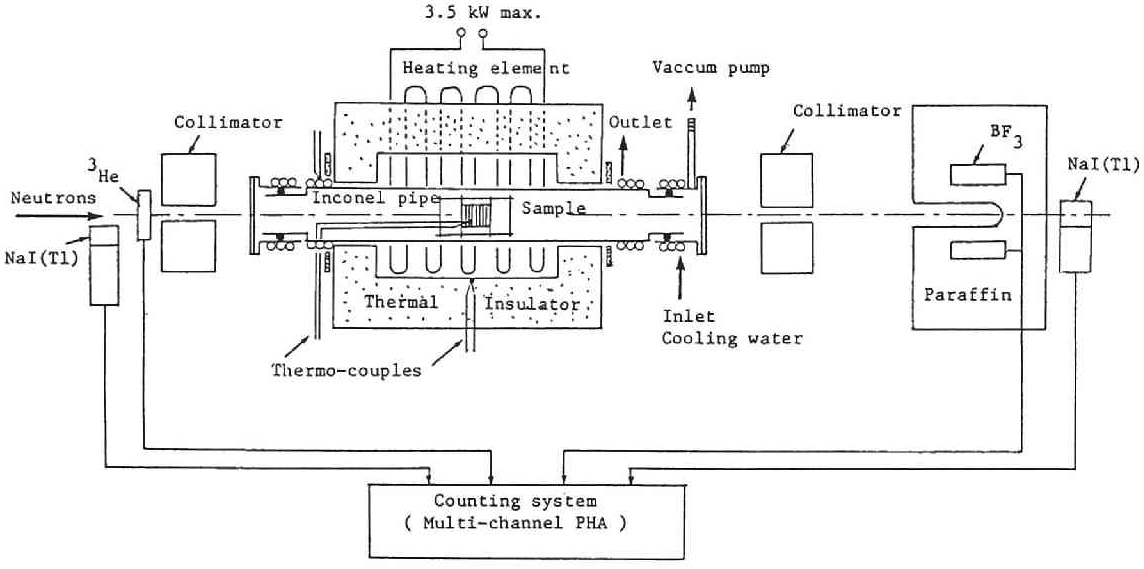

Fig. 10-1 Experimental arrangement of EATCS measurement.

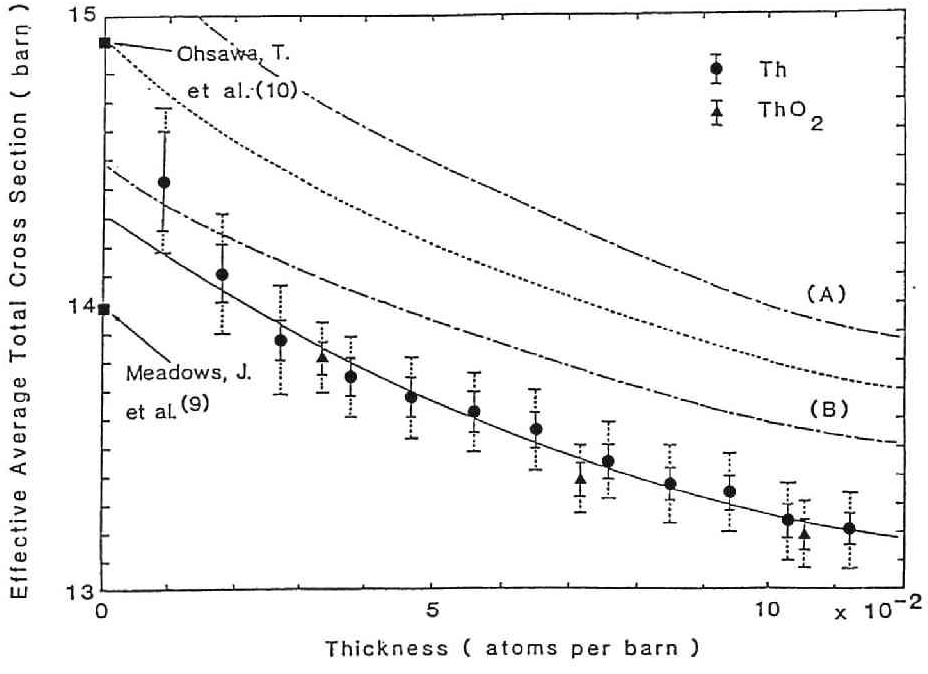

Fig. 10-2 EATCS of Th and ThO_2 at room temperature. The solid curve is a fitting to the experiment of Th with a parabolic function. The dotted and dot-dash curves are theoretical calculations and the details are found in the text.

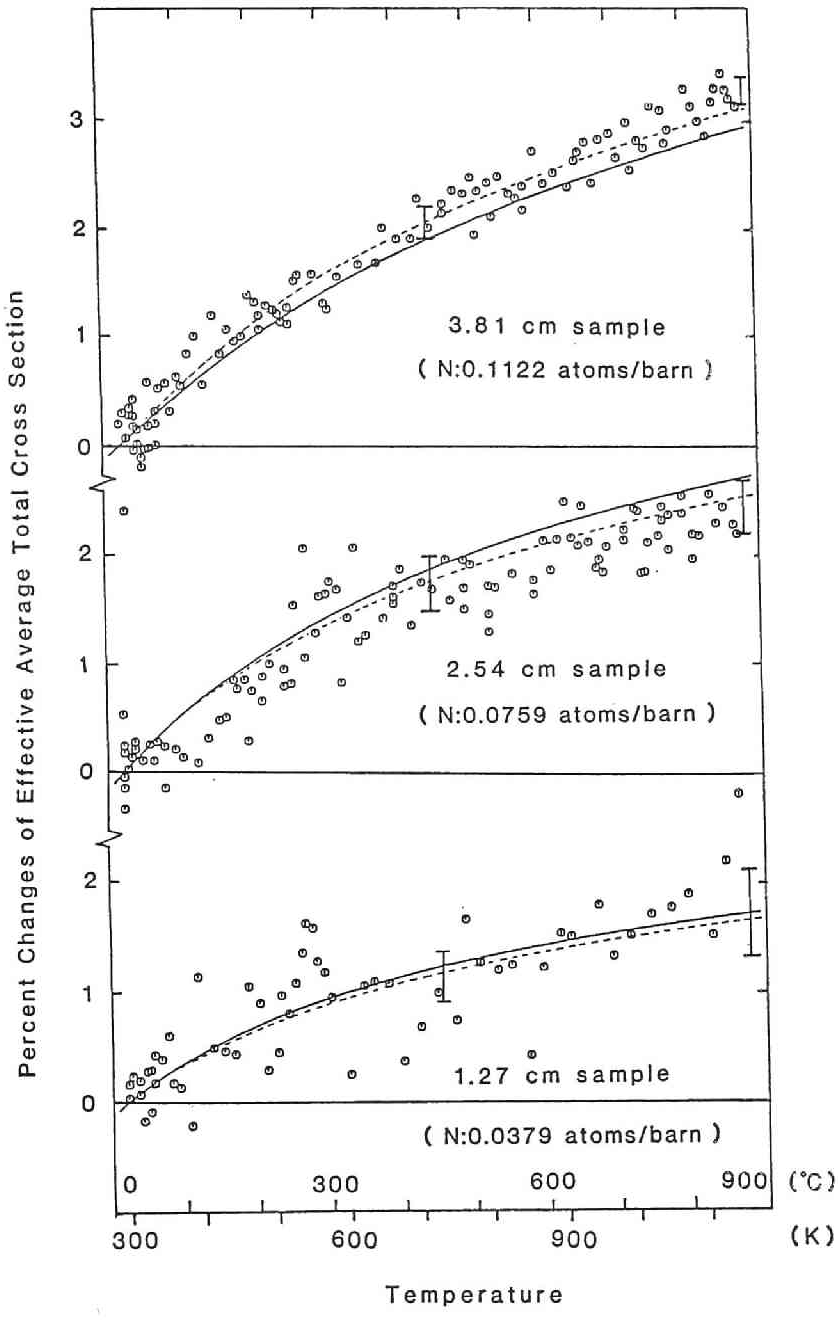

Fig. 10-3 Percent changes of EATCS with temperature for Th. Vertical bars show the confidence band of experiment. Curves are the predicted EATCS using the scaling law and the thickness dependences shown by the solid and dotted curves in Fig.10-2 respectively.

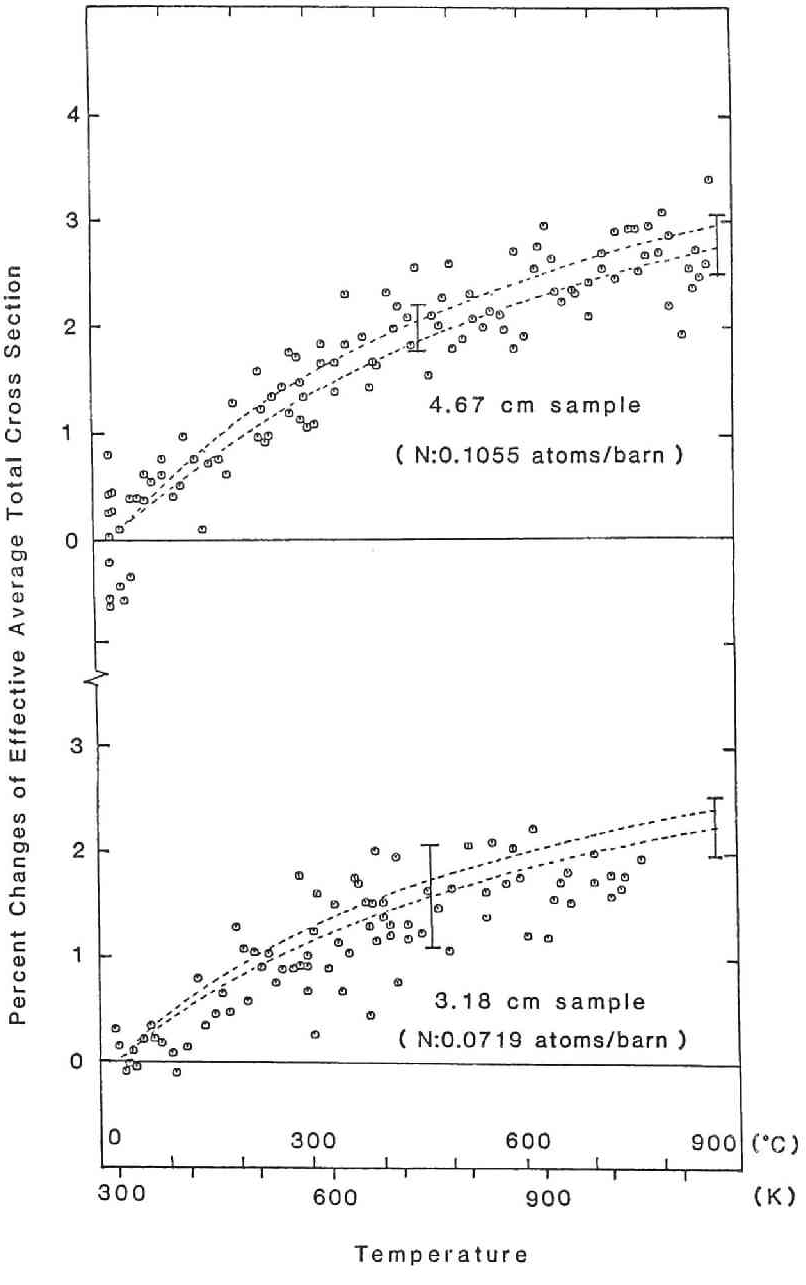

Fig. 10-4 Percent changes of EATCS with temperature for ThO_2. Vertical bars show the confidence band of experiment. Curves are the predictions using the scaling law and the thickness dependence shown by the dotted curve in Fig.10-2. The upper dotted curves are obtained by adopting a real temperature and the lower adopting an effective temperature for the prediction.

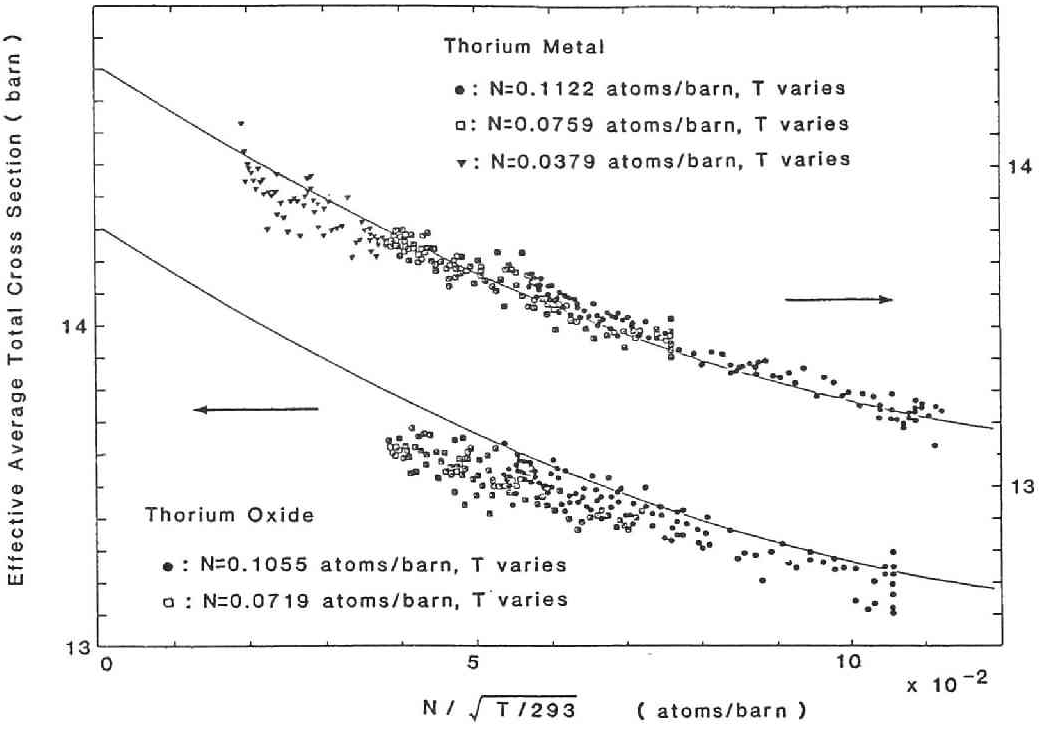

Fig. 10-5 Changes of EATCS for Th and ThO_2 as a function of the dependence and thickness of the sample.

Table 10-1 Evaluated values of the unresolved resonance parameters for ^{232}Th (11)

Quantity	Evaluated Value
a (fm)	9.72 ± 0.3
$\langle D(0,1/2) \rangle$ (eV)	16.57 ± 0.9
$\langle D(1,1/2) \rangle$ (eV)	16.57 ± 0.9
$\langle D(1,3/2) \rangle$ (eV)	8.285
$\langle \Gamma_n^0(1/2) \rangle$ (meV)	1.419 ± 0.08
$\langle \Gamma_n^1(1/2) \rangle$ (meV)	2.4855
$\langle \Gamma_n^1(3/2) \rangle$ (meV)	1.24275
$\langle \Gamma_\gamma \rangle$ (meV)	$21. \pm 0.77$
S_0	$0.8559 \pm 0.09 \times 10^{-4}$
S_1	$1.5 \pm 0.4 \times 10^{-4}$

Chapter 11 Concluding Remarks

In order to meet the requirements of reliable neutron-cross-section data for the research and development of nuclear energy, this study has extended the application of filtered neutrons to precise measurements of neutron cross sections by making effective use of excellent characteristics - clean and intense - of the neutrons. The experiments in the main part were carried out by employing a photo-neutron source with an electron linear accelerator. The other experiments were carried out using the reactor-based filtered neutrons. The subjects of the application were taken up with a view to show the capabilities of filtered neutrons for precise measurements and simultaneously to provide refined experimental data for several materials mainly of technological importance. The conclusions obtained in the applications are summarized in the following items:

(1) In order to provide relaible data for an optimal design of a Sc-filter, the neutron total cross section has been measured near the 2-keV cross-section minimum using the time-of-flight method and the neutrons filtered with Sc itself. The minimum value of the cross section obtained is 0.21 $\pm$ 0.03 barn, which is only one third of a recent measurement with the similar technique. The lower value of this study indicates that one may use a much thicker filter in a filtered-beam facility to reduce further the background in experiments. A trial of fitting the present result with the Breit-Wigner multi-level formula shows that the lower value is consistent with the dominant contribution of the spin-antiparallel interaction for thermal neutrons.

(2) Silicon is another filter material whose cross section values near the minima are scarce. A similar measurement to that of Sc has been carried out for Si near the minima. The cross section near the 146-keV minimum is 0.187 $\pm$ 0.006 barn, which is much lower than - approximately 50 % of - the JENDL-2 evaluation. The measurement newly found another marked window near 53.5 keV which was not considered in the evaluation. The value is 0.265 $\pm$ 0.008 barn and this minimum should be also taken into consideration in a filter design.

(3) An applicability study of the accelerator-based Fe-filtered beam technique has been carried out in a transmission measurement and has shown that the technique is intrinsically capable of yielding an accuracy of 0.1 %, which is considerably better than a typical value of about 1 % in this energy range and comparable to that achieved in precise measurements of thermal-neutron cross sections. Along with the feasibility study, the technique has been applied to the total cross sections of Be, C and O, giving the data with an accuracy of approximately 0.2 %. The result for Be, 5.903 $\pm$ 0.011 barns, agrees with the ENDF/B-V value by 0.4 %, and 4.5 % larger than the JENDL-2 value. For C, the result obtained, 4.684 $\pm$ 0.009 barns, is larger than the evaluations by 0.7 to 1.2 %. For O, the result, 3.736 $\pm$ 0.007 barns, is 1.6 % larger than the ENDF/B-III.

(4) The accelerator-based Fe-filtered beam, which was shown to be capable of transmission measurements of a 0.1-% intrinsical accuracy, has been applied to the total cross section of the n-p interaction. The result is 17.740 $\pm$ 0.023 barns at the effective energy of 23.645 $\pm$ 0.068 keV and provides a precise value in the keV region with an accracy comparable to that of the most precise experiments in other energy ranges. The value was used to discuss the empirical parameters used in the effective-range formula of the n-p interaction.

(5) The accelerator-based Fe-filtered beam has been applied to point capture cross-section measurements. The accuracy attained is about 5 % and is considerably better than the discrepancies which exist between the presently-available experimental data. It has been shown that this technique may be used as one of the effective techniques to settle the problem of the discrepancies between the existing data. The sample materials taken up for measurements are a fertile material ^{238}U, a structural material ^{93}Nb, and four nuclei of atomic-mass-numbers near those of fission products ^{115}In, ^{127}I, ^{165}Ho and ^{181}Ta.

(6) The 144-keV Si-filtered beam at the 10-MW MURR has been used to measure the inelastic-scattering cross section of ^{232}Th. The result is 0.74 $\pm$

0.05 barn and first provided an experimental data below 250 keV. This value is in good agreement with the evaluation JENDL-2 and with a coupled-channel calculation where the inelastic scattering through the direct-exitation process of the collective rotational motion of a deformed nucleus is included as well as that through the compound-nucleus-formation process.

(7) The 24-keV Fe-filtered beam at the reactor has been applied to an experimental study of a relationship between the Doppler and self-shielding effects by measuring the effective average total cross sections of the Th-metal and ThO_2. The present study experimentally verified the Bee's theoretical prediction that the temperature and thickness dependences of the EATCS are scaled by one parameter $N/\sqrt{\Theta}$ in the high temperature limit, N being the thickness and Θ the effective temperature. The difference of EATCS between Th and ThO_2 is small and within the error of this experiment at least above room temperature, though some dependence on atomic binding was expected.

General conclusions of this study and a few recommendations for the future applications of the filtered neutrons for precise cross-section measurements are summarized as follows:

(1) The study has shown that the filtered neutrons are capable of precise measurements of neutron cross sections in the keV range, where the means of neutron production are scarce, with precisions as high as those of the most precise measurements in other energy ranges. The experimental techniques applying filtered neutrons may be used to meet the technological requirements on more precise cross-section data.

(2) The accelerator-based filtered neutrons with employing the time-of-flight technique have been found to almost completely remove perplexing problems of the background in experiments. This leads to obtain a precise cross section. It is recommended to apply the filtered-neutron technique in parallel with the measurements of cross-section curves in order to normalize the curves and improve the reliability of the absolute values. The technique is especially suited to the experiment with an electron linear

accelerator since the thick filter also reduces the gamma-flash disturbance to the detector system. The beam width is not necessarily short as the energy resolution is determined by the filter material.

(3) Reactor-based filtered neutrons are intense and steady. However, much care is necessary in the removal and the subtraction of background since the time-of-flight technique can not be usually applied at reactors. The filtered neutrons at reactors are suited to measurements of a small change of cross sections such as the temperature dependence, and to measurements where the intensity and steadiness of the neutrons are needed.

(4) There are several possibilities of other filter materials than those used in this study. Applications of these materials are recommended for precise measurements at different energies. Seperated isotopes of an even-even nucleus may have marked interference minima and the cross-section measurements of these materials are expected to extend the variety of filter materials. These filteres may be expensive; however, they also have other fields of application such as in a medical facility of the neutron therapy.

Acknowledgment

The author wishes to express his sincere gratitude to Prof. Toshikazu Shibata, Prof. Itsuro Kimura and all of the members of the Division of Nuclear Reactor of the Research Reactor Institute of Kyoto University for their continued encouragement during a long period before the completion of this study.

The accelerator-based filtered-neutron technique was introduced to KURRI-LINAC by Dr. Robert C. Block, Professor of the Rensselaer Polythechnic Institute, in 1974 during his stay at KURRI. He conducted the experiment in Chapter 6 and showed the technique was suited to experiments using a medium-scale electron linear accelerator.

Dr. Nobuhiro Yamamuro, Professor (presently Emeritus Professor) of Tokyo Institute of Technology, conducted a series of the capture-cross-section measurements at KURRI-LINAC from 1974 to 1982. He developed the pulse-height-weighting technique introducing C_6F_6 and C_6D_6 scintillation detectors. The experiment in Chapter 7 is a study by the combination of the pulse-height-weighting and filtered-neutron techniques.

The experiments in Chapters 9 and 10 were carried at the Research Reactor Facility of the University of Missouri (MURR) during the author's stay from July 1981 to April 1982 under the cooperation with Dr. Robert M. Brugger, Director of the Facility. The staff of MURR helped the author to make his stay very fruitful. The theoretical analysis in Chapter 9 was carried out by Mr. Takaaki Ohsawa of Kyushu University.

The author is deeply grateful to the staff of KURRI-LINAC: Dr. Katsuhei Kobayashi who was in the closest cooperation in almost all experiments at the linac; Messrs. Yasuhiro Kimura, Kiyoshi Takami, Shuji Yamamoto and Toshihiko Kozuka for their continued effort of the maintainance works of the linac and for their very-willing technological survices in the laboratory equipment.

The author wishes to express his gratitude for the continued encouragement and for the guidance and co-operation in the research works of neutron thermalization which is another field of his research activity, to the following doctors: Dr. Kenji Sumita, Professor of Osaka University; Dr. Akito Takahashi, Associate Professor of Osaka University; Mr. Shigeyasu Sakamoto,

Associate Professor of Tokai University; and Dr. Otohiko Aizawa, Associate Professor of Musashi Institute of Technology.

He also wishes to express his gratitude to Dr. Hiroshi Nishihara, Professor of Kyoto University and Dr. Keisuke Kobayashi, Associate Professor of Kyoto University, for their critical reading of the manuscript of this thesis and giving helpful advice to him.

The list of the publications relevant to the present study

Full papers :

1) Robert C. BLOCK, Yoshiaki FUJITA, Katsuhei KOBAYASHI, Tohru OOSAKI: " Precision Neutron Total Cross Section Measurements Near 24 keV ", J. Nucl. Sci. Technol., 12(1), 1 (1975).
2) Yoshiaki FUJITA, Katsuhei KOBAYASHI, Tohru OOSAKI , Robert C. BLOCK: " Measurement of the Neutron-Proton Total Cross Section Using 24 keV Iron Filtered Neutrons ", Nucl. Phys., A258, 1 (1976).
3) Katsuhei KOBAYASHI, Yoshiaki FUJITA, Yoshihiro OGAWA: " Measurements of Neutron Total Cross Section Minima in Natural Iron and Silicon ", Annals of Nucl. Energy, 4, 499 (1977).
4) Nobuhiro YAMAMURO, Takeshi DOI, Toshiharu MIYAGAWA, Yoshiaki FUJITA, Katsuhei KOBAYASHI , Robert C. BLOCK: " Measurements of Neutron Capture Cross Sections with Fe-Filtered Beam ", J. Nucl. Sci. Technol., 15(9), 637 (1978).
5) Yoshiaki FUJITA; " Measurements of Neutron Total Cross Section of Scandium Near 2 keV ", J. Nucl. Sci. Technol., 20(3), 191 (1983).
6) Yoshiaki FUJITA, Takaaki OHSAWA, Robert M. BRUGGER, Don M. ALGER, William H. MILLER : " Measurement of the Nuclear Inelastic Scattering Cross Section of ^{232}Th for 144 keV Si-Filtered Neutrons ", J. Nucl. Sci. Technol., 20(12), 983 (1983).
7) Yoshiaki FUJITA, Robert M. BRUGGER, Don M. ALGER and William H. MILLER; " Measurement of a Relationship between the Doppler and the Self-Shielding Effects in ^{232}Th for 24 keV Neutrons ", J. Nucl. Sci. Technol., 21(2), 83 (1984).

Short Note :

1) Yoshiaki FUJITA, Katsuhei KOBAYASHI, Itsuro KIMURA , Saim A. SELVI: " Measurements of Cross Section Minima of Si Near 146 and 53.5 keV ", to be submitted to J. Nucl. Sci. Technol.

Exposition :

1) Yoshiaki FUJITA and Nobuhiro YAMAMURO; " Filtered Neutron Beam and Its Application " (in Japanese), J. of Atomic Energy Soc. of Japan, 23(2), 3 (1981).